

LIVIA MARIA BRUMATTI DE SOUZA

**ASSESSMENT OF EXTREME CLIMATE IMPACTS ON LARGE-SCALE
COMMODITY AND FAMILY FARMING AGRICULTURE IN BRAZIL**

Thesis presented to the Applied Meteorology
graduate program of the Universidade Federal de
Viçosa in partial fulfillment of the requirements
for the degree of *Doctor Scientiae*.

Adviser: Gabrielle Ferreira Pires

Co-advisers: Lívia Cristina Pinto Dias
Lineu Neiva Rodrigues
Gabriel Medeiros Abrahão

**VIÇOSA – MINAS GERAIS
2023**

**Ficha catalográfica elaborada pela Biblioteca Central da Universidade
Federal de Viçosa - Campus Viçosa**

T

S729a
2023
Souza, Livia Maria Brumatti de, 1992-
Assessment of extreme climate impacts on large-scale
commodity and family farming agriculture in Brazil / Livia
Maria Brumatti de Souza. – Viçosa, MG, 2023.
1 tese eletrônica (136 f.): il. (algumas color.).

Texto em inglês.

Orientador: Gabrielle Ferreira Pires.

Tese (doutorado) - Universidade Federal de Viçosa,
Departamento de Engenharia Agrícola, 2023.

Referências bibliográficas: f. 129-136.

DOI: <https://doi.org/10.47328/ufvbbt.2023.356>

Modo de acesso: World Wide Web.

1. Climatologia agrícola. 2. Produtos agrícolas.
3. Agricultura familiar. I. Pires, Gabrielle Ferreira, 1987-.
II. Universidade Federal de Viçosa. Departamento de Engenharia
Agrícola. Programa de Pós-Graduação em Meteorologia
Aplicada. III. Título.

CDD 22. ed. 632.1


LIVIA MARIA BRUMATTI DE SOUZA

**ASSESSMENT OF EXTREME CLIMATE IMPACTS ON LARGE-SCALE
COMMODITY AND FAMILY FARMING AGRICULTURE IN BRAZIL**


Thesis presented to the Applied Meteorology
graduate program of the Universidade Federal de
Viçosa in partial fulfillment of the requirements
for the degree of *Doctor Scientiae*.

APPROVED: May 23, 2023

Assent:

Documento assinado digitalmente
 LIVIA MARIA BRUMATTI DE SOUZA
Data: 07/06/2023 10:00:13-0300
Verifique em <https://validar.iti.gov.br>

Livia Maria Brumatti de Souza
Author

Documento assinado digitalmente
 GABRIELLE FERREIRA PIRES
Data: 07/06/2023 10:11:30-0300
Verifique em <https://validar.iti.gov.br>

Gabrielle Ferreira Pires
Adviser

To my parents Lilia e Air

ACKNOWLEDGEMENTS

A Deus por todas as bênçãos derramadas durante esta caminhada e toda minha vida.

Aos meus pais e meu irmão por todo o suporte e conselhos, e que mesmo distantes fisicamente se fizeram presente. Por acreditarem e incentivarem meus sonhos.

Ao Luiz por ser companheiro de todas as horas, que me apoiou, incentivou, e que me fez acreditar que era possível até quando eu mesma não acreditava. Por todo o carinho e amor diário que fizeram os momentos difíceis mais suportáveis e os momentos bons mais incríveis. Pelas discussões e contribuições científicas que enriqueceram esse trabalho.

Aos meus amigos que fizeram dessa caminhada mais leve, e que mesmo distantes se fizeram presentes: Lara, Yan, Fernando, Vitor e Ana Maria.

Aos amigos do CLIMAP, Lais, Humberto, Nathan, Vivi, Taison e Raoni, que estiveram sempre presente em cada etapa dessa trajetória, pelas discussões científicas, pelas horas de descontração e convivência que fizeram dessa caminhada mais leve. Em especial, ao Nathan, pela dedicação e proatividade que enriqueceram este trabalho.

Aos amigos do Biosfera-Atmosfera, Aninha, Raphael Pousa, Emily, Flávia e Verônica, pelas trocas científicas, pelos momentos de descontração no almoço, café da tarde e saídas.

A minha orientadora, Gabrielle Pires, por ser inspiração e exemplo de pesquisadora. Por todos os ensinamentos, suporte e paciência nesta trajetória que se iniciou há 9 anos atrás na iniciação científica. Por ser a orientadora humana que entende o lado do aluno, mas que também é exigente e nos impulsiona a ser cada vez melhor.

Aos meus coorientadores, Gabriel, Livia e Lineu, por todas as discussões científicas e sugestões que melhoraram esse trabalho. Ao Gabriel, pelos conselhos e pela paciência.

Ao Álvaro pelas contribuições científicas à esse trabalho.

A todos os professores que fizeram parte desta trajetória pelos conhecimentos compartilhados.

A Graça Freitas por todo auxílio e suporte nessa trajetória acadêmica.

A Universidade Federal de Viçosa pela oportunidade de realizar o doutorado, e por ter sido casa desde a graduação.

O presente trabalho foi realizado com apoio da Coordenação de Aperfeiçoamento de Pessoal de Nível Superior – Brasil (CAPES) – Código de Financiamento 001.

A Coordenação de Aperfeiçoamento de Pessoal de Nível Superior (CAPES), pela concessão da bolsa de estudos.

ABSTRACT

SOUZA, Livia Maria Brumatti de, D.Sc., Universidade Federal de Viçosa, May 2023. **Assessment of extreme climate impacts on large-scale commodity and family farming agriculture in Brazil.** Adviser: Gabrielle Ferreira Pires. Co-advisers: Livia Cristina Pinto Dias, Lineu Neiva Rodrigues and Gabriel Medeiros Abrahão.

The changes in extreme climate patterns threaten several sectors that are climate dependent, as agriculture. Climate extremes could affect agricultural production resulting in yield and area losses. Losses in the main crops of family farming of the Brazilian semiarid region and large-scale commodity agriculture of the Mato Grosso and MATOPIBA can compromise national and international food security. Unfortunately, climate change will likely aggravate this situation in the future. This study aims to evaluate the extreme climate impacts on large-scale commodity and family farming agriculture in Brazil during the past and future periods. First, I evaluated the extreme climate impacts on large-scale commodities (soybean and maize second season) and family farming agriculture (maize, bean, and cassava) during 2003-2019. Drought events predominate during this period in both regions, and vapor pressure deficit was the index that better represent the relationship between extreme climate indexes and crop yield in both agriculture types. Family farming crops were more exposed to extreme climate events than commodity agriculture crops, and they are more vulnerable to extreme climate due to low technological levels. In family farming agriculture, maize was the crop most affected by climate extremes, followed by beans and cassava. In commodity agriculture, off-season maize yield was more impacted by drought and hot events than soybean. During this period, family farmers' agricultural output presented negative trends, while commodity farmers agricultural output presented positive trends. These results illustrate an alarming and worrying situation for family farmers of the semiarid region. Second, to improve future climate risk assessment, the best bias correction method (linear scaling and quantile mapping) was investigated and what are the best models of CMIP6/IPCC for climate (precipitation, minimum and maximum temperatures) and extreme climate variables (maximum consecutive dry days, CDD, and extreme degree days, EDD) in Brazilian regions. The results showed that non-parametric quantile mapping methods (empirical quantile and robust empirical quantile) were the best bias correction methods for almost all variables. Linear scaling presented a slightly better performance in some models and regions for the CDD index with minimal improvement, demonstrating that bias correction cannot improve indexes not well represented by climate models. The best models varied according to the variable, but ACCESS-ESM1-5, EC-Earth3-Veg, CanESM5, EC-Earth3, and

CMCC-ESM2 predominated in the variables' ranking after bias correction. Third, in a complementary analysis, the extreme climate impacts were estimated for the main crops of commodity and family farming agriculture under four climate change scenarios (SSP1-2.6, SSP2-4.5, SSP3-7.0, and SSP5-8.5) in 2021-2100 period. Our results demonstrated increasing trends of hot and dry events during crop growing seasons of both agricultural types in most scenarios and periods, culminating in yield losses. Family farmers will experience a more extreme climate and greater yield losses than commodity farmers. Both agriculture types will need to increase their resilience to deal with climate change, regardless of the scenario, however, more attention and immediate actions are needed for family farmers.

Keywords: Extreme climate. Family farming. Commodity agriculture. Bias correction.

RESUMO

SOUZA, Livia Maria Brumatti de, D.Sc., Universidade Federal de Viçosa, maio de 2023. **Avaliação dos impactos dos eventos climáticos extremos na agricultura de larga-escala de commodity e familiar no Brasil.** Orientadora: Gabrielle Ferreira Pires. Coorientadores: Livia Cristina Pinto Dias, Lineu Neiva Rodrigues e Gabriel Medeiros Abrahão.

As mudanças nos padrões climáticos extremos ameaçam diversos setores dependentes do clima, como a agricultura. Os eventos extremos podem afetar a produção agrícola, resultando em perdas de produtividade e área. A ocorrência de perdas nas principais culturas da agricultura familiar do semiárido brasileiro e da agricultura de larga escala de commodities no Brasil central pode comprometer a segurança alimentar nacional e internacional. Infelizmente, essa situação provavelmente será agravada no futuro pelas mudanças climáticas. Este estudo tem como objetivo avaliar os impactos dos eventos extremos na agricultura familiar e de commodities no Brasil durante o período histórico e futuro. Primeiro, foi avaliado os impactos dos eventos extremos na agricultura de commodities (soja e milho de segunda safra) e na agricultura familiar (milho, feijão e mandioca) durante o período 2003-2019. Os eventos de seca predominaram neste período em ambas as regiões, e o déficit de pressão de vapor foi o índice que melhor representou a relação entre os índices climáticos extremos e a produtividade das culturas em ambos os tipos de agricultura. As culturas da agricultura familiar foram mais expostas aos eventos extremos do que as culturas da agricultura de commodities, e são mais vulneráveis a esses eventos devido ao baixo nível tecnológico. Na agricultura familiar, o milho foi a cultura mais afetada pelos extremos climáticos, seguidos do feijão e da mandioca. Na agricultura de commodities, o milho de segunda safra foi mais impactado pela seca e pelos eventos de calor do que a soja. Nesse período, a produção agrícola dos produtores da agricultura familiar apresentou tendências negativas enquanto a produção agrícola dos produtores de commodities apresentou tendências positivas. Esses resultados ilustram uma situação alarmante e preocupante para os agricultores familiares do semiárido. Em segundo lugar, para melhorar a avaliação de risco climático futuro, foi investigado qual é o melhor método de correção de viés (escalonamento linear e mapeamento de quantis) e quais são os melhores modelos do CMIP6/IPCC para as variáveis climáticas (precipitação, temperaturas mínima e máxima) e para as variáveis climáticas extremas (número máximo de dias consecutivos secos, CDD, e graus dias extremo, EDD) nas regiões brasileiras. Os resultados mostraram que os métodos não-paramétricos de mapeamento de quantis (quantil empírico, QUANT e quantil empírico robusto, RQUANT) foram os melhores métodos de correção de viés para quase todas as variáveis. O

método de escalonamento linear apresentou um desempenho um pouco melhor em alguns modelos e regiões para o índice CDD com uma melhora mínima, demonstrando que a correção de viés não é capaz de melhorar índices mal representados por modelos climáticos. Os melhores modelos variaram de acordo com a variável, mas ACCESS-ESM1-5, EC-Earth3-Veg, CanESM5, EC-Earth3 e CMCC-ESM2 predominaram entre os melhores em todas as variáveis após a correção de viés. Em terceiro lugar, em uma análise complementar, foi estimado o impacto dos eventos extremos nas principais culturas da agricultura familiar e na agricultura de commodities em quatro cenários de mudanças climáticas (SSP1-2.6, SSP2-4.5, SSP3-7.0 e SSP5-8.5) durante o período de 2021-2100. Os resultados indicaram tendências crescentes de eventos quentes e secos durante a estação de crescimento de ambos os tipos de agricultura na maioria dos cenários e períodos, culminando em perdas de produtividade. Os agricultores familiares podem experimentar um clima mais extremo e mais perdas de produtividade do que os produtores de commodities. Ambos os tipos de agricultura precisarão aumentar sua resiliência para lidar com as mudanças climáticas, independente do cenário, porém, mais atenção e ações imediatas são necessárias para os agricultores familiares.

Palavras-chave: Eventos extremos. Agricultura familiar. Agricultura de commodities. Correção de viés.

LIST OF ILLUSTRATIONS

CHAPTER 1

- Figure 1.1** – Geographical location of the main producing regions of commodity (MT and MATOPIBA) and family farming agriculture (semiarid region, defined by SUDENE, (2017))...... 23
- Figure 1.2** – Crop sowing dates (a-e), harvest dates (f-j) and maximum exposure time (MET) (k-o) for each crop. 28
- Figure 1.3** – Critical values of extreme climate indices in 2003-2019 period. Upper limit (97.5%) of 95% confidence interval was considered for CDD (days), EDD (degree days), VPD (kPa) and VPD_lim (days). Lower limit (2.5%) of 95% confidence interval was considered for PRCPTOT. 30
- Figure 1.4** – Scores of influences of extreme climate indices on crops yields, for a) family farming of semiarid region and b) commodity agriculture of MT and MATOPIBA, represented as the standard deviations of each index. 34
- Figure 1.5** – Temporal evolution of extreme climate indices (c, d, e, f, g) and changes on yield (a) and planted area (b) for each crop during 2003-2019. Crops represented with orange palette are from family farming agriculture of semiarid region and crops represented with green palette are from commodity agriculture of MT and MATOPIBA. 35
- Figure 1.6** – Regression lines for log(Yield) and the Harvested area/Planted area ratio for each crop. Crops represented with orange palette are from family farming in Semiarid region and crops represented with green palette are from commodity agriculture in MT and MATOPIBA. The shadow on regression lines represents the 95% confidence interval. 36
- Figure S1.1** – Critical (lower and upper limits of 95% confidence interval) and average values of extreme climate indices for Maize 1st season on 2003-2019 period..... 44
- Figure S1.2** – Critical (lower and upper limits of 95% confidence interval) and average values of extreme climate indices for Bean on 2003-2019 period..... 45
- Figure S1.3** – Critical (lower and upper limits of 95% confidence interval) and average values of extreme climate indices for Cassava on 2003-2019 period..... 46
- Figure S1.4** – Critical (lower and upper limits of 95% confidence interval) and average values of extreme climate indices for Soybean on 2003-2019 period. 47
- Figure S1.5** – Critical (lower and upper limits of 95% confidence interval) and average values of extreme climate indices for Maize 2nd season on 2003-2019 period. 48
- Figure S1.6** – Critical (lower and upper limits of 95% confidence interval) and average values of onset, end, and duration of wet season on 2003-2019 period..... 49
- Figure S1.7** – Rainy season onset (a), duration (b) and end (c) for MT (dark blue) and MATOPIBA (light blue) for 2003-2019 period. Horizontal lines represent the average of the period for each region. 50

CHAPTER 2

Figure 2.1 – Political Brazilian regions and states.	54
Figure 2.2 – Flowchart of the methodology.	55
Figure 2.3 – Percentual bias (PBIAS, %) of precipitation for each bias correction method, raw model data, ACCESS-CM2, BCC-ESM2-MR, CMCC-ESM2, EC-Earth3-Veg, GFDL-ESM4, INM-CM5-0, MIROC6, MPI-ESM1-2-HR, MRI-ESM2-0 models.	64
Figure 2.4 – Percentual bias (PBIAS, %) of precipitation for each bias correction method, raw model data, NorESM2-MM, ACCESS-ESM1-5, CanESM5, EC-Earth3, EC-Earth3-Veg-LR, INM-CM4-8, MPI-ESM1-2-LR, and NorESM2-LM models.	65
Figure 2.5 – KGE and PBIAS results for each variable (PREC, TMAX, TMIN, CDD and EDD), model and Brazilian region for QUANT method.	66
Figure 2.6 – Ranking of models' performance for a) PREC, b) TMIN, c) TMAX, d) CDD and e) EDD for NT, NE, CW, SE, and ST regions.	67
Figure S2.1 – KGE of precipitation for each bias correction method, raw model data, and ACCESS-CM2, BCC-ESM2-MR, CMCC-ESM2, EC-Earth3-Veg, GFDL-ESM4, INM-CM5-0, MIROC6, MPI-ESM1-2-HR, MRI-ESM2-0 models.	71
Figure S2.2 – KGE of precipitation for each bias correction method, raw model data, and NorESM2-MM, ACCESS-ESM1-5, CanESM5, EC-Earth3, EC-Earth3-Veg-LR, INM-CM4-8, MPI-ESM1-2-LR and NorESM2-LM models.	72
Figure S2.3 – KGE of maximum temperature for each bias correction method, raw model data, and ACCESS-CM2, BCC-ESM2-MR, CMCC-ESM2, EC-Earth3-Veg, GFDL-ESM4, INM-CM5-0, MIROC6, MPI-ESM1-2-HR, MRI-ESM2-0 models.	73
Figure S2.4 – KGE of maximum temperature for each bias correction method, raw model data, and NorESM2-MM, ACCESS-ESM1-5, CanESM5, EC-Earth3, EC-Earth3-Veg-LR, INM-CM4-8, MPI-ESM1-2-LR and NorESM2-LM models.	74
Figure S2.5 – Percentual bias (PBIAS) of maximum temperature for each bias correction method, raw model data, and ACCESS-CM2, BCC-ESM2-MR, CMCC-ESM2, EC-Earth3-Veg, GFDL-ESM4, INM-CM5-0, MIROC6, MPI-ESM1-2-HR, MRI-ESM2-0 models.	75
Figure S2.6 – Percentual bias (PBIAS) of maximum temperature for each bias correction method, raw model data, and NorESM2-MM, ACCESS-ESM1-5, CanESM5, EC-Earth3, EC-Earth3-Veg-LR, INM-CM4-8, MPI-ESM1-2-LR and NorESM2-LM models.	76
Figure S2.7 – KGE of minimum temperature for each bias correction method, raw model data, and ACCESS-CM2, BCC-ESM2-MR, CMCC-ESM2, EC-Earth3-Veg, GFDL-ESM4, INM-CM5-0, MIROC6, MPI-ESM1-2-HR, MRI-ESM2-0 models.	77
Figure S2.8 – KGE of minimum temperature for each bias correction method, raw model data, and NorESM2-MM, ACCESS-ESM1-5, CanESM5, EC-Earth3, EC-Earth3-Veg-LR, INM-CM4-8, MPI-ESM1-2-LR and NorESM2-LM models.	78

Figure S2.9 – Percentual bias (PBIAS) of minimum temperature for each bias correction method, raw model data, and ACCESS-CM2, BCC-ESM2-MR, CMCC-ESM2, EC-Earth3-Veg, GFDL-ESM4, INM-CM5-0, MIROC6, MPI-ESM1-2-HR, MRI-ESM2-0 models.	79
Figure S2.10 – Percentual bias (PBIAS) of minimum temperature for each bias correction method, raw model data, and NorESM2-MM, ACCESS-ESM1-5, CanESM5, EC-Earth3, EC-Earth3-Veg-LR, INM-CM4-8, MPI-ESM1-2-LR and NorESM2-LM models.	80
Figure S2.11 – KGE of CDD for each bias correction method, raw model data, and ACCESS-CM2, BCC-ESM2-MR, CMCC-ESM2, EC-Earth3-Veg, GFDL-ESM4, INM-CM5-0, MIROC6, MPI-ESM1-2-HR, MRI-ESM2-0 models.	81
Figure S2.12 – KGE of CDD for each bias correction method, raw model data, and NorESM2-MM, ACCESS-ESM1-5, CanESM5, EC-Earth3, EC-Earth3-Veg-LR, INM-CM4-8, MPI-ESM1-2-LR and NorESM2-LM models.	82
Figure S2.13 – Percentual bias (Pbias) of CDD for each bias correction method, raw model data, and ACCESS-CM2, BCC-ESM2-MR, CMCC-ESM2, EC-Earth3-Veg, GFDL-ESM4, INM-CM5-0, MIROC6, MPI-ESM1-2-HR, MRI-ESM2-0 models.	83
Figure S2.14 – Percentual bias (Pbias) of CDD for each bias correction method, raw model data, and NorESM2-MM, ACCESS-ESM1-5, CanESM5, EC-Earth3, EC-Earth3-Veg-LR, INM-CM4-8, MPI-ESM1-2-LR and NorESM2-LM models.	84
Figure S2.15 – KGE of EDD for each bias correction method, raw model data, and ACCESS-CM2, BCC-ESM2-MR, CMCC-ESM2, EC-Earth3-Veg, GFDL-ESM4, INM-CM5-0, MIROC6, MPI-ESM1-2-HR, MRI-ESM2-0 models.	85
Figure S2.16 – KGE of EDD for each bias correction method, raw model data, and NorESM2-MM, ACCESS-ESM1-5, CanESM5, EC-Earth3, EC-Earth3-Veg-LR, INM-CM4-8, MPI-ESM1-2-LR and NorESM2-LM models.	86
Figure S2.17 – Percentual bias (Pbias) of EDD for each bias correction method, raw model data, and ACCESS-CM2, BCC-ESM2-MR, CMCC-ESM2, EC-Earth3-Veg, GFDL-ESM4, INM-CM5-0, MIROC6, MPI-ESM1-2-HR, MRI-ESM2-0 models.	87
Figure S2.18 – Percentual bias (Pbias) of EDD for each bias correction method, raw model data, and NorESM2-MM, ACCESS-ESM1-5, CanESM5, EC-Earth3, EC-Earth3-Veg-LR, INM-CM4-8, MPI-ESM1-2-LR and NorESM2-LM models.	88
Figure S2.19 – KGE and PBIAS result for each variable (PREC, TMAX, TMIN, CDD and EDD), model and Brazilian region without bias correction.	89
Figure S2.20 – KGE and PBIAS result for each variable (PREC, TMAX, TMIN, CDD and EDD), model and Brazilian region for PTF method.	90
Figure S2.21 – KGE and Pbias result for each variable (PREC, TMAX, TMIN, CDD and EDD), model and Brazilian region for RQUANT method.	90
Figure S2.22 – KGE and Pbias result for each variable (PREC, TMAX, TMIN, CDD and EDD), model and Brazilian region for SSPLIN method.	91

Figure S2.23 – KGE and Pbias result for each variable (PREC, TMAX, TMIN, CDD and EDD), model and Brazilian region for LS method.	92
--	----

CHAPTER 3

Figure 3.1 – VPD values during crop growing season, periods, and scenarios. The crops are represented in the lines: a) Maize 1st season, b) Bean, c) Cassava, d) Soybean, and e) Maize 2nd season. The vertical dashed lines represent the periods 2021-2050 and 2071-2100. The scenarios lines and the shadow on it represent the ensemble of the 4 models and their variability, respectively.	100
--	-----

Figure 3.2 – VPD_lim values during crop growing season, periods, and scenarios. The crops are represented in the lines: a) Maize 1st season, b) Bean, c) Cassava, d) Soybean, and e) Maize 2nd season. The vertical dashed lines represent the periods 2021-2050 and 2071-2100. The scenarios lines and the shadow on it represent the ensemble of the 4 models and their variability, respectively.	101
--	-----

Figure 3.3 – EDD values during crop growing season, periods, and scenarios. The crops are represented in the lines: a) Maize 1st season, b) Bean, c) Cassava, d) Soybean, and e) Maize 2nd season. The vertical dashed lines represent the periods 2021-2050 and 2071-2100. The scenarios lines and the shadow on it represent the ensemble of the 4 models and their variability, respectively.	102
--	-----

Figure 3.4 – CDD values during crop growing season, periods, and scenarios. The crops are represented in the lines: a) Maize 1st season, b) Bean, c) Cassava, d) Soybean, and e) Maize 2nd season. The vertical dashed lines represent the periods 2021-2050 and 2071-2100. The scenarios lines and the shadow on it represent the ensemble of the 4 models and their variability, respectively.	103
--	-----

Figure 3.5 – PRCPTOT values during crop growing season, periods, and scenarios. The crops are represented in the lines: a) Maize 1st season, b) Bean, c) Cassava, d) Soybean, and e) Maize 2nd season. The vertical dashed lines represent the periods 2021-2050 and 2071-2100. The scenarios lines and the shadow on it represent the ensemble of the 4 models and their variability, respectively.	104
--	-----

Figure 3.6 – Yield change from 2003-2019 to 2021-2050 for each crop, scenario and ensemble models.	107
--	-----

Figure 3.7 – Yield change from 2003-2019 to 2071-2100 for each crop, scenario, and ensemble models.	109
---	-----

Figure S3.1 – Yield change CanESM5 (2021-2050).	118
---	-----

Figure S3.2 – Yield change CanESM5 (2071-2100).	119
---	-----

Figure S3.3 – Yield change CMCC-ESM2 (2021-2050).	120
---	-----

Figure S3.4 – Yield change CMCC-ESM2 (2071-2100).	121
---	-----

Figure S3.5 – Yield change EC-Earth3 (2021-2050).	122
---	-----

Figure S3.6 – Yield change EC-Earth3 (2071-2100).	123
---	-----

Figure S3.7 – Yield change EC-Earth3-Veg (2021-2050).	124
---	-----

Figure S3.8 – Yield change EC-Earth3-Veg (2071-2100).	125
---	-----

LIST OF TABLES

CHAPTER 1

Table 1.1 -Maize1st season fixed effect estimators.	31
Table 1.2 - Bean fixed effect estimators	31
Table 1.3 – Cassava fixed effect estimators.....	32
Table 1.4 – Soybean fixed effect estimators.	33
Table 1.5 – Maize 2nd season fixed effects estimators.....	33
Table S1.1 – Results from Hausman, Chow, and Breusch-Pagan tests for log(yield) models.....	43

CHAPTER 2

Table 2.1 – CMIP6 model's description used in this study.	56
Table 2.2 – Climate and climate extreme variables.	57

CHAPTER 3

Table 3.1 – Trends of climate indexes for each crop, scenario, and period.	105
Table S3.1 – Fixed effect model estimators of Maize 1st season.	115
Table S3.2 – Fixed effect model estimators of bean.	115
Table S3.3 – Fixed effect model estimators of cassava.	116
Table S3.4 – Fixed effect model estimators of soybean.	116
Table S3.5 – Fixed effect model estimators of maize 2nd season.	117

SUMMARY

General introduction	16
Chapter 1: Historical evolution of extreme events impacts on family farming and commodity agriculture in Brazil: lessons from the past to build resilience in Brazilian agricultural systems.....	19
1.1 -Introduction	20
1.2- Data and methods	21
1.2.1 – Study areas	21
1.2.2 – Crop Sowing and Harvest dates	23
1.2.3 – Extreme climate indexes	24
1.2.4 – Evaluation of extreme climate impact on agricultural outputs	25
1.2.5 – Evaluation of agricultural outputs trends	26
1.3- Results	26
1.3.1 – Crop calendar	26
1.3.2 – Extreme climate indexes	28
1.3.3 – Extreme climate impacts on yield.....	30
1.3.4 – Regions levels trend.....	36
1.4 – Discussion.....	37
1.4.1 – Meteorological phenomena behind agricultural losses.....	37
1.4.2 – Crops vulnerability to extreme climate.....	38
1.4.3 – Contrasting family farming and commodity agriculture historical evolution	40
1.5 – Conclusion	41
1.6 – Supplementary Materials	43
Chapter 2: Uncovering the need for bias correction in CMIP6 models for Brazil's climate assessment	51
2.1 – Introduction	52
2.2 – Data and methods	53
2.2.1 – Study area	53
2.2.2 – Climate data	55
2.2.3 – Bias correction methods.....	57
2.2.3.1 – Linear Scaling (LS)	57
2.2.3.2 – Quantile Mapping (QM): Parametric transformation Function (PTF).....	58
2.2.3.3 - Quantile Mapping (QM): Empirical quantiles (QUANT)	59

2.2.3.4 - Quantile Mapping (QM): Robust empirical quantiles (RQUANT).....	59
2.2.3.5 - Quantile Mapping (QM): Smoothing splines (SSPLIN)	59
2.2.4 – Performance evaluation of bias correction methods.....	59
2.2.5 – Ranking of the models' performance	60
2.3 – Results	60
2.3.1 – PREC	60
2.3.2 – TMIN and TMAX.....	61
2.3.3 – EDD	62
2.3.4 – CDD	63
2.4 – Discussion.....	67
2.5 – Conclusion.....	69
2.6 - Supplementary material	71
Chapter 3: Future alternative pathways to Brazilian agriculture under climate change scenarios: contrasting semiarid family farmers and Mato Grosso and MATOPIBA commodity farmers.....	93
3.1 – Introduction	93
3.2 – Data and methods	95
3.2.1 – Study areas.....	95
3.2.2 – Climate data and scenarios	96
3.2.3 – Climate indexes and trend analysis.....	97
3.2.4 – Yield model and projections under climate change scenarios.....	98
3.3 – Results	99
3.3.1 – Future trends in extreme climate indexes during crop growing season.....	99
3.3.2 – Future yield changes	106
3.3.2.1 – Family farming agriculture of the semiarid region	106
3.3.2.2 – Commodity agriculture of the MT and MATOPIBA.....	108
3.4 – Discussion.....	109
3.5 – Conclusion.....	114
3.6 - Supplementary Material	115
General Conclusions.....	126
REFERENCES	129

General introduction

Extreme events defined as climate events with the occurrence of values close to the highest or lowest observed values of climate variables (IPCC, 2012). These events occur due to natural climate variability, but changes in frequency, intensity, and duration could occur in some regions due to climate change (IPCC, 2022). These extreme climate events could impact many sectors that are dependent on climate, as agriculture, energy, etc.

Brazil stands out in food production, being one of the main producers and exporters of some crops, with agribusiness contributing to 24.8% of the country's gross domestic product (GDP) in 2022 (CEPEA, 2023). Two agriculture types stand out in the country: family farming agriculture and large-scale commodity agriculture.

Family farming agriculture corresponds to 77% of the Brazilian agricultural establishments occupying an area of about 81 Mha and employing 67% of all jobs in the country's agriculture (IBGE - Instituto Brasileiro de Geografia e Estatística, 2017). 38% of these agricultural establishments are concentrated in the Brazilian semiarid region (IBGE - Instituto Brasileiro de Geografia e Estatística, 2017), which is formed by 1,262 municipalities in the northern part of Minas Gerais state and the northeast Brazilian region (SUDENE, 2017). The production system is based on family labor and limited technological use, and the production is aimed at subsistence and supplying the internal market.

Large-scale commodity agriculture is mostly concentrated in the central Brazilian region. It is characterized by the intensive use of technology in the field, such as machinery, adapted cultivars, expert labor, nutrients, and irrigation, which contribute to the cultivation of many harvests in the same agricultural year, increasing the yield of the crops cultivated in this system in the last years. The main purpose of the cultivation in this agriculture type is to supply the international market.

In the last years, many studies have identified changes in the rainfall pattern and the occurrence of extreme climate in the main producing regions of these agriculture types: semiarid and central Brazilian regions (Salvador and de Brito, 2018; Leite-Filho *et al.*, 2019; Costa *et al.*, 2020; Marengo *et al.*, 2022b) threatening their agricultural production. The occurrence of extreme climate during crop growing season could result in production losses (Lesk *et al.*, 2016; Matiu *et al.*, 2017; Vogel *et al.*, 2019), and the magnitude of these losses depend on the type, intensity, and duration of the climate extreme and in what plant phenological stage they occur (Rosenzweig *et al.*, 2001; Hatfield and Prueger, 2015; Vogel *et*

al., 2019). Production losses in both agriculture types could threaten food security and compromise the entire production chain (da Silva *et al.*, 2017).

In the future, extreme climate are predicted to increase the frequency, intensity, and duration (IPCC, 2022), increasing the exposure of the farmers of both agriculture types to these events and demanding elaboration of adaptation strategies to minimize the adverse impacts on production. Climate models are a reliable tool to predict future climate change impacts and elaborate adaptation measures, however, these models present biases associated with models' imperfections that could reduce the accuracy of climate risk assessment. The application of bias correction methods improves climate risk assessment in areas such as agriculture and hydrology (Ines and Hansen, 2006; Teutschbein and Seibert, 2012). In the literature, there are several bias correction techniques with different assumptions, such as correction of mean, variance, or distribution bias (Lenderink *et al.*, 2007; Teutschbein and Seibert, 2012; Pierce *et al.*, 2015; Enayati *et al.*, 2021), which create the question of what is the best bias correction method for a specific region. For Brazil, it is unknown what is the best bias correction method for climate and extreme climate variables and which are the best models for each variable and Brazilian region. This information will contribute to improving the future climate risk assessment in the country.

Fewer studies evaluated the direct impact of extreme climate on Brazilian agriculture, and most of them are concentrated in commodity agriculture. Rattis *et al.* (2021) showed that droughts decreased soybean and off-season maize yield in rainfed and irrigated systems in central Brazil in the last years, and Fonseca *et al.* (2022) showed the impacts of these droughts on sowing dates in the region. There is a lack of studies for family farmers in the semiarid region, where the most intense and prolonged droughts occurred in the last decade. Many studies evaluated the future impact of climate change on commodity agriculture (Pires *et al.*, 2016; Andrea *et al.*, 2019; Brumatti *et al.*, 2020; Hampf *et al.*, 2020; Zilli *et al.*, 2020; Fernandes *et al.*, 2022) and a few studies focused in the crops of the northeast region (Silva *et al.*, 2010; Martins *et al.*, 2019), however, all of these studies evaluate the impact of mean climate change instead of the direct impact of extreme climate.

Family farming and commodity Brazilian agriculture have several different aspects that influence how farmers are affected and respond to extreme climate. To understand how extreme climate impacted family farming and commodity agriculture in the past, identifying their vulnerability, and how they could be affected by extreme climate in the future is essential to create adaptation strategies and increase the resilience of both agriculture types.

In this way, this thesis investigates the impacts of extreme climate on the main crops of commodity agriculture of central Brazil and family farming of the Brazilian semiarid region. In Chapter 1, I investigate how these two agriculture types were affected by extreme climate in the past. Chapter 2 evaluates the best bias correction method and the best models for climate and extreme climate variables in Brazil to improve climate risk assessment. And Chapter 3 investigates how extreme climate could change during the crop growing season and how these changes could affect crop yields of commodity and family farming agriculture during 2021-2100 under four scenarios of Coupled Model Intercomparison Project 6 (CMIP6/IPCC).

Chapter 1: Historical evolution of extreme events impacts on family farming and commodity agriculture in Brazil: lessons from the past to build resilience in Brazilian agricultural systems.

Abstract

The increase in frequency, intensity, and duration of extreme precipitation and temperature events threatens numerous sectors of the economy that depend on climate, especially agriculture. Extreme weather events during the crop cycle lead to production losses regarding commodity and family farming. Brazilian agriculture can compromise national and international food security. Understanding how extreme temperature and rainfall events have impacted commodity and family farming agriculture in the central and semiarid Brazilian regions is vital to identify the vulnerabilities, and hence, increasing the resilience of these agricultural types. In this context, I aimed to evaluate how extreme climate impacted the agricultural outputs of family farming and commodity agriculture during 2003-2019. Using econometric models, I calculated extreme climate indexes and determined how they affected agricultural outputs. I found that drought events predominated during the study period and that extreme vapor pressure deficit (VPD) was the extreme climate index that most impacted crops yield in both agriculture types. Family farming crops were more exposed to extreme climate events than commodity agriculture crops, and they are more vulnerable to extreme climate due to low technological levels. In family farming agriculture, maize was the crop most affected by extreme climate, followed by bean and cassava. In commodity agriculture, drought and hot events impacted off-season maize yield more than soybean. The fluctuations in agricultural outputs of family farming crops could be explained by the large-scale climate phenomena predominating in the semiarid region and their lower adaptive capacity to droughts. These results illustrate an alarming and worrying increasing level of food insecurity in such a vulnerable region as the semiarid and the many challenges that might be ahead with increasing climate change.

1.1 -Introduction

Extreme climate events are predicted to increase their frequency, intensity, and duration in the next years, and many of these changes are observed yearly worldwide (IPCC - Intergovernmental Panel on Climate Change, 2022).

Agricultural systems are particularly affected by extreme climate, even though the impacts depend on the type, intensity, and duration of the extreme event, as well as on the crop, cultivar, and plant phenological stage (Rosenzweig *et al.*, 2001; Hatfield and Prueger, 2015; Vogel *et al.*, 2019). In general, dry and hot events lead to the closure of plant stomata and reduced photosynthesis, causing yield losses especially if extreme weather occurs during phenological phases more sensitive to water stress, such as the reproductive phase (Rosenzweig *et al.*, 2001; Li *et al.*, 2019; Grossiord *et al.*, 2020). Intense damages are expected when dry events are combined with extreme maximum temperatures (Rosenzweig *et al.*, 2001; Hatfield and Prueger, 2015; Li *et al.*, 2019). In addition to yield losses, a reduction in the planted and harvested areas is also a consequence of extreme weather conditions, leading to a drop in total production (Lesk *et al.*, 2016), decreasing food supply, causing market shocks and price fluctuations (Gbegbelegbe *et al.*, 2014; da Silva *et al.*, 2017).

While Brazil is one of the main agricultural producers/exporters in the world and impacts both national and international markets and food security, it has also been experiencing important extreme events that have affected its economy and population (Cunha *et al.*, 2019; Rattis *et al.*, 2021). Generally, a warming trend was detected in nearly all territories, while precipitation trends varied substantially throughout the country (Avila-Diaz *et al.*, 2020; Cortez *et al.*, 2022). More specifically, the north-eastern region of Brazil, where 38% of national family farmers are located (Melo and Voltolini, 2019), showed an expressive increase in the frequency, intensity, and duration of droughts (Brito *et al.*, 2018; Bezerra *et al.*, 2019; Costa *et al.*, 2020), which dramatically impacted agriculture in the last years. Moreover, central regions that concentrate most of the commodity cultivation in the country have also experienced recent extreme weather. In MATOPIBA – a region of intense agriculture activity formed by Maranhão, Tocantins, Piauí, and Bahia states – extreme rainfall has increased during the wet season, while dry periods are longer (dos Reis *et al.*, 2020; Marengo *et al.*, 2022). In the Midwest region, severe droughts were registered during 2011-2019, with a degree of severity only lower than in the northeast region (NE) (Cunha *et al.*, 2019).

Therefore, Brazilian agriculture and economy might have already been and continue to be affected by extreme weather events, especially extreme temperatures, and rainfall. In a complex and dynamic agricultural context, two main cultivation types: commodity and family farming agriculture. The main producing regions of these agricultural types are in central and northeast Brazilian regions, where changes in extreme climate events have been observed.

Recent studies have investigated long-term observed variations in climate and agriculture, indicating that drought events explain the variations in yield in the main producing regions of soybean and off-season maize in the last years (Rattis *et al.*, 2021) and that it can impact sowing dates and sowing windows (Fonseca *et al.*, 2022), with potential harms to harvested areas. However, these studies mainly focus on large-scale commodity agriculture, leaving an important gap regarding family farming agriculture in Brazil. To ensure food security, it is necessary to increase the resilience of the agricultural sector to factors that jeopardize the availability of food and the entire production chain, such as extreme climate. Understanding how precipitation and temperature extremes impacted agricultural yields of commodity and family farming agriculture in the past, contrasting the impacts, and identifying the vulnerability of these two agriculture types over the years is crucial to create adaptation strategies and increasing their resilience.

In this context, this study aims to evaluate the impact of extreme climate events on the agricultural outputs of the main crops and regions of family farming and commodity agriculture in Brazil, important information that could contribute to the development of climate-smart agriculture in the country.

1.2- Data and methods

1.2.1 – Study areas

Two agricultural regions stand out in the country. First, central Brazil is specialized in commodity agriculture production, including the states of Mato Grosso (MT) and MATOPIBA (Figure 1.1). MT had the highest production of soybean in 2021 (IBGE, 2021) while the MATOPIBA is a region that rapidly expanded and increased their production in the last years. The main crops produced are soybeans and maize (while other crops, such as cotton and beans are also common), largely cultivated in multiple cropping systems (2 to 2.5 harvests per year). Multiple cropping imposes a high technology input (machinery, enhanced cultivars, nutrients,

expert labor, and irrigation in ~5% of the area). It directs most of its production to the international market, fuelling the national economy.

On the other hand, the Brazilian semiarid region is home to a great share of family farming agriculture in the country, formed by 1,262 municipalities in the north-eastern Brazilian region and the northern part of Minas Gerais state with 99% of these municipalities having at least 50% of the agricultural establishments classified as family farming (IBGE - Instituto Brasileiro de Geografia e Estatística, 2017) (Figure 1.1). Family farming represents 77% of Brazilian agricultural establishments, with 38% of rural family properties located in semiarid region, covering almost 22 Mha, contributing to the nourishment of the producing families and 2.5% of the production value of total Brazilian agricultural properties (IBGE - Instituto Brasileiro de Geografia e Estatística, 2017). Many crops are cultivated in the semiarid region (sugarcane, peanut, sorghum, and cotton), but the more prominent are maize, bean, and cassava (Silva and Neto, 2019). The production system is based on family labor and low technology use, and the production is aimed at subsistence (which creates a connection between agricultural production and food security, Alvalá *et al.*, 2017) and the production surplus is to supply the internal market. The semiarid region is characterized by high climate variability and suffered from unprecedented drought, environmental changes, degradation, low-income, and poverty increase in recent decades.

These two agricultural types (large-scale commodity agriculture and local family farming) are inserted in dramatically different socio-economic conditions and are expected to have different resilience and adaptation capacities to extreme climate and weather, and therefore will necessitate specific support and information in the future.

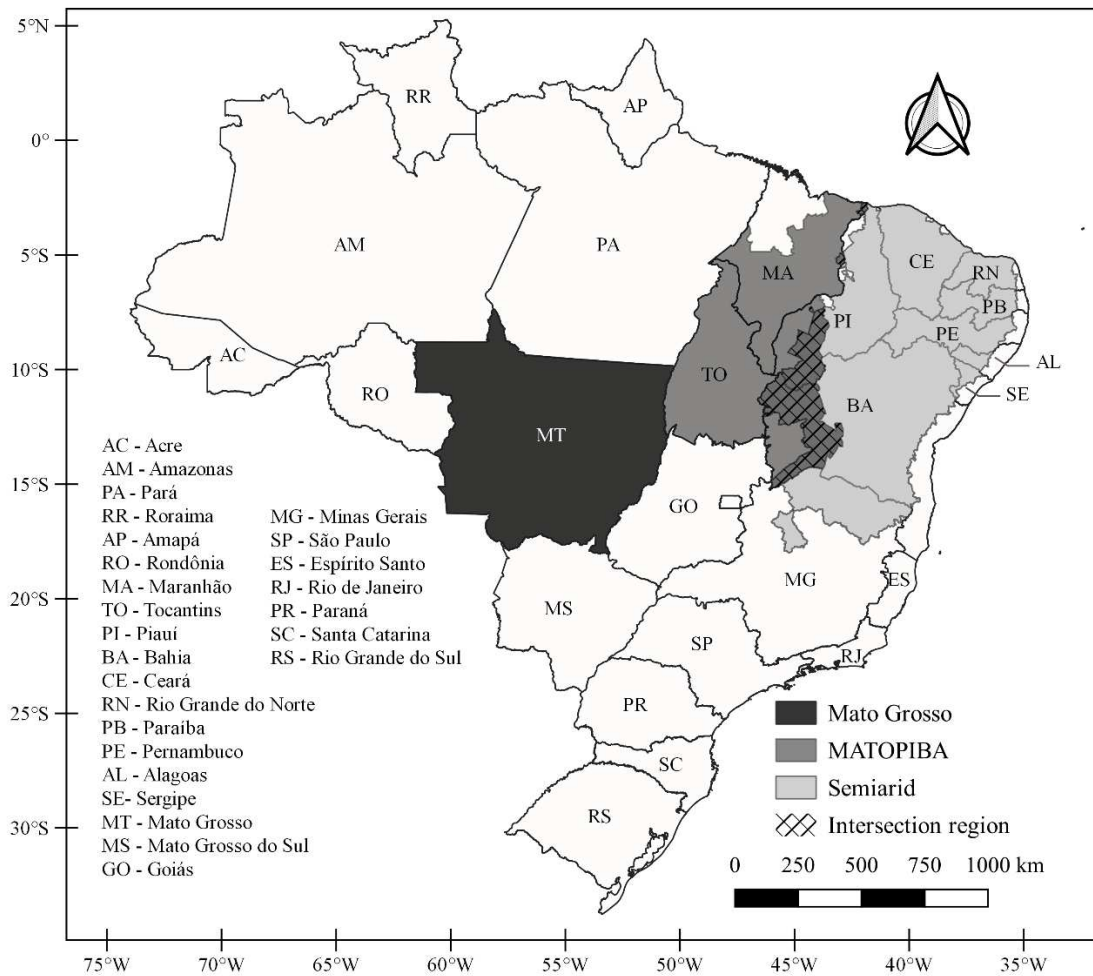


Figure 1.1 – Geographical location of the main producing regions of commodity (MT and MATOPIBA) and family farming agriculture (semiarid region, defined by SUDENE, (2017)).

1.2.2 – Crop Sowing and Harvest dates

To estimate the period that crops were growing in each region I followed the Climatic Risk Agricultural Zoning data from *AgriTempo* (www.agritempo.gov.br), which includes the sowing windows of all crops studied here. The *AgriTempo* data is available for each municipality and crop. It is a good indicator of effective sowing and harvest dates because some farmers follow its recommendations to avoid yield losses and attend to agricultural credit programs' demands.

I determined the maximum exposure time (MET) as the sum of the period that crops could be growing in the field. More specifically, MET includes the sowing window (usually

three months) and the average crop cycle length (varies among crops, but on average ranged from 80-240 days), while the crop harvest date is the last day of MET.

The maximum sowing window of each crop and municipality was summed with the average cycle length of each maturity group selected. The maturity groups were chosen considering the usual configuration in the field. Generally, soybean, maize and off-season maize are short-cycle cultivars (I selected maturity group I for these crops, with an average cycle length of 120 days); cassava has a long cycle (around 240 days); and beans, cowpea type (the most common type in the region) with a short cycle (maturity group II, with an average cycle length of 80 days).

1.2.3 – Extreme climate indexes

Five extreme climate indexes related with agricultural production (VPD, VPD_lim, EDD, PRCPTOT and CDD, defined below) were calculated during the MET for each municipality and crop using gridded rainfall and temperature data. I used the Climate Hazards group Infrared Precipitation with Stations (CHIRPS) dataset (Funk *et al.*, 2015) for daily rainfall data. This dataset was developed based on satellite and meteorological stations information and is available in a spatial resolution of 0.05° ($\sim 5.5 \times 5.5$ km), covering 1981-2022. In this study, I analyzed daily precipitation for the 2003-2019 period. This period was selected due to the temporal availability of all datasets used in this study.

Daily relative humidity, maximum and minimum temperatures are derived from Xavier *et al.* (2022) dataset. This dataset was constructed from interpolation of meteorological stations data from *Instituto Nacional de Meteorologia* (INMET), *Agência Nacional de Águas* (ANA) and *Departamento de Água e Energia Elétrica de São Paulo* (DAAE) for Brazil. Data is available on 0.1° ($\sim 11 \times 11$ km) from 1980 until July/2020, I used data from 2003 to 2019, to follow the crops agricultural calendar.

Vapor pressure deficit (VPD), defined as the difference between saturated air vapor pressure and actual air vapor pressure, has an important relationship with plant transpiration and is good indicator to associate the impact of combined dry and hot conditions on plants (Grossiord *et al.*, 2020). Based on relative humidity, minimum and maximum temperature, I calculated daily VPD according to Allen *et al.* (2006). Even though VPD was calculated for the

maximum exposure time for each municipality and crop, the average during the MET was considered as the extreme index for each harvest.

Another important climate index to agriculture, that I propose, is VPD_{lim}, which is derived from VPD, but instead of water stress intensity, it indicates the frequency of occurrence of water stress on crops. VPD_{lim} represents the number of days, during the MET, when the daily VPD is above a limit value that leads crops to close the stomata and reduce transpiration, indicating water stress. I assumed as the threshold for VPD values that will account for an increase in VPD_{lim} in crops are: soybean and cassava 2.0 kPa (El-Sharkawy, 1993; Fletcher *et al.*, 2007; Sinclair *et al.*, 2017), for maize 1.7 kPa (Gholipour *et al.*, 2013; Sinclair *et al.*, 2017), and cowpea bean 2.2 kPa (Belko *et al.*, 2012; Sinclair *et al.*, 2017).

Extreme degree days (EDD) is a heat stress metric in crops. They were calculated as the degree days above a critical temperature for each crop and municipality, according to the method of Schlenker and Roberts (2009). The critical temperature for soybean, cowpea bean, and cassava is 30 °C (Hillocks *et al.*, 2001; Schlenker and Roberts, 2009; Silva *et al.*, 2010) and for maize is 29 °C (Schlenker and Roberts, 2009).

I considered that PRCPTOT represents the total rainfall during MET and is an important index to identify the harvests when rainfall diminishes. Still regarding water stress, the consecutive dry days (CDD) indicate the dry spell occurrence during MET.

In addition to the climate indexes described, I also calculated the onset (ORS), demise (ERS), and duration of the rainy season (DRS) for MT and MATOPIBA, where multiple cropping is common and is particularly affected by those parameters (Abrahão and Costa, 2018). These rainy season parameters were calculated using the Anomalous Accumulation method, with reference rainfall of 2.5 mm.dia⁻¹ (Arvor *et al.*, 2014; Abrahão and Costa, 2018; Fonseca *et al.*, 2022).

These climate indexes represent the main climate occurrences that resulted in crops failure in both agricultural types in the last years and should capture this effect on crops.

1.2.4 – Evaluation of extreme climate impact on agricultural outputs

I estimate crop log (yield) as a function of the various extreme indices described in section 2.3 and the trend, to discount the effect of technological trend. I adjusted econometric

models to identify which climate extreme index most impacts crop yields, as commonly applied in many previous studies that relate climate with economic activities (Schlenker and Roberts, 2009; Powell and Reinhard, 2015; Cohn *et al.*, 2016; Castro *et al.*, 2019; Rattis *et al.*, 2021). I show the results for the best model as determined by Breusch-Pagan, Chow, and Hausman tests.

Total production, planted and harvested area for each crop and municipality is derived from *Sistema IBGE de Recuperação Automática* (SIDRA/IBGE), Table 1612 for bean, cassava, and soybean, and Table 839 for 1st season and 2nd season maize. The yield of each crop is the ratio between total production and planted area data. Here, I considered that all production and planted area of cassava, bean, and maize 1st season in the semiarid region was from family farming, since 99% of their municipalities had at least 50% of the agricultural establishment classified as family farming (IBGE - Instituto Brasileiro de Geografia e Estatística, 2017).

1.2.5 – Evaluation of agricultural outputs trends

I constructed regression lines to evaluate the trends of crops log (Yield) and losses in the planted area over time for each crop of agriculture type. The regression lines were constructed with the average agricultural outputs for the regions and crops for each harvest. The losses in the planted area were estimated with the ratio of the harvested area and planted area of each municipality and year. Ratio values lower than 1 indicate losses in planted areas.

1.3- Results

1.3.1 – Crop calendar

Maize first season in the semiarid region is cultivated in the municipalities of Bahia (BA), Minas Gerais (MG), Ceará (CE), Rio Grande do Norte (RN), Paraíba (PB), Pernambuco (PE), Alagoas (AL), and Sergipe (SE) states. The pattern of sowing dates varied throughout the states. In BA, MG municipalities, and parts of CE, and PE, maize is planted around October (~ day 300). In other states, maize is sowed at the beginning of the civil year, varying from January to March (Figure 1.2-a). The harvest dates varied from January to May (BA, MG, CE, and PE) and from May to September (the north portion of semiarid) (Figure 1.2-f).

Cowpea bean is cultivated in most semiarid, except in the central part of BA and the eastern part of Piauí (PI). The sowing pattern varied spatially. In western Bahia and PI municipalities, cowpea bean is sowed from September to December, while in the municipalities of CE, RN, PE, PB, SE, and eastern BA the sowing dates varied from January to March (Figure 1.2-b). Consequently, the last harvest date possible for cowpea bean in the first region varied from January to March, while other regions varied from April to August (Figure 1.2-g).

The long cassava cultivar is mainly concentrated in the north-eastern part of the semiarid region, including the states of CE, RN, PB, PE and AL. All municipalities in this region sow cassava at the beginning of the civil year, in January, and harvest at the end of the same year, these municipalities are more concentrated in CE and PE state (Figure 1.2-c,h). Few municipalities harvest cassava at the beginning of the next civil year.

Municipalities in Mato Grosso (MT) mainly sow soybean between the end of September and the middle of October, while in MATOPIBA sowing dates vary from October to November (Figure 1.2-d). The last day to harvest soybean is around the middle of April in MT, TO, and western BA, and around the beginning of June in PI and MA (Figure 1.2-i). The higher MET occurs north of MT, south of MA, and eastern PI (Figure 1.2-n).

Off-season maize is sowed in January in MT and MATOPIBA (Figure 1.2-e) and stays in the field until May and June (Figure 1.2-j). The greatest MET of second crop maize occurs north of MT (Figure 1.2-o).



Figure 1.2 – Crop sowing dates (a-e), harvest dates (f-j) and maximum exposure time (MET) (k-o) for each crop.

1.3.2 – Extreme climate indexes

Climate extreme indexes values varied according to the region and crop. I considered as critical values of VPD, VPD_lim, CDD, and EDD the upper limit of the 95% confidence interval for the 2003-2019 period, since the highest value of these climate extreme indexes are more damaging for crops. The inverse was considered for PRCPTOT (the lower limit of 95% confidence interval) since the lower availability of rainfall to crops cultivated in rainfed systems could be largely damaging. Figure 1.3 illustrates the critical values of climate extreme indexes for each crop and region.

Family farming crops (maize 1st season, bean, and cassava) are more exposed to higher values of CDD, VPD, VPD_lim, and EDD and lower values of PRCPTOT compared to commodity crops (Figure 1.3). Among family farming crops, cassava is more exposed to extreme climate than maize and bean due to its longer cycle (Figure 1.3-k-o). Critical values of CDD ranged from 50 to greater than 60 days during cassava MET. For EDD, VPD, and VPD_lim, these values varied from 240 to > 300 degrees days, from 1.2 to >1.7 kPa and 8 to > 40 days, respectively. PRCPTOT values ranged from 480 to 1040 mm. The average values of the period are demonstrated in Figure S1.3 for the municipalities that cultivated cassava.

In general, some municipalities that cultivate maize 1st season showed higher values of CDD (~35 days), EDD (~ 200 degrees days), VPD (~ 1.3 kPa) and VPD_lim (~ 30 days) and lower values of PRCPTOT (~ 500 mm) than the municipalities that cultivate bean. The municipalities located in the northern semiarid show the critical values of the period to maize and bean. The average values of the period are demonstrated in Figures S1.1 and S1.2 for the municipalities that cultivated maize and bean.

Among the crops of commodity agriculture, soybean cultivated in MT and MATOPIBA was exposed to higher values of VPD and VPD_lim during the period analyzed, mainly in the MATOPIBA region, when compared with off-season maize in these regions. However, off-season maize was exposed to higher CDD and EDD values, and lower water availability than soybean (Figure 1.3). The average values of the period are demonstrated in Figures S1.4 and S1.5 for soybean and maize off-season.

The region that is the most exposed to the critical values of the rainy season to soy-maize double cropping systems was MATOPIBA, with the highest number of pixels with late onset, early end, and shorter duration of the rainy season for the period (Figure S1.6). Almost all states presented the critical values, except for the Tocantins state.

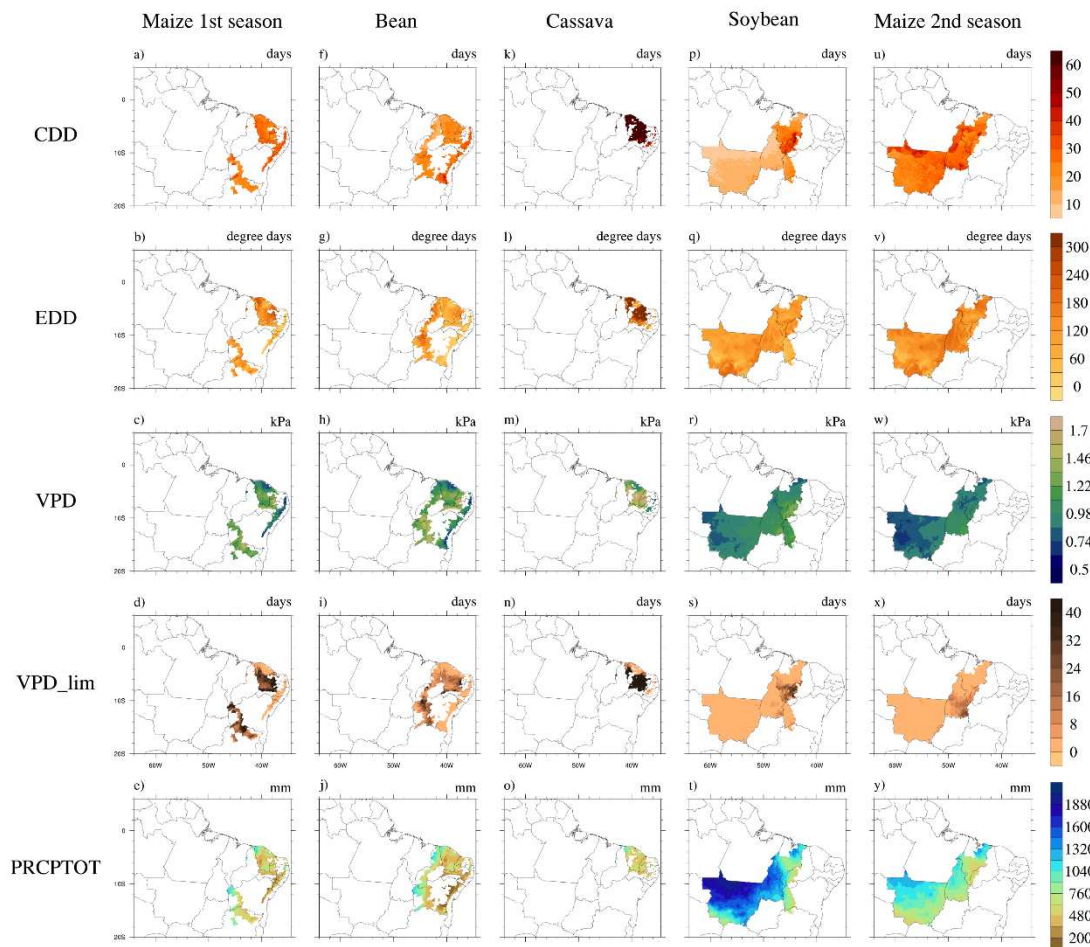


Figure 1.3 – Critical values of extreme climate indices in 2003-2019 period. Upper limit (97.5%) of 95% confidence interval was considered for CDD (days), EDD (degree days), VPD (kPa) and VPD_lim (days). Lower limit (2.5%) of 95% confidence interval was considered for PRCPTOT.

1.3.3 – Extreme climate impacts on yield

The Hausman, Chow, and Breusch-Pagan tests indicated the best model to relate each extreme climate index with $\log(\text{crops yield})$ of crops. Fixed effect (FE) was the best model to represent all family farming crops and commodity maize and their relationship with climate indexes and technological trend throughout time (Table S1.1). However, in the case of soybean, even though most indexes still adhered to FE, statistical tests indicated that random effect (RE) was the best model to represent yield and DRS climate index. Nonetheless, I also chose to represent this index with FE models considering it is more conservative than random effect in controlling non-observed variables. Therefore, yield *versus* extreme indexes were all represented using FE models.

Among all extreme indexes, VPD stands out with the higher effects on family farming yield losses, followed by VPD_lim, CDD, and EDD. PRCPTOT, as expected, showed a positive effect on these crops' yield (Tables 1.1-1.3). All the estimators of fixed effect models of family farming agriculture presented significance with a 0.1% level. The model constructed with EDD and the trend was the one that explains the greater amount of variance in maize 1st season ($R^2=0.20$) (Table 1.1). For bean, the models constructed with the trend, PRCPTOT and EDD presented greater and similar variance ($R^2=0.13$) (Table 1.2). In cassava, the model constructed with VPD and the trend had greater variance ($R^2=0.07$) (Table 1.3).

Table 1.1 -Maize 1st season fixed effect estimators.

Maize 1st season					
	Log_yield	Log_yield	Log_yield	Log_yield	Log_yield
<i>Predictors</i>	<i>Estimates</i>	<i>Estimates</i>	<i>Estimates</i>	<i>Estimates</i>	<i>Estimates</i>
year	-0.0154 ***	-0.0200 ***	-0.0388 ***	-0.0529 ***	-0.0428 ***
VPD	-2.3877 ***				
EDD		-0.0126 ***			
VPD lim			-0.0225 ***		
CDD				-0.0171 ***	
Prec total					0.0020 ***
Observations	10196	10196	10196	10196	10196
R ² / R ² adjusted	0.164 / 0.105	0.204 / 0.148	0.110 / 0.047	0.070 / 0.004	0.187 / 0.129

* $p < 0.1$ ** $p < 0.05$ *** $p < 0.001$

Table 1.2 - Bean fixed effect estimators

Bean					
	Log_yield	Log_yield	Log_yield	Log_yield	Log_yield
<i>Predictors</i>	<i>Estimates</i>	<i>Estimates</i>	<i>Estimates</i>	<i>Estimates</i>	<i>Estimates</i>
year	-0.0253 ***	-0.0286 ***	-0.0402 ***	-0.0427 ***	-0.0362 ***
VPD	-1.2781 ***				
EDD		-0.0093 ***			
VPD lim			-0.0153 ***		
CDD				-0.0201 ***	
Prec total					0.0013 ***
Observations	12432	12432	12432	12432	12432
R ² / R ² adjusted	0.111 / 0.049	0.130 / 0.070	0.073 / 0.009	0.079 / 0.016	0.136 / 0.076

* $p < 0.1$ ** $p < 0.05$ *** $p < 0.001$

Table 1.3 – Cassava fixed effect estimators.

Cassava					
	Log_yield	Log_yield	Log_yield	Log_yield	Log_yield
Predictors	Estimates	Estimates	Estimates	Estimates	Estimates
year	-0.0140 ***	-0.0147 ***	-0.0169 ***	-0.0201 ***	-0.0202 ***
VPD	-0.4068 ***				
EDD		-0.0013 ***			
VPD lim			-0.0020 ***		
CDD				0.0005	
Prec total					0.0002 ***
Observations	4718	4718	4718	4718	4718
R ² / R ² adjusted	0.066 / -0.008	0.065 / -0.009	0.058 / -0.017	0.050 / -0.026	0.063 / -0.011

* $p < 0.1$ ** $p < 0.05$ *** $p < 0.001$

Similarly, VPD, followed by VPD_lim, CDD, and EDD were the indexes that most affected crop yield of commodity agriculture (Tables 1.4 and 1.5). Among the two crops, maize was more affected by these extreme indexes than soybean. In addition, the delay of the rainy season onset (ORS) causes soybean yield loss. In contrast, PRCPTOT and the duration of the rainy season (DRS) positively affected it, confirming that increases in water availability and duration benefit soybeans that are commonly sowed as the first crop in multiple cropping systems. On the other hand, second season maize, showed a positive relationship with ORS and a negative relationship with ERS and DRS. All the estimators of fixed effect models constructed with soybean log(yield) and extreme climate indexes presented significance at 0.1%, while all the estimators of fixed effect models constructed with off-season maize log(yield) and extreme climate presented significance at 5% (Tables 1.4-1.5).

The model constructed with VPD and the off-season maize trend was the one that explains the greater amount of variance ($R^2=0.42$), while for soybean, the model constructed with EDD and the trend was the one with greater amount of variance ($R^2=0.26$) (Tables 1.4-1.5).

Table 1.4 – Soybean fixed effect estimators.

Soybean								
	Log_yield	Log_yield	Log_yield	Log_yield	Log_yield	Log_yield	Log_yield	Log_yield
Predictors	Estimates	Estimates	Estimates	Estimates	Estimates	Estimates	Estimates	Estimates
year	0.0118 ***	0.0121 ***	0.0119 ***	0.0082 ***	0.0084 ***	0.0085 ***	0.0085 ***	0.0084 ***
VPD	-0.5482 ***							
EDD		-0.0028 ***						
VPD lim			-0.0124 ***					
CDD				-0.0039 ***				
Prec total					0.0002 ***			
ORS						-0.0014 ***		
ERS							0.0026 ***	
DRS								0.0020 ***
Observations	3881	3881	3881	3881	3881	3881	3881	3881
R ² / R ² adjusted	0.113 / 0.032	0.257 / 0.190	0.146 / 0.068	0.066 / -0.019	0.100 / 0.018	0.070 / -0.015	0.114 / 0.033	0.119 / 0.040

* $p < 0.1$ ** $p < 0.05$ *** $p < 0.001$

Table 1.5 – Maize 2nd season fixed effects estimators.

Maize 2nd season								
	Log_yield	Log_yield	Log_yield	Log_yield	Log_yield	Log_yield	Log_yield	Log_yield
Predictors	Estimates	Estimates	Estimates	Estimates	Estimates	Estimates	Estimates	Estimates
year	0.0491 ***	0.0486 ***	0.0452 ***	0.0441 ***	0.0427 ***	0.0453 ***	0.0457 ***	0.0465 ***
VPD	-1.4188 ***							
EDD		-0.0036 ***						
VPD lim			-0.0203 ***					
CDD				-0.0083 ***				
Prec total					0.0004 ***			
ORS						0.0036 ***		
ERS							-0.0013 **	
DRS								-0.0020 ***
Observations	2013	2013	2013	2013	2013	2013	2013	2013
R ² / R ² adjusted	0.422 / 0.343	0.405 / 0.324	0.370 / 0.284	0.351 / 0.263	0.356 / 0.269	0.347 / 0.258	0.333 / 0.243	0.344 / 0.255

* $p < 0.1$ ** $p < 0.05$ *** $p < 0.001$

As the results show, VPD was the variable that most impacted crops yield during 2003-2019. Importantly, its impact on family farming crops is greater than in commodity agriculture (Figure 1.4), affecting primarily maize, followed by bean, and cassava. Regarding commodity agriculture, maize is also clearly more affected than soybean (Figure 1.4).

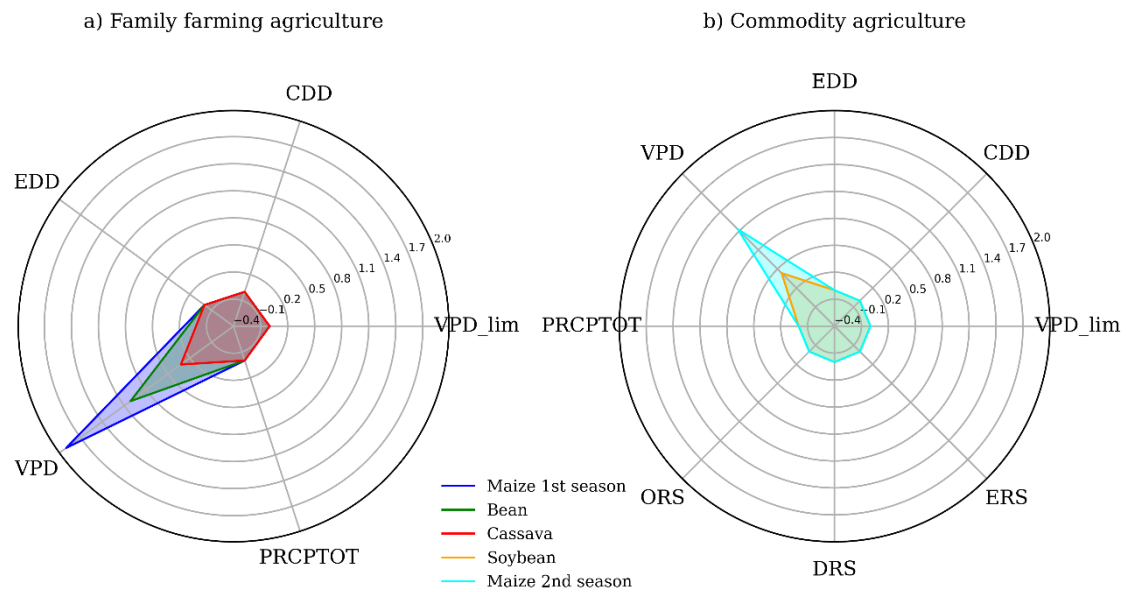


Figure 1.4 – Scores of influences of extreme climate indices on crops yields, for a) family farming of semiarid region and b) commodity agriculture of MT and MATOPIBA, represented as the standard deviations of each index.

The annual evolution of climate indexes and crop yields draws important patterns for family farming (Figure 1.5). During the period analysed, severe maize, bean and cassava yield losses (up to 25%) occurred from 2009/2010 harvest on (Figure 1.5-a), when PRCPTOT decreased and EDD and VPD increased (Figure 1.5-a, c, g). Yield and planted area losses intensified during the 2011/2012 to 2015/2016 harvests, when VPD, VPD_lim, and EDD reach their highest value (Figure 1.5-c, d, e), while PRCPTOT (Figure 1.5-g) reached its lower value of the period. The greatest lost on yield (~25%, Figure 1.5-a) and planted area (~25-50%, Figure 1.5-b) occurred in 2011/2012, but followed closely by the 2015/2016 harvest. On the other hand, during 2005/2006, 2007/2008, 2010/2011, and 2017/2018 harvests, mostly in La Niña years, family farming crops yield increased – but mainly maize – increased shortly above the average (Figure 1.5-a). In these years the reverse behavior in the climate indexes was shown: PRCPTOT increased and VPD, VPD_lim and EDD decreased.

The pattern observed on large-scale crops yields of MT and MATOPIBA region was a prevalence of reduction on soybean and off-season maize yield until the 2011/2012 and a prevalence of an increase after this harvest (Figure 1.5-a). In these crops, no planted area losses during the study period were reported (Figure 1.5-b).

The 2015/2016 harvest was the one that do not follow this pattern found for commodity agriculture crops. The yield growth trend has been halted and losses on maize second season

and soybean were of about 20% (Figure 1.5-a). In this harvest, were observed the lowest values of PRCPTOT for both crops in the period of 2003-2019, and the highest VPD, VPD_lim, and EDD values (Figure 1.5-c, d, e, g). In addition, reductions in the duration of rainy season were observed in both regions (Figure S1.7-b), driven by the delay of the rainy season, mainly in MATOPIBA region (Figure S1.7-a). Both regions presented delayed onset dates on this harvest when compared with the average of the period (Figure S1.7). This agricultural year was the one with the shortest rainy season to MATOPIBA and MT, with reductions of 49 and 18 days, respectively, in relation with the average duration of the period (Figure S1.7-b).

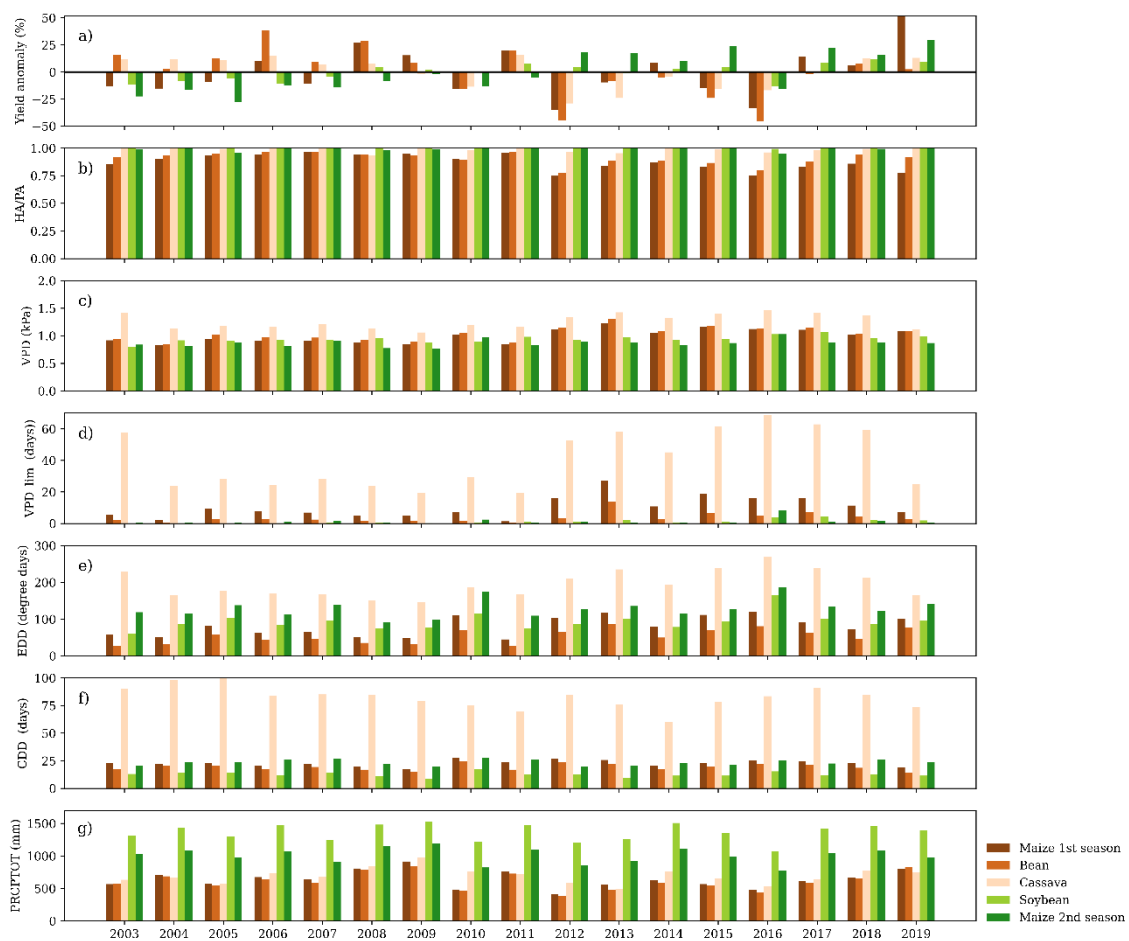


Figure 1.5 – Temporal evolution of extreme climate indices (c, d, e, f, g) and changes on yield (a) and planted area (b) for each crop during 2003-2019. Crops represented with orange palette are from family farming agriculture of semiarid region and crops represented with green palette are from commodity agriculture of MT and MATOPIBA.

1.3.4 – Regions levels trend

Technological trend ($\log(\text{crops yield}) \times \text{year}$) and harvested-planted area ratio of all family farming crops showed a significant negative trend (Figure 1.6), indicating an important production decrease in such a vulnerable region. Family farming maize 1st season presented the largest decrease in planted area, followed by bean and cassava.

Commodity agriculture, on the other hand, show an increasing technological trend with minimum changes in the harvested – planted area ratio, illustrating the increase in total production that these systems achieved in recent years (Figure 1.6).

The positive technological trend on crops of commodity agriculture and the negative technological trend on crops of family farming agriculture were also captured by the econometric models (Tables 1.1-1.5).

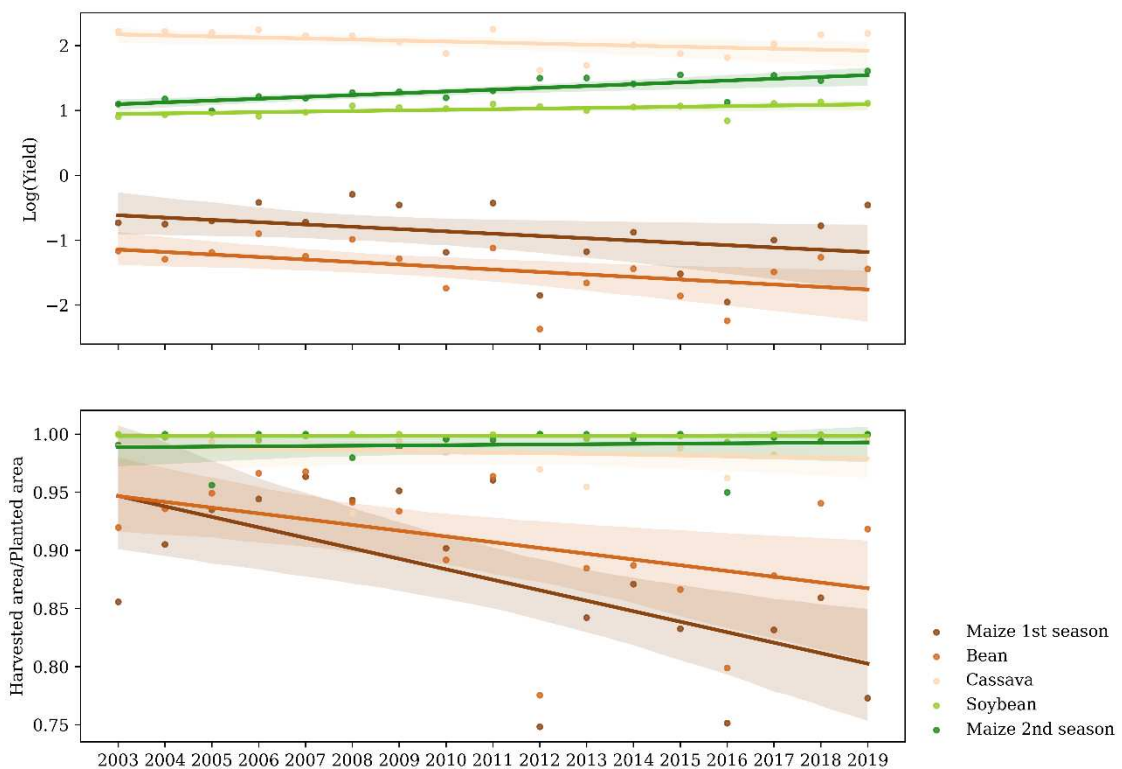


Figure 1.6 – Regression lines for $\log(\text{Yield})$ and the Harvested area/Planted area ratio for each crop. Crops represented with orange palette are from family farming in Semiarid region and crops represented with green palette are from commodity agriculture in MT and MATOPIBA. The shadow on regression lines represents the 95% confidence interval.

1.4 – Discussion

1.4.1 – Meteorological phenomena behind agricultural losses

During the 2003-2019 period, family farming and commodity crops were exposed to a combination of extreme climate events, especially after 2011, when the intensity and frequency of hot and dry events increased (greater values of EDD, VPD, and VPD_lim and lower values of PRCPTOT). Indeed, the most severe and intense droughts in the Brazilian territory over the last six decades occurred during 2011-2019 (Cunha *et al.*, 2019), with expected impacts in agricultural yield and planted area.

The 2009/2010 losses of family farming production were related to lower rainfall caused by a combination of a northward shift of the Intertropical Convergence Zone (ITCZ) position (Marengo *et al.*, 2017) and the unfavorable phase of Madden Julian Oscillation (MJO) to convection activity and rainfall (Alvarez *et al.*, 2016). During 2011/2012, an anomalous La Niña event, with cooling concentrated in central equatorial Pacific combined with warmer conditions in the tropical north Atlantic, lead to a northward shift of ITCZ and reduced rainfall on Northeastern Brazil (Rodrigues and McPhaden, 2014). The 2015/2016 drought was caused by a strong El Niño event, with great repercussion in the continent (Jiménez-Muñoz *et al.*, 2016; Cunha *et al.*, 2019). The warmer tropical Pacific sea surface temperature (SST) lead to changes in the Walker circulation, with a descending air flux in Northeastern, inhibiting the ITCZ movement to the south, resulting in less rainfall in the region (Cai *et al.*, 2020). In addition to the strong El Niño of 2015/2016, the intense social and economic impacts were an association of this event with the previous droughts that occurred in the region (Marengo *et al.*, 2017).

The strong El Niño of 2015/2016 also affected commodity agriculture, when in addition to lower PRCPTOT and higher VPD, the behavior of rainy season changed, reaching the shortest duration of the entire study period. In MATOPIBA, this event caused the largest delay of rainy season onset observed in 2003-2019. Indeed, in Western Bahia, a prominent agricultural region in MATOPIBA, 2015/2016 El Niño caused a strong delay in the rainy season onset but the sowing dates of rainfed farmers were not delayed, and even with that, the first crop presented yield losses (Fonseca *et al.*, 2022), probably due to water stress and higher temperatures during the growing season. However, in years with delay in the first crop sowing dates due to the rainy season delay, the off-season maize is submitted to a period of water stress in the end of cycle, and hence yield losses (Nóia Júnior and Sentelhas, 2019; Brumatti *et al.*, 2020). The delay in rainy season onset compromises the viability of double cropping systems

(Pires *et al.*, 2016; Abrahão and Costa, 2018; Brumatti *et al.*, 2020; Rattis *et al.*, 2021). According to Rattis *et al.*, (2021), double cropping systems were less adopted in the MATOPIBA region during 2012-2016 due to extreme climatic conditions.

In addition to the impacts of large-scale climate events on rainy season behavior, its onset and duration are also affected by land use and climate change (Leite-Filho *et al.*, 2019; Marengo *et al.*, 2022). In deforested areas inside Amazonia (including MT), rainy season starts later and is shorter (Leite-Filho *et al.*, 2019). Moreover, during the last decade, MATOPIBA presented drier and warmer conditions associated with land-use change and climate change, which contributes to a delay of rainy season onset in the region (Marengo *et al.*, 2022).

1.4.2 – Crops vulnerability to extreme climate

High VPD, VPD_lim, EDD, and CDD and low PRCPTOT values during 2003-2019 resulted from hot and dry conditions, affecting national agriculture, but most importantly, the semiarid region. VPD computes the difference from the maximum amount of water the air can hold and the actual conditions. It describes the drying power of the atmosphere and how much humidity it demands from the surface. This deficit controls plant transpiration and yield: high VPD leads to stomata closure to reduce water loss, therefore impacting photosynthesis, crop growth and yield (Rosenzweig *et al.*, 2001; Grossiord *et al.*, 2020). This important link between the atmosphere and the plants best described yield loss throughout the study period. In addition to the higher values of VPD, the frequency of VPD values that cause damage to crops (VPD_lim) increased during MET from 2011 on, demonstrating that crops are exposed to more intense and frequent drought and dry events, especially in family farming agriculture of the semiarid region. Other indexes, such as EDD, CDD, and PRCPTOT, reinforce this result, however, they do not explain plants' relation with climate variables as well as VPD, especially the combination of dry and hot events that predominated in the last decades in both agricultural regions.

The level of the impact on each crop and region is related to the exposure level to extreme conditions, the phenological stages when extreme climate events occur and the tolerance of crops to drought and high temperature.

The results strongly indicate that family farming crops are more exposed to hot and dry events during MET when compared with commodity crops. The most impacted crop yield was maize, followed by bean and cassava.

Cassava had the longer MET (~1 year) when compared to other crops, and therefore is exposed for long periods to adverse conditions. Despite that, cassava was the family farming crop with least impact on yield since it is a very tolerant crop, supporting extreme conditions throughout its development, such as high temperatures, prolonged drought periods, elevated levels of soil salinity and prolonged solar radiation exposure (Pushpalatha and Gangadharan, 2020). The fine and deep root system and the crop capability to maintain photosynthetic rate of about 50% under prolonged droughts (Pushpalatha and Gangadharan, 2020), contributes to cassava resilience in dry conditions. Thus, according to our results, cassava was more tolerant to unfavorable climatic conditions than maize and bean.

Bean and maize are sowed in similar periods among different municipalities in the semiarid, but maize is on the field longer than beans and is more exposed to adverse conditions. In that sense, maize was the family farmers crop most affected by extreme climate indexes throughout the semiarid. Maize yield failure is common in the region, and this contributes to the predomination of significantly lower yield values (~1 ton/ha, Silva and Neto, (2019)) than maize cultivated in central Brazil (~ 5 ton/ha, IBGE, (2022)). Family farmers in the semiarid have historically cultivated crops poorly adapted to drought, such as maize and bean. Cultivation of these crops in the region is linked to traditional and cultural beliefs that shape the regional agriculture and economy (Marengo et al., 2022). Despite the higher risk of maize failure, for example, the farmers continue to plant this crop because even if crop failure occurs, the straw is used for animal feed (Silva and Neto, 2019). Adaptation measures could be a solution to attenuate yield losses of maize and bean; however, adopting these measures is scarce in the region due to low technological input in farms. Adopting of alternative species more tolerant to drought, such as forage palm, agave, and sorghum could be another solution. Sorghum cultivation has grown in the region in last years, and is used for human consumption, animal feed, and the biomass could be used as forage (Marengo et al., 2022).

Commodity crops were less exposed to droughts and higher temperatures than family farming. Furthermore, the positive trend in the crops yield of commodity agriculture could be explained by the increase in technological trends during the studied period. These agricultural lands present a high technological level, with adapted and highly productive cultivars, while encompassing large irrigation poles that expanded in the last years, such as western Bahia, Alto Rio das Mortes, and Alto Teles Pires (ANA, 2021). The lower exposition due to a milder climate and the high technological level confirm that these crops and regions are less vulnerable to extreme climate conditions than family farming crops. Despite the increased yield in soybean

and off-season maize in MT and MATOPIBA, all the technology available was not sufficient to offset the impacts of the 2015/2016 El Niño.

Among the crops of commodity agriculture, soybean was more exposed to higher values of VPD and VPD_{lim} than maize off-season. However, the fixed effect model demonstrates that off-season maize yield was more impacted by these variables than soybean. It could be related to the fact that the adoption of irrigation practice is more common in soybean than in off-season maize in these regions and the damages of higher VPD and VPD_{lim} are attenuated in this crop. Besides reducing the water stress in crops, the irrigation practice reduces the high-temperature extremes in irrigated croplands (Vogel *et al.*, 2019), explaining the lower impact of EDD on soybean yield compared to off-season maize. Moreover, in years with delayed onset of the rainy season, the late sowing of soybean submits the off-season maize growing season to more adverse climate conditions (Nóia Júnior and Sentelhas, 2019).

Our results for commodity crops corroborated with the results of Rattis *et al.* (2021). These authors found that drought events decreased soybean and maize yield in these regions; and that VPD and precipitation explain the variations in these crops' yield during the last decades. Besides that, other studies have shown that the rainy season onset has been delayed in the last decades in the main producing regions of commodity crops (Leite-Filho *et al.*, 2019; Marengo *et al.*, 2022) and that this has affected rainfed agriculture of the region, especially in MATOPIBA (Fonseca *et al.*, 2022), corroborating with our findings.

1.4.3 – Contrasting family farming and commodity agriculture historical evolution

An important characteristic that stands out when contrasting these two agricultural types is that main family farming crops yields and planted areas have a decreasing trend. In contrast, large-scale commodity crops increase production throughout the studied period. This is naturally related to the difference in the technological level among regions. Our results endorse that, even though the literature identifies historical extreme climate conditions and predict their intensification in the future in both regions, family farming is experiencing an alarming and increasing level of food insecurity. Without adaptation measures, the population could opt to migrate to other regions. However, as demonstrated by Delazeri *et al.* (2022), in low-income rural areas of the NE region, rural outmigration is limited because of the reduced capacity to afford migration costs, then this population tends to stay in rural areas and is even more exposed to the frequent and intense extreme climate events leading to losses in agricultural production.

The losses in agricultural production increase the population's poverty and food insecurity and limit their capacity to adapt to climate change and extreme climate events, closing this unfortunate positive feedback.

In the Northeast region of Brazil, there are some policy programs of the Brazilian Federal Government and projects that work on the mitigation of the impacts of drought, such as *Garantia-Safra*, *Adapta sertão*, *Pronaf semiarido*, *Agro nordeste*, *ABC plan* and *drought stipend* (Marengo et al., 2022). However, according to Marengo et al. (2022), most programs are more reactive than preventive in dealing with droughts. That isolated government support to small farmers may not help them to build resilience to this climatic event in the long term.

There are some adaptation measures to help family farmers increase their resilience to extreme climate events, such as: increasing the access of farmers to cultivars and species adapted to dry and hot conditions and technical assistance; adoption of water and soil management techniques; adoption of water management techniques, such as dams or reservoirs; crop diversification and changes in crop calendar; development and adoption of a drought monitoring system, based in satellite sensor and crop and hydrological modeling; and combine technology-based solutions with regional social, economic and cultural aspects (Angelotti and Giongo, 2019; Marengo et al., 2022).

Commodity agriculture could adapt to extreme climate events by delaying first crop sowing dates (Pires *et al.*, 2016), and adopting short cycles cultivars of soybean and maize to adapt to a shorter rainy season (Abrahão and Costa, 2018; Brumatti *et al.*, 2020), and consequently, reduce the time exposure of crops to extreme climate events in the field. In addition, the farmers could invest in creating and adopting of a forecast system, mainly for the onset of the rainy season, to prevent losses during the initial plant development stages.

1.5 – Conclusion

This study assessed the extreme climate impacts on family farming agriculture of the semiarid region and the large-scale commodity agriculture of MT and MATOPIBA. Both agricultural types suffered from drought and hot events during 2003-2019, but their exposure and vulnerability to extreme climate caused different impacts on crops yield and planted area. Commodity agriculture lands were less exposed and more adapted than family farmers to extreme climate events due to the high level of technology, with the use of irrigation and adapted

cultivars, for example. The negative trends in agricultural outputs of family farming agriculture indicate that climate impact superposes the scarce or inexistent adaptation measures and leads to losses in the agricultural outputs of the region's main crops.

These results illustrate an alarming and worrying increasing level of food insecurity in such a vulnerable region as the semiarid. Importantly, such farms respond to a great share of the internal market, producing food consumed both in the semiarid and other regions of the country. Contrastingly, only a small share of the annual commodity crops production is consumed internally. Maize and soybean are the main commodities exported by Brazil, and their total production and export rates break records every year. Unfortunately, climate projections indicate that extreme climate will potentially exacerbate these conditions and, even though they might affect both agricultural types, impacts will also be greater in the semiarid.

Regional public policies and programs have still not achieved the goal of maintaining production and increasing resilience to climate extremes, indicating we still have to overcome these challenges in order to guarantee food security. There is an urgent need to create or expand existent adaptation programs to extreme climate, such as *Adapta Sertão* and ABC plan, to help family farmers build resilience, guarantee food security and develop climate-smart agriculture in the country.

1.6 – Supplementary Materials

Table S1.1 – Results from Hausman, Chow, and Breusch-Pagan tests for log(yield) models.

	Climate indices	Breusch-Pagan	Chow	Hausman	Result
Maize 1st season	VPD	Rho*	Rho*	Rho*	Fixed Effect
	VPD_lim	Rho*	Rho*	Rho*	Fixed Effect
	EDD	Rho*	Rho*	Rho*	Fixed Effect
	CDD	Rho*	Rho*	Rho*	Fixed Effect
	PRCPTOT	Rho*	Rho*	Rho*	Fixed Effect
	year	Rho*	Rho*	Rho*	Fixed Effect
Bean	VPD	Rho*	Rho*	Rho*	Fixed Effect
	VPD_lim	Rho*	Rho*	Rho*	Fixed Effect
	EDD	Rho*	Rho*	Rho*	Fixed Effect
	CDD	Rho*	Rho*	Rho*	Fixed Effect
	PRCPTOT	Rho*	Rho*	Rho*	Fixed Effect
	year	Rho*	Rho*	Rho*	Fixed Effect
Cassava	VPD	Rho*	Rho*	Rho*	Fixed Effect
	VPD_lim	Rho*	Rho*	Rho*	Fixed Effect
	EDD	Rho*	Rho*	Rho*	Fixed Effect
	CDD	Rho*	Rho*	Rho*	Fixed Effect
	PRCPTOT	Rho*	Rho*	Rho*	Fixed Effect
	year	Rho*	Rho*	Rho*	Fixed Effect
Soybean	VPD	Rho*	Rho*	Rho*	Fixed Effect
	VPD_lim	Rho*	Rho*	Rho*	Fixed Effect
	EDD	Rho*	Rho*	Rho*	Fixed Effect
	CDD	Rho*	Rho*	Rho***	Fixed Effect
	PRCPTOT	Rho*	Rho*	Rho*	Fixed Effect
	ORS	Rho*	Rho*	Rho*	Fixed Effect
	ERS	Rho*	Rho*	Rho*	Fixed Effect
	DRS	Rho*	Rho*	Aho	Random Effect
	year	Rho*	Rho*	Aho	Random Effect
Maize 2nd season	VPD	Rho*	Rho*	Rho*	Fixed Effect
	VPD_lim	Rho*	Rho*	Rho*	Fixed Effect
	EDD	Rho*	Rho*	Rho*	Fixed Effect
	CDD	Rho*	Rho*	Rho*	Fixed Effect
	PRCPTOT	Rho*	Rho*	Rho*	Fixed effect
	ORS	Rho*	Rho*	Rho*	Fixed Effect
	ERS	Rho*	Rho*	Rho*	Fixed Effect
	DRS	Rho*	Rho*	Rho*	Fixed Effect
	year	Rho*	Rho*	Rho*	Fixed Effect

Rho: reject null hypothesis; Aho: accept null hypothesis. ***p<0.1, **p<0.05, *p<0.01

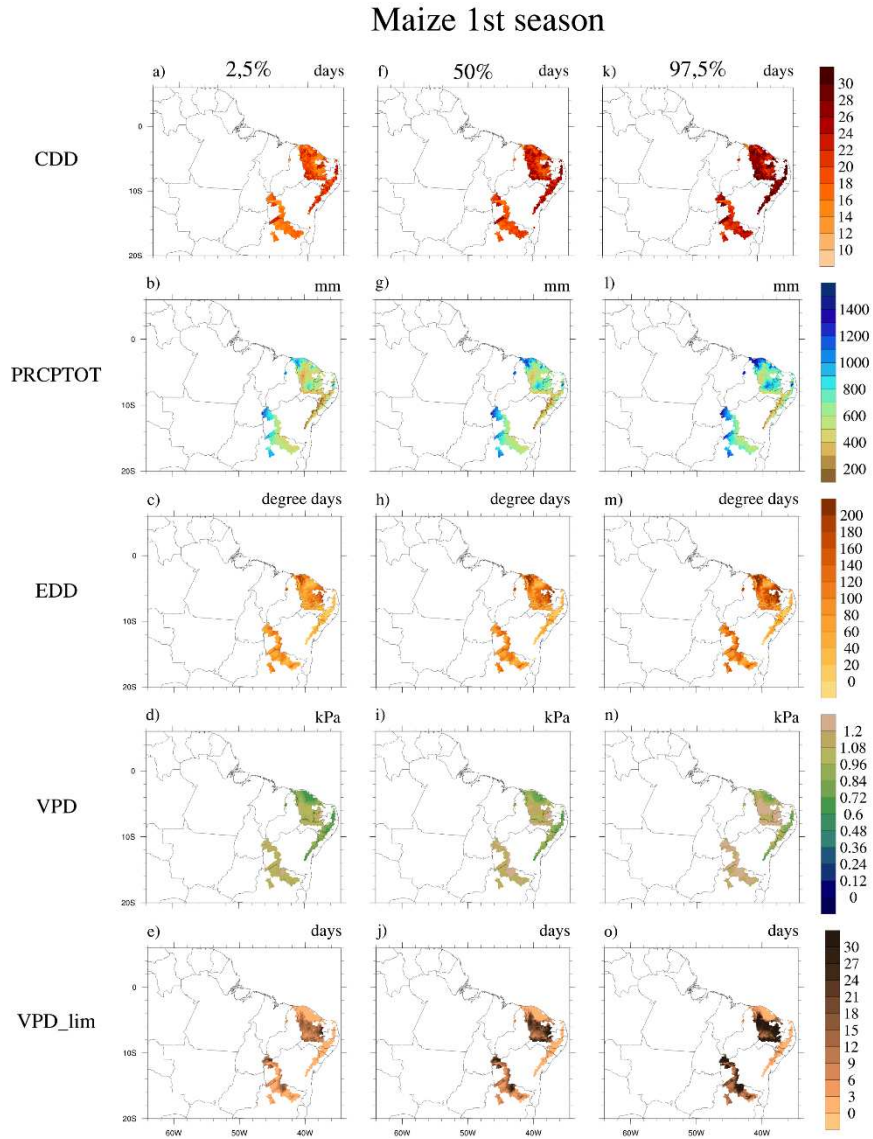


Figure S1.1 – Critical (lower and upper limits of 95% confidence interval) and average values of extreme climate indices for Maize 1st season on 2003-2019 period.

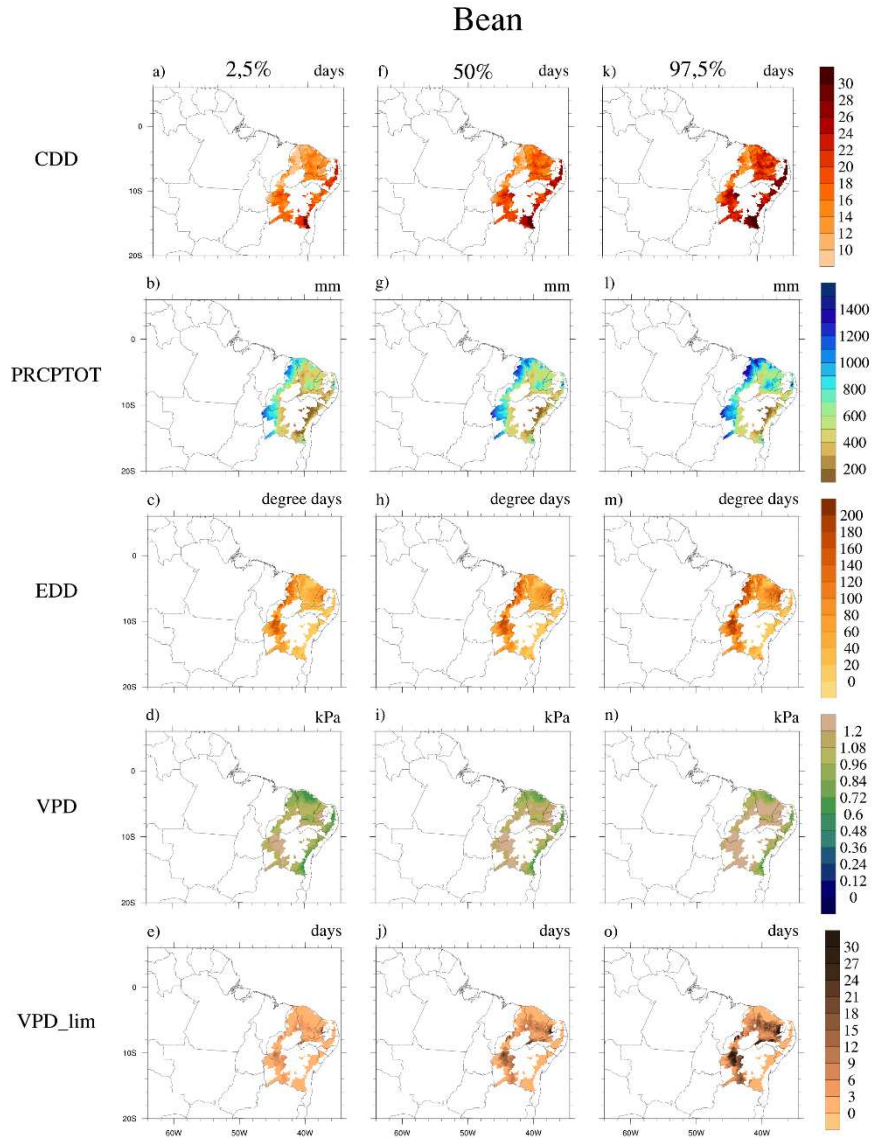


Figure S1.2 – Critical (lower and upper limits of 95% confidence interval) and average values of extreme climate indices for Bean on 2003-2019 period.

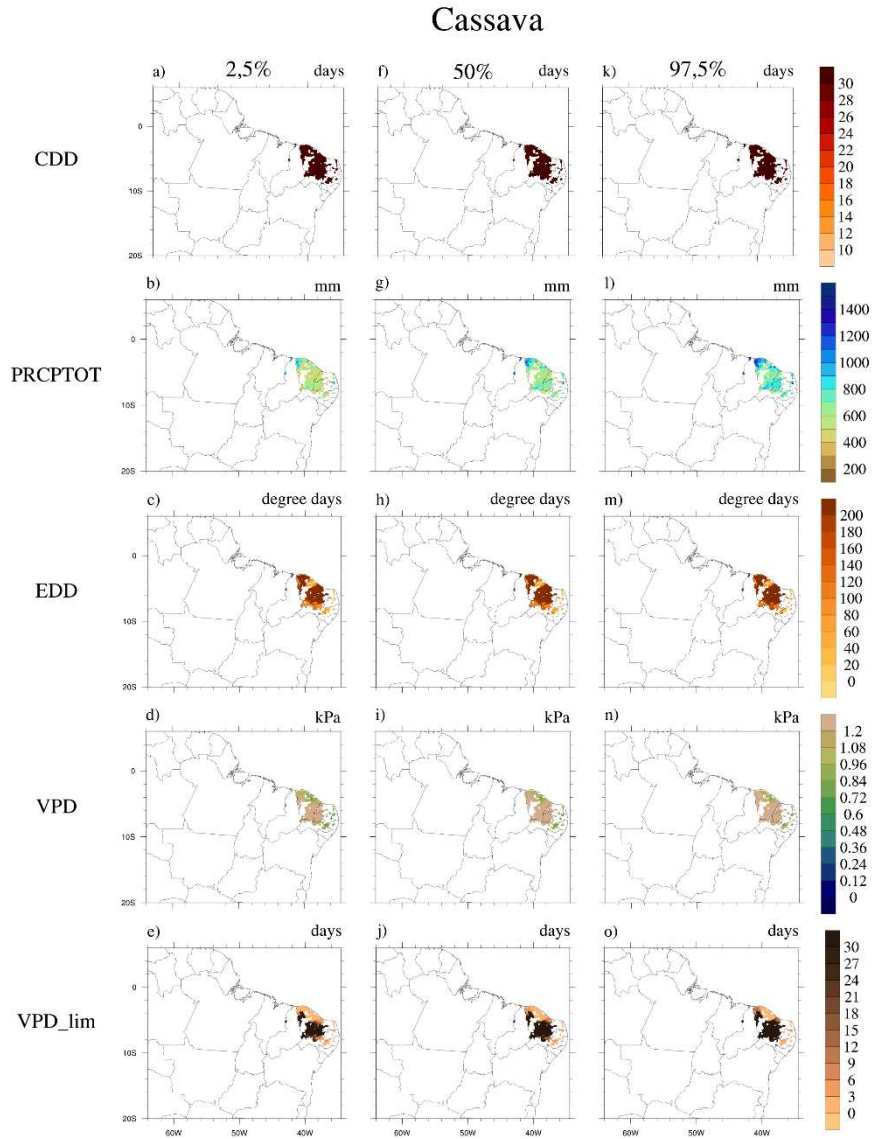


Figure S1.3 – Critical (lower and upper limits of 95% confidence interval) and average values of extreme climate indices for Cassava on 2003-2019 period.

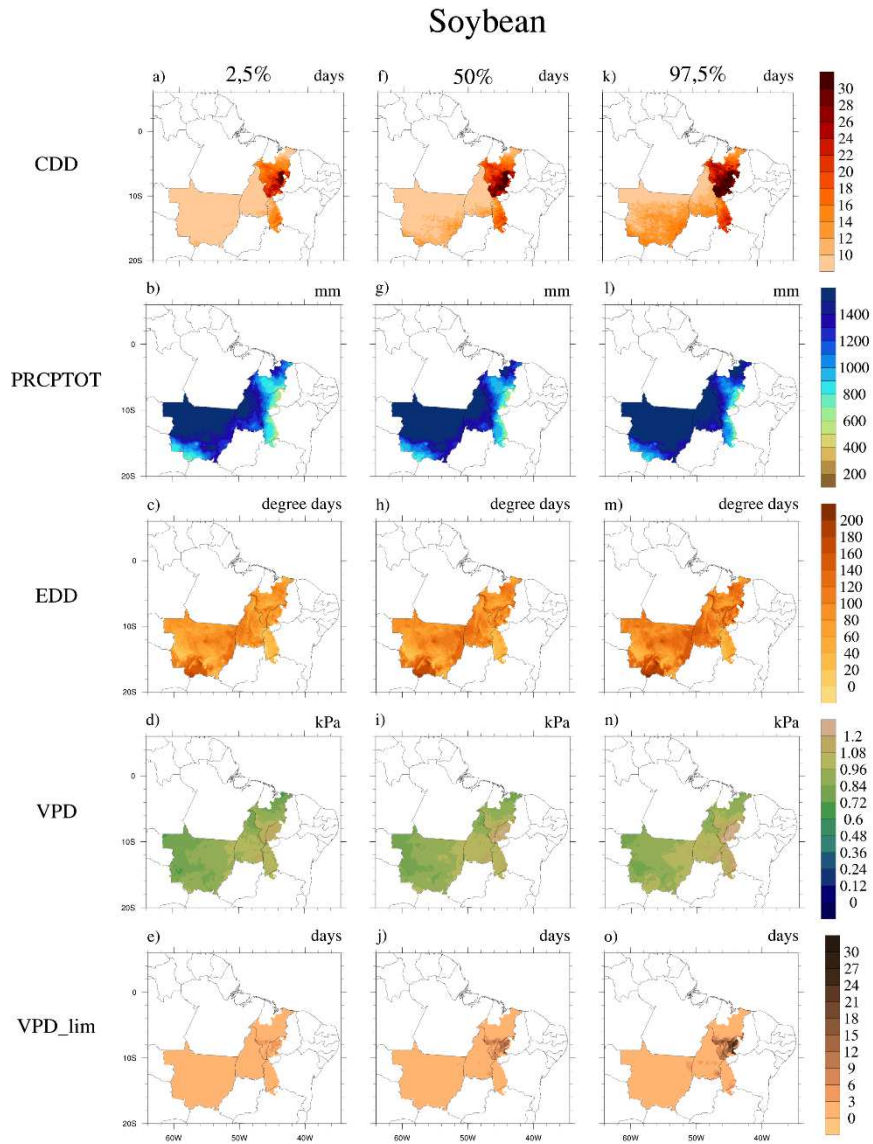


Figure S1.4 – Critical (lower and upper limits of 95% confidence interval) and average values of extreme climate indices for Soybean on 2003-2019 period.

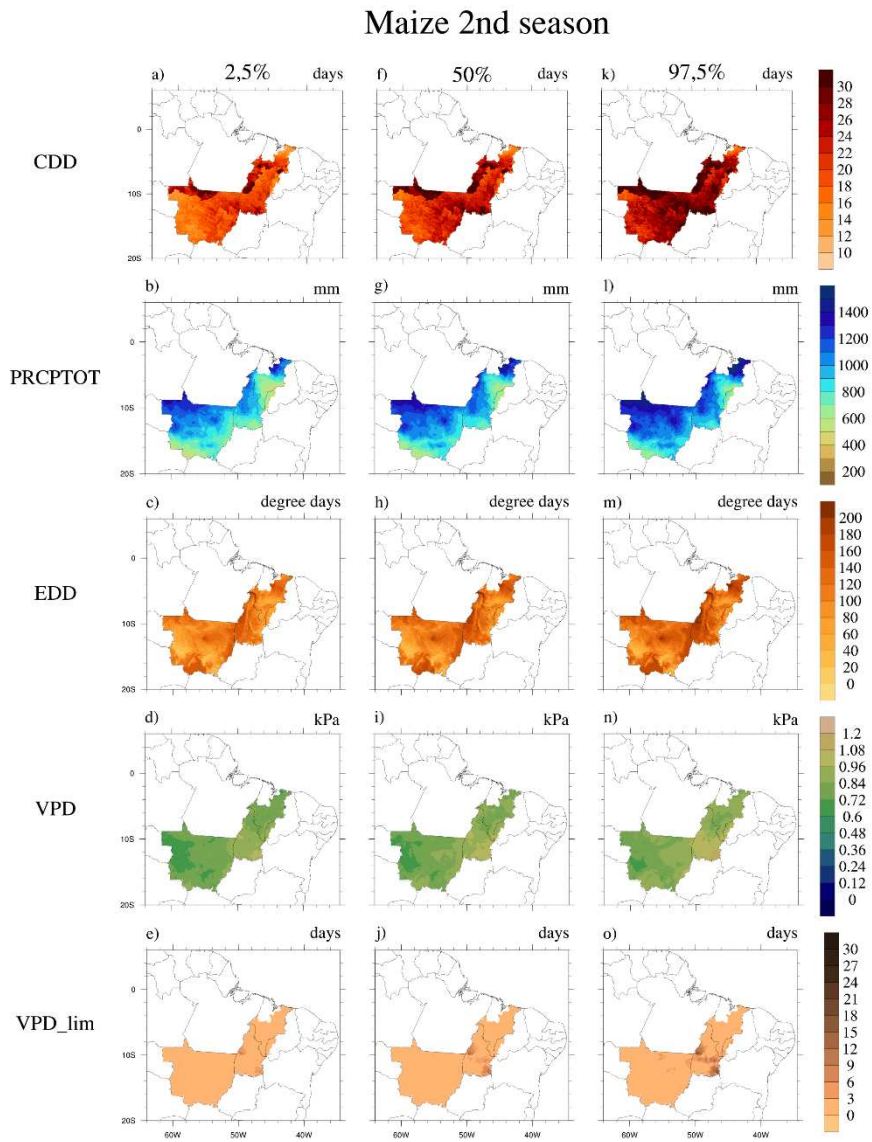


Figure S1.5 – Critical (lower and upper limits of 95% confidence interval) and average values of extreme climate indices for Maize 2nd season on 2003-2019 period.

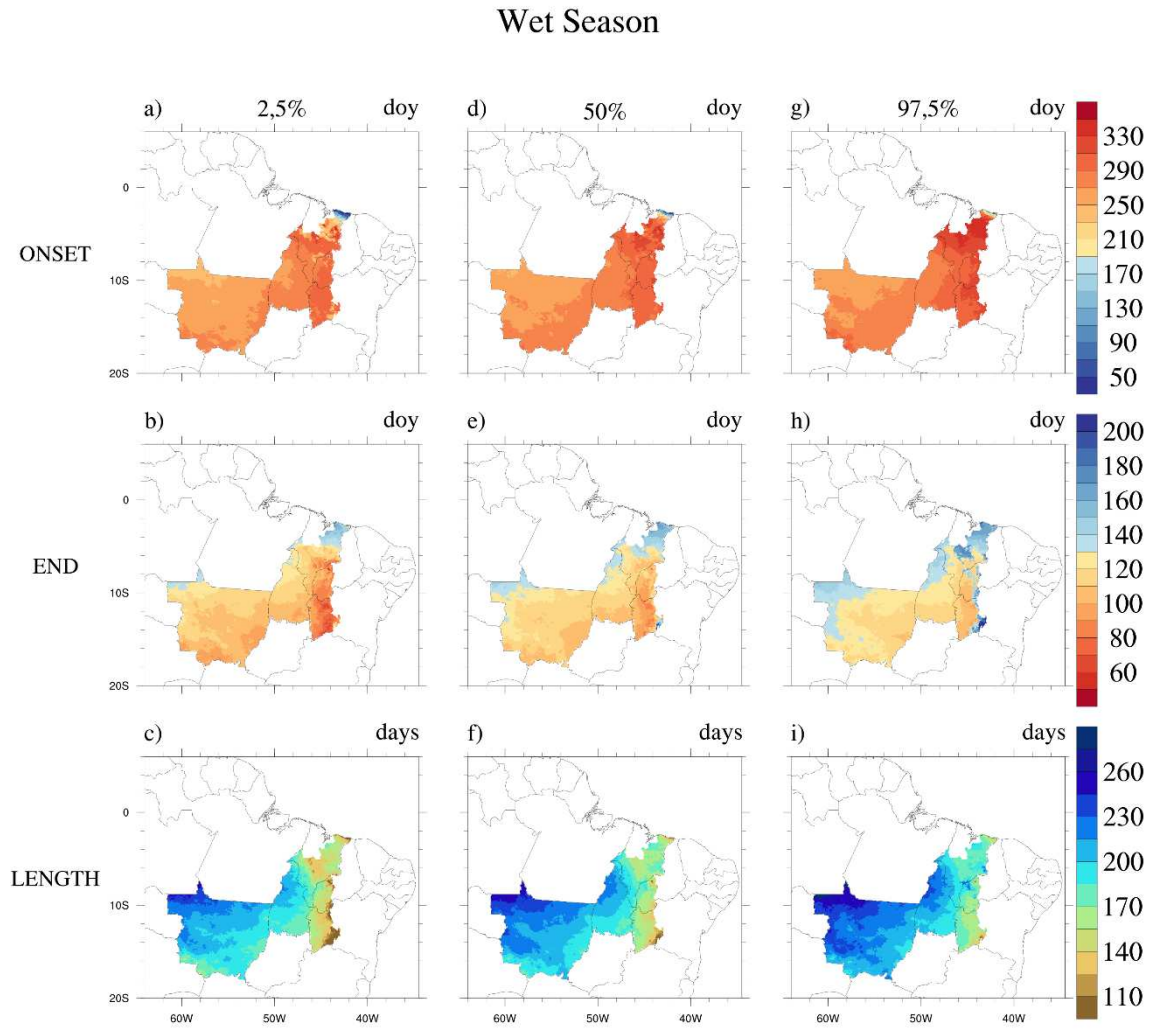


Figure S1.6 – Critical (lower and upper limits of 95% confidence interval) and average values of onset, end, and duration of wet season on 2003-2019 period

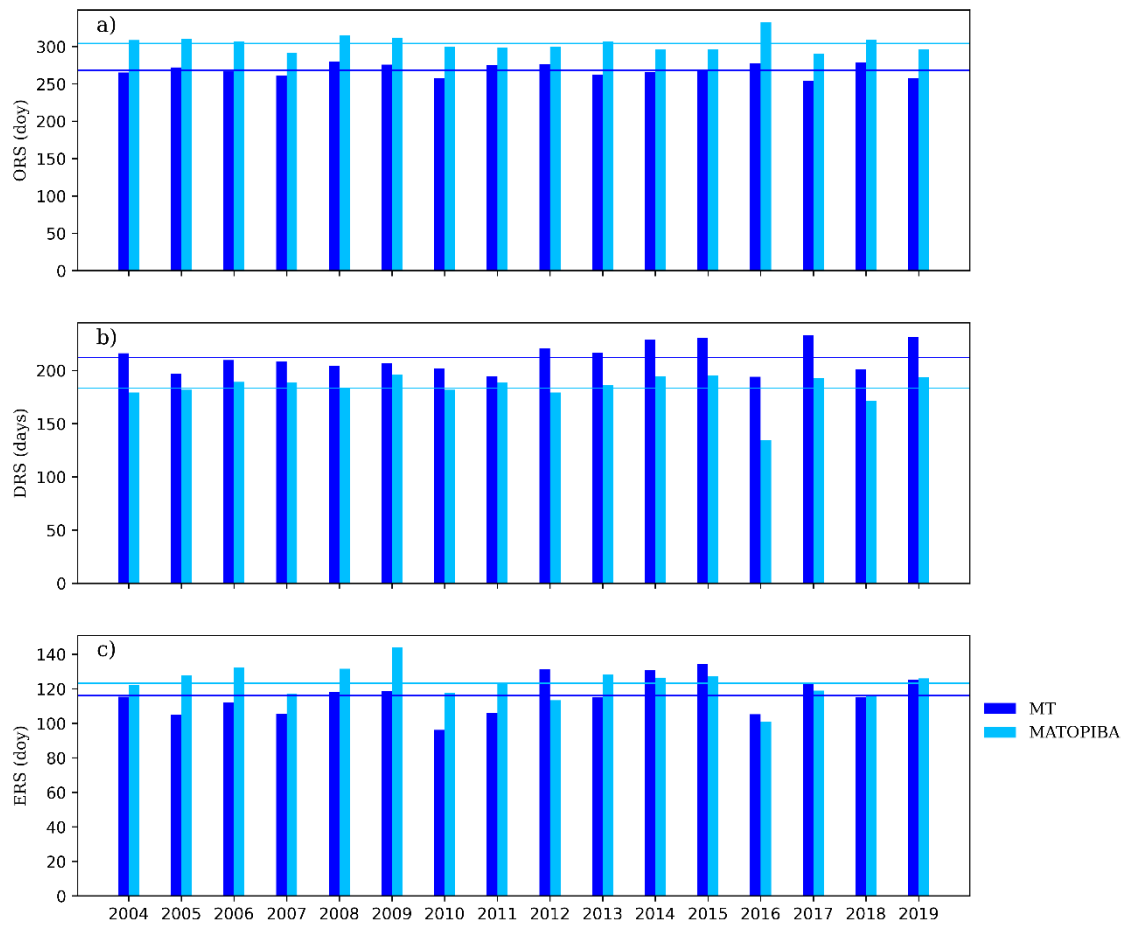


Figure S1.7 – Rainy season onset (a), duration (b) and end (c) for MT (dark blue) and MATOPIBA (light blue) for 2003-2019 period. Horizontal lines represent the average of the period for each region.

Chapter 2: Uncovering the need for bias correction in CMIP6 models for Brazil's climate assessment

Abstract

In the last years, the impacts of climate change have become increasingly evident, affecting both population and economic sectors, highlighting the need to create adaptation strategies in the face of the predicted intensification of its impacts in the future. Climate models' projections are commonly used to assess the future effects of climate change and develop adaptation strategies. However, these projections may have biases affecting climate risk assessment in hydrology and agriculture. In this way, our study aimed to evaluate the best bias correction method from the Coupled Model Intercomparison Project Phase 6 (CMIP6) for Brazil's climate and extreme climate variables and select the best models for each variable. I evaluated the performance and error of two types of bias correction methods commonly applied in the literature: linear scaling and quantile mapping for precipitation, minimum and maximum temperatures, the maximum number of consecutive dry days (CDD), and extreme degree days (EDD). Our results showed that the non-parametric quantile mapping methods performed better for most variables. In some models and regions, the linear scaling method performed slightly better for the CDD index, however, the improvement was minimal compared to the raw data, indicating that bias correction methods cannot achieve good performance in indexes that climate models do not well represent. The best models varied according to the variable, but ACCESS-ESM1-5, EC-Earth3-Veg, CanESM5, EC-Earth3, and CMCC-ESM2 predominated in the variables' ranking after bias correction. Our study supplies insight into the best method of bias correction and the best models for each variable and Brazilian region. This level of detailed information promotes a better choice between models and methods in climate risk assessment studies regarding agriculture, energy production, society, and disasters.

2.1 – Introduction

The aggravation of the climate crisis with the increase of socio-economic, natural, and human damages and the predicted future intensification of climate change creates the need to adapt and reduce these impacts through adaptation strategies (IPCC -Intergovernmental Panel on Climate Change, 2022). The climate model projections are reliable tools to evaluate the level of climate change impact in the future and are commonly used to create adaptation strategies in many sectors, such as agriculture, energy production, and disaster prevention.

Several studies assessed the impact of climate change in these sectors, especially agriculture, which plays a critical role in the Brazilian economy. Unfortunately, models predict a bleak future for this industry in the mid to late 21st century (Costa *et al.*, 2019; Brumatti *et al.*, 2020; Commar *et al.*, 2023). Moreover, the energy production sector also might face challenges (Arias *et al.*, 2020; Commar *et al.*, 2023). Furthermore, projections indicate that extreme events will become more severe, frequent, and extended, contributing to natural disasters impacting society (Medeiros *et al.*, 2022; Reboita *et al.*, 2022). Regrettably, the lack of specific evaluations of indices for these sectors and regions, coupled with the failure to assess model bias, poses a significant challenge to the reliability of these models for planning purposes.

Climate model projections have many uncertainties associated with the conceptualization and representation of the processes in the models, non-linearity of processes in the climate system, scenarios, and initial conditions of projections (Taylor *et al.*, 2012; Sillmann *et al.*, 2013). These uncertainties, particularly those related to imperfections of models, can introduce biases that reduce the accuracy of climate risk assessment in agriculture and hydrology. Therefore, minimizing these biases is crucial for achieving more reliable projections and estimates.

Many techniques are used to reduce these models' biases as dynamical and statistical downscaling and bias correction methods, which will be the focus of this study. A wide range of bias correction methods with different assumptions is used in the literature, such as the correction of mean, variance, or distribution bias (Lenderink *et al.*, 2007; Teutschbein and Seibert, 2012; Pierce *et al.*, 2015; Enayati *et al.*, 2021), which create the question about what is the best method for a specific region.

Several studies have evaluated the best bias correction method. Teutschbein and Seibert (2012) evaluated the performance of bias correction methods in five Sweden catchments for

temperature and precipitation variables. These authors found that all bias correction methods improved the models' performance of both variables on the monthly scale. However, the quantile mapping method had the best result, while linear scaling underperformed. Enayati *et al.* (2021) concluded that the empirical quantiles (QUANT) and robust empirical quantiles (RQUANT) were the best bias correction methods for precipitation and temperature variables in Iran. For Brazil, recent studies have made available a dataset of CMIP6 models' ensemble with bias corrected. However, they do not assess the best bias correction method and models for each climate variable (Thrasher *et al.*, 2022; Ballarin *et al.*, 2023). These authors assumed one bias correction method, as well as in hydrological studies where linear scaling is commonly used (Andrade *et al.*, 2021; Santos *et al.*, 2021; Siqueira *et al.*, 2021). Therefore, the assessment of the best bias correction method and the best models for each climate and extreme climate variable remains unknown in Brazil.

In this way, to accurately assess climate risk in Brazil's hydrology and agriculture, it is crucial to apply bias correction methods to climate and extreme climate variables. However, choosing the most suitable correction method for each region and selecting the best CMIP6 models remains unknown. Therefore, our study aimed to identify the best bias correction method and models for climate and extreme climate variables in each Brazilian region to support climate impact studies.

2.2 – Data and methods

2.2.1 – Study area

This study was developed in Brazil, and all the analyses were calculated for each pixel and each political region: north (NT), northeast (NE), center west (CW), southeast (SE), and south (ST) (Figure 2.1) for the period 1981-2010.

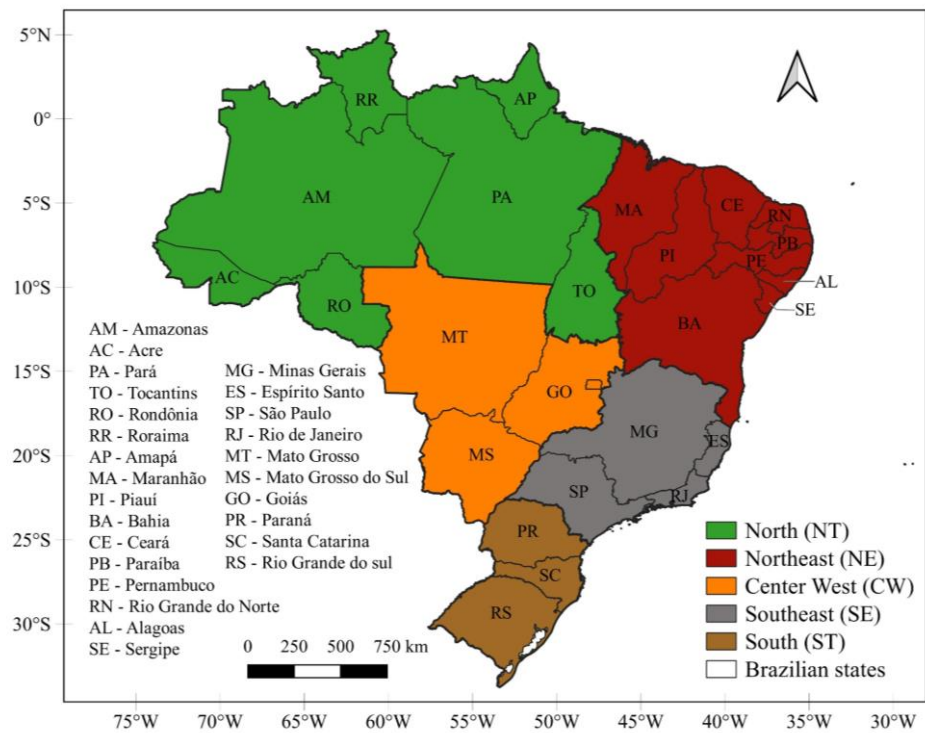


Figure 2.1 – Political Brazilian regions and states.

Our methodology was summarized and presented in Figure 2.2 and detailed in the following items.

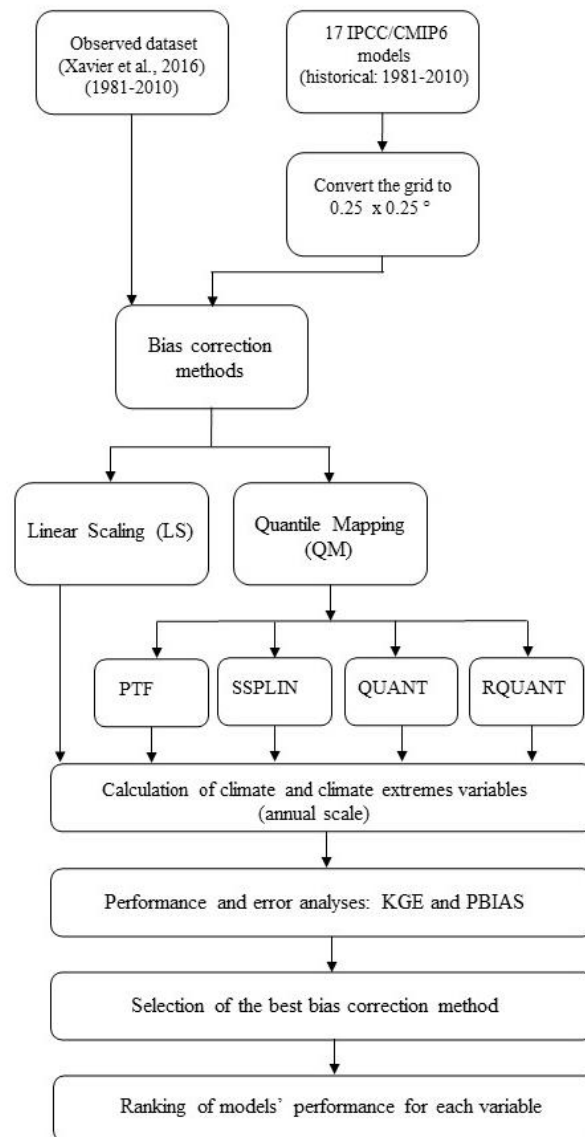


Figure 2.2 – Flowchart of the methodology.

2.2.2 – Climate data

I used the Brazilian gridded observation dataset at $0.25^{\circ} \times 0.25^{\circ}$ (lat/lon) with daily observed precipitation ($\text{mm} \cdot \text{day}^{-1}$), minimum and maximum temperatures ($^{\circ}\text{C}$) data for the period 1981-2010 from Xavier *et al.* (2016), and historical simulations from the IPCC/CMIP6 models as the simulated climate to the same period. Xavier *et al.* (2016) interpolated data from meteorological stations of *Agência Nacional de Águas (ANA)*, *Departamento de Águas e Energia Elétrica de São Paulo (DAAE)*, and *Instituto Nacional de Meteorologia (INMET)*.

I selected models comprising daily data of the specified variables for the historical period and for SSP1-2.6, SSP2-4.5, SSP3-7.0, and SSP5-8.5 scenarios in May/2021 (Table 2.1). I prioritize using the r1i1p1f1 variant label of models instead of using many ensemble members because the variability between models is greater than the variability between ensemble members. Choosing the same ensemble member guarantees that all models were initialized in the same conditions.

The horizontal resolution of the models (which ranged from $0.7^\circ \times 0.7^\circ$ to $2.79^\circ \times 2.81^\circ$, Table 2.1) was changed to match the spatial resolution of the observed dataset ($0.25^\circ \times 0.25^\circ$) using the largest area fraction remapping, preserving the same grid values of the original model resolution.

Table 2.1 – CMIP6 model's description used in this study.

Model number	Model	Institution	Country	Horizontal Resolution (lat × lon)
1	ACCESS-CM2	CSIRO	Australia	$1.25^\circ \times 1.87^\circ$
2	ACCESS-ESM1-5	CSIRO	Australia	$1.25^\circ \times 1.87^\circ$
3	BCC-CSM2-MR	BCC	China	$1.13^\circ \times 1.13^\circ$
4	CanESM5	CCCma	Canada	$2.79^\circ \times 2.81^\circ$
5	CMCC-ESM2	CMCC	Italy	$0.94^\circ \times 1.25^\circ$
6	EC-Earth3	EC-Earth-Consortium	Europe	$0.70^\circ \times 0.70^\circ$
7	EC-Earth3-Veg	EC-Earth-Consortium	Europe	$0.70^\circ \times 0.70^\circ$
8	EC-Earth3-Veg-LR	EC-Earth-Consortium	Europe	$1.12^\circ \times 1.12^\circ$
9	GFDL-ESM4	NOAA-GFDL	USA	$1.00^\circ \times 1.25^\circ$
10	INM-CM4-8	INM	Russia	$1.50^\circ \times 2.00^\circ$
11	INM-CM5-0	INM	Russia	$1.50^\circ \times 2.00^\circ$
12	MIROC6	MIROC	Japan	$1.41^\circ \times 1.41^\circ$
13	MPI-ESM1-2-HR	DKRZ	Germany	$0.94^\circ \times 0.94^\circ$
14	MPI-ESM1-2-LR	MPI-M	Germany	$1.87^\circ \times 1.87^\circ$
15	MRI-ESM2-0	MRI	Japan	$1.13^\circ \times 1.13^\circ$
16	NorESM2-LM	NCC	Norway	$1.90^\circ \times 2.50^\circ$
17	NorESM2-MM	NCC	Norway	$0.94^\circ \times 1.25^\circ$

I also used annual extreme climate variables as consecutive dry days (CDD) and extreme degree days (EDD) (Table 2.2).

CDD is the maximum consecutive days of a determined period (when daily precipitation is below 1 mm.d⁻¹), calculated from daily precipitation data of observed and IPCC/CMIP6 models. EDD indicates crops' exposure to higher temperatures during the growing season, calculated using daily minimum and maximum temperatures and a threshold temperature (Flach *et al.*, 2021). I assumed that the threshold temperature is 29 °C (Schlenker and Roberts, 2009) because it is a critical temperature for maize and is close to the critical temperature of other important crops for Brazil as soybean, cassava, and bean (30 °C) (Hillocks *et al.*, 2001; Schlenker and Roberts, 2009; Silva *et al.*, 2010). These two extreme climate indexes represent dry spells (CDD) and exposure to higher temperature (EDD) during crop-growing seasons. Despite the agricultural approach, the CDD index could be used in studies with different approach as hydrology. Combining these two indices, I can evaluate models' reliability on climate impact in agriculture.

Table 2.2 – Climate and climate extreme variables.

Variable name	Variable abbreviation	Unit
Daily precipitation	PREC	mm
Minimum temperature	TMIN	°C
Maximum temperature	TMAX	°C
Maximum consecutive dry days	CDD	Days
Extreme degree days	EDD	Degree days

2.2.3 – Bias correction methods

I evaluated two types of bias correction methods: linear scaling and quantile mapping., which differ mainly in the complexity and the type of correction.

2.2.3.1 – Linear Scaling (LS)

The LS method is considered a simple bias correction method, and its main purpose is to correct the mean bias. In contrast, the variables' frequency or intensity distribution bias is not corrected (Ines and Hansen, 2006). Daily precipitation (P, mm.day⁻¹) was corrected using the ratio between the long-term monthly mean of observed ($\overline{P_{obs}}$, mm.month⁻¹) and simulated ($\overline{P_{sim}}$, mm.month⁻¹) data (Equation 1), while daily temperature (T, °C) was corrected using the difference of the long-term monthly mean of observed ($\overline{T_{obs}}$, °C) and simulated ($\overline{T_{sim}}$, °C) data (Equation 2) (Lenderink *et al.*, 2007; Teutschbein and Seibert, 2012). Equation 2 was applied to minimum and maximum temperatures.

$$P_{\text{corr}}(t) = P(t) \times \left(\frac{\overline{P_{\text{obs}}}}{\overline{P_{\text{sim}}}} \right), t = 1, \dots, 365 \quad \text{Equation 1}$$

$$T_{\text{corr}}(t) = T(t) + (\overline{T_{\text{obs}}} - \overline{T_{\text{sim}}}), t = 1, \dots, 365 \quad \text{Equation 2}$$

2.2.3.2 – Quantile Mapping (QM): Parametric transformation Function (PTF)

Quantile Mapping (QM) is a bias correction method that uses transfer functions created with time series of observed and simulated data to adjust the distribution of simulated data to match the distribution of observations. In this procedure, the simulated distribution is fitted for each quantile. The quantile-quantile relation is obtained from the inverse Cumulative Distribution Functions (CDFs) of both simulated and observed time series (Equation 3) (Gudmundsson *et al.*, 2012). All QM methods were calculated using the R package qmap (Gudmundsson *et al.*, 2012).

$$X_o = F_o^{-1}[F_m(X_m)], \quad \text{Equation 3}$$

Where F_m is the CDF of the modeled variable X_m , and the F_o^{-1} is the quantile function (or inverse CDF).

Two approaches are available to adjust the simulated distribution according to the observed distribution: parametric and non-parametric. The parametric approach relies on a predefined transformation function to adjust data. On the other hand, the non-parametric uses empirical data distributions to correct bias, and therefore are more flexible (Enayati *et al.*, 2021).

The parametric transformation function (PTF) has many predefined functions, such as linear, scale, power, etc. In this study, PTF considers a linear transformation function (Equation 4) that assumes a linear relationship between quantile functions of the observed and simulated time series in the historical period.

$$X_o = a + bX_m \quad \text{Equation 4}$$

Where X_m is the modeled CDF, X_o is the observed CDF, a and b are parameters obtained from fitting a linear least squares regression.

2.2.3.3 - Quantile Mapping (QM): Empirical quantiles (QUANT)

The empirical quantiles (QUANT) method is a non-parametric approach, then the transformation function does not follow a theoretical function. In the QUANT method, the empirical CDFs of observed and simulated time series are estimated for regularly spaced quantiles ($q=0.01$), and the differences between the CDFs are estimated for each time interval and are smoothed using a linear interpolation (Osuch *et al.*, 2017; Qian and Chang, 2021).

2.2.3.4 - Quantile Mapping (QM): Robust empirical quantiles (RQUANT)

As well as the QUANT method, the robust empirical quantiles method (RQUANT) follows a non-parametric approach to correct the bias of climate variables. This method estimates the quantile-quantile relation of observed and simulated time series using local linear least squares regression (Enayati *et al.*, 2021; Qian and Chang, 2021).

2.2.3.5 - Quantile Mapping (QM): Smoothing splines (SSPLIN)

The SSPLIN method is a QM method based on a non-parametric approach and QUANT and RQUANT methods. This method applies a smoothing spline to the quantile-quantile relation of observed and simulated time series (Gudmundsson *et al.*, 2012; Enayati *et al.*, 2021).

2.2.4 – Performance evaluation of bias correction methods

After bias correction, I calculated the climate and extreme climate variables for the annual scale for the simulated and observed datasets to apply the performance and error metrics. Then, in the annual scale, the climate variables were: daily mean precipitation, daily mean minimum and maximum temperatures, and the extreme climate (CDD and EDD) calculated to the civil year (beginning on January 1 and ending on December 31). The performance evaluation was done for the 1981-2010 period.

The best bias correction method is determined by the Kling-Gupta Efficiency index (KGE) as a performance metric and Percentage bias (PBIAS) as an error measure.

KGE (Gupta *et al.*, 2009; Kling *et al.*, 2012) is calculated considering the Euclidian distance of correlation (r), bias ratio (α), and the variability ratio (γ) of observed and simulated data (Equation 5). KGE values close to 1 indicate a better performance of the simulated variable. Althoff and Rodrigues, (2021) found that KGE had a more reliable criterion as a performance metric than other metrics in hydrological studies. Moreover this metric is commonly applied in climate studies (Zuluaga *et al.*, 2022; Avila-Diaz *et al.*, 2023)

$$KGE = 1 - \sqrt{(r - 1)^2 + (\alpha - 1)^2 + (\gamma - 1)^2} \quad \text{Equation 5}$$

PBIAS is the difference between the simulated (P_i) and observed variable (O_i), divided by the observed variable, and multiplied by 100 (Equation 6). PBIAS indicates the variation of the simulated data in relation to observed data, then values close to zero indicate a smaller error in simulated data.

$$PBIAS = \frac{\sum_{i=1}^n (P_i - O_i)}{\sum_{i=1}^n O_i} \times 100 \quad \text{Equation 6}$$

2.2.5 – Ranking of the models' performance

To select the best CMIP6 model, I ranked the models from the best to worst KGE values for each Brazilian region and variable after applying the bias correction that performed better in our analysis.

2.3 – Results

In general, all methods improved most model representation. Still, the performance between the quantile mapping (QM) methods (QUANT, SSPLIN, and RQUANT, PTF) and the linear scaling (LS) method differed along the entire Brazilian territory, models and variables (Figures S2.1, S2.2).

2.3.1 – PREC

Compared to the QM methods, the bias correction applied to PREC had notably lower performance in the LS method, particularly in the NT region. As a result, LS worsened the performance of some models in this region, namely CanESM5, MIROC6, MPI-ESM1-2-HR,

MPI-ESM1-2-LR, MRI-ESM2-0, NorESM2-LM, and NorESM2-MM (Figures S2.19, S2.23). The Brazilian region that performed better after LS was CW, but the models still presented lower performance than QM (Figure S2.23).

QM methods improved the performance in some models and regions for PREC, especially in NE (Figures 2.5 and S2.20-2.22). For example, most CMIP6 models tend to overestimate PREC in NE by more than 30% (Figure S2.19), and after QM bias correction the error is reduced to $\pm 6\%$ in models (Figures 2.4 and S2.20-S2.22).

The PTF method tends to overestimate PREC along the NE region ($PBIAS > 15\%$) while it underestimates the same variable along other Brazilian regions ($PBIAS < -6\%$) in some models (Figures 2.3, 2.4). The worst KGE values (~ -1) for this method are in NT, more precisely in AM and PA states, while the best KGE values (0.4-0.6) are in the states of CW region, as MT and GO in most models (Figures S2.1, S2.2). The non-parametric QM methods performed better than the PTF method for PREC, especially in QUANT and RQUANT.

Among the non-parametric methods, QUANT and RQUANT presented the best and most similar results in PREC, with error variations only in some models and regions (Figures 2.5, S2.21, and S2.22). On the other hand, SSPLIN performed worse than QUANT and RQUANT in some models (CMCC-ESM2, ACCESS-CM2, INM-CM4-8, and INM-CM5-0) with KGE values close to -1 in some pixels (Figures S2.1, S2.2).

Despite similar results found for QUANT and RQUANT, I choose QUANT as the best bias correction method for PREC due to faster calculation. The five models that performed better for PREC, QUANT, and all Brazilian territory were: CMCC-ESM2, CanESM5, EC-Earth3-Veg, MRI-ESM2-0, and MIROC6 (Figure 2.6-a). The CMCC-ESM2 model performed better in all Brazilian regions, with the best performance of PREC in the NT and ST regions, while BCC-CSM2-MR showed the lowest performance.

2.3.2 – TMIN and TMAX

Similarly to PREC, all bias correction methods for temperature improved most models' data. Even though the LS method performed better to TMIN and TMAX than to PREC (Figure S2.23), it was outperformed by QM methods. In the LS method, some models presented the worst KGE values (~ -1) for maximum and minimum temperature in AM and PA states, while

QM methods presented greater KGE values for the same states (Figures S2.3, S2.4, S2.7, and S2.8).

Among QM methods, most models presented the worst performance in the CW region for TMIN and ST region for TMAX. This pattern is also observed in the LS method. Despite the difference in KGE, the error of both methods ranged between $\pm 3\%$ for minimum and maximum temperatures (Figures S2.5, S2.6, S2.9, and S2.10). QM methods presented a similar performance for TMIN and TMAX, with differences only in some models and pixels with KGE values close to -1 in the SSPLIN method (Figures S2.5, S2.6, S2.9, and S2.10). Then, the best methods were QUANT, RQUANT, and PTF for these variables.

I considered the QUANT as the best method to select the best models. To TMIN and TMAX, in the five best positions of models' ranking, four models repeated in ranking both variables: ACCESS-ESM1-5, CanESM5, EC-Earth3-Veg, and EC-Earth3 (Figure 2.6 -b,c). The models that completed the ranking were: BCC-CSM2-MR and MPI-ESM1-2-LR to TMIN and TMAX, respectively. The best models for TMIN and TMAX were ACCESS-ESM1-5 and CanESM5, while the worst were NorESM2-LM and INM-CM5-0, respectively.

2.3.3 – EDD

Extreme climate indexes showed similar bias patterns to the climate variables used to calculate them, with the EDD index performing better than the CDD index after the bias correction. The bias correction improved the performance of the EDD when compared with the raw model's data (Figures 2.5, S2.19-S2.23), and achieved better results with QM methods than LS in most models and regions (Figures 2.5, S2.20, S2.21, and S2.22). In the QM methods, some models showed lower performance only in ST region, while models poor performance spread to other regions besides ST with the LS method. For example, many models overestimated EDD for SSPLIN (PBIAS 10-20%) and PTF (PBIAS > 20%) in ST, while the error in other regions ranged from - 5% to + 5%. QUANT and RQUANT presented the best performance and the lower error for all regions and most models (Figures 2.5, S2.21).

Considering QUANT the best bias correction method, the best five models for EDD and all Brazilian territory were: ACCESS-ESM1-5, EC-Earth3-Veg, CanESM5, EC-Earth3, and INM-CM4-8 (Figure 2.6-e). The best and the worst models for EDD were ACCESS-ESM1-5 and MIROC6, respectively.

2.3.4 – CDD

The CDD index performed poorly in all methods, regions, and nearly all models. All QM methods overestimated the CDD compared to the observed index in all regions and most models (Figures S2.20, S2.21, and S2.22). Most models had difficulty in the representation of this index (without the application of bias correction methods), especially in the NT and NE regions in almost all models (negative KGE values), with an overestimation of the index of more than 30% (Figure S2.19). QM methods increased the CDD performance of some models in the NT region, while the difference was minimal in other regions compared to the raw data. The LS method for this variable performed slightly better when compared to QM methods. Even with the increase in performance, the KGE values remained low for this index in all methods.

To the CDD index, the five models that performed better in the QUANT method were: EC-Earth3, ACCESS-ESM1-5, MIROC6, INM-CM5-0, and CMCC-ESM2 (Figure 2.6-d). The best model was EC-Earth3, while the worst model was NorESM2-LM.

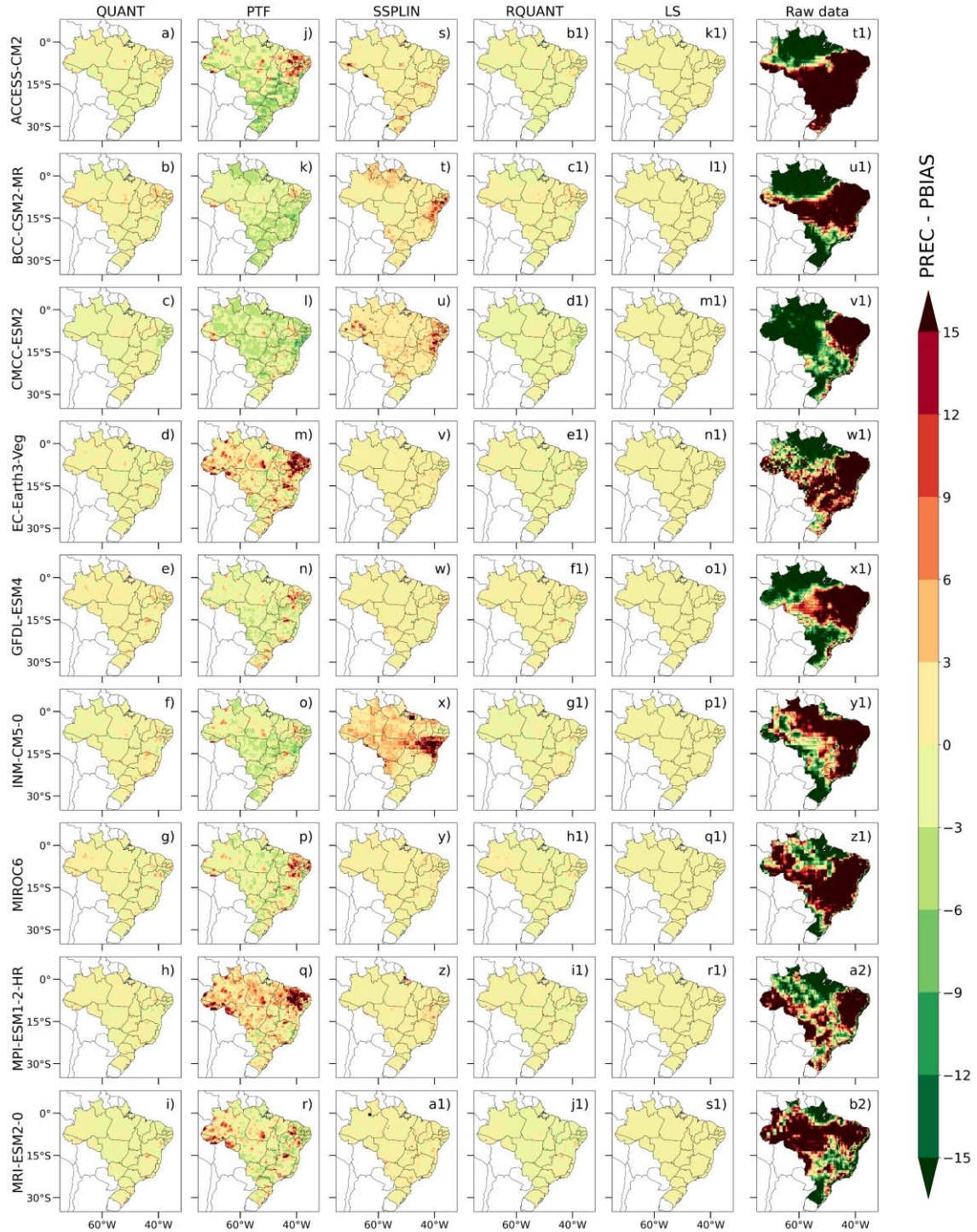


Figure 2.3 – Percentual bias (PBIAS, %) of precipitation for each bias correction method, raw model data, ACCESS-CM2, BCC-ESM2-MR, CMCC-ESM2, EC-Earth3-Veg, GFDL-ESM4, INM-CM5-0, MIROC6, MPI-ESM1-2-HR, MRI-ESM2-0 models.

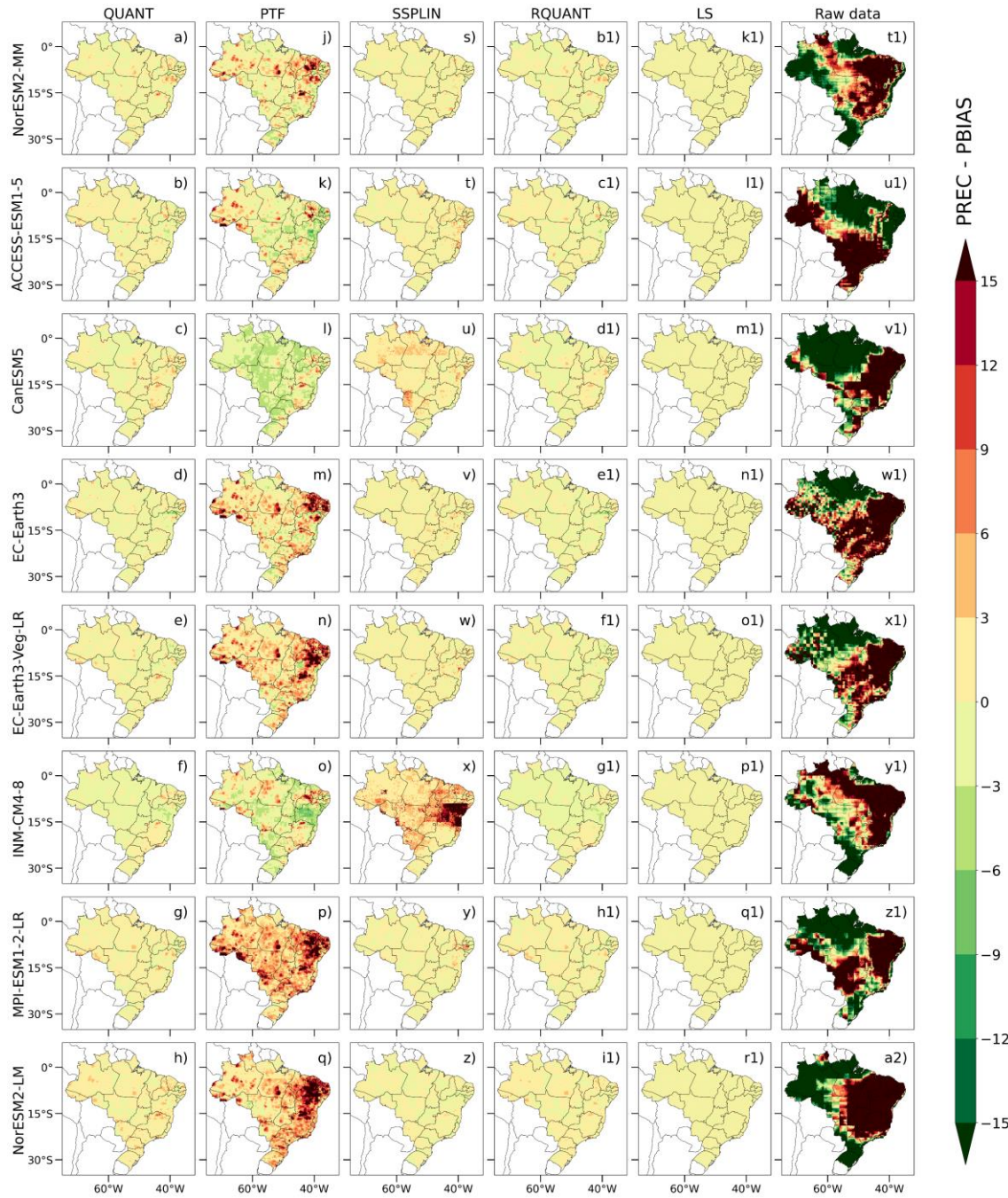


Figure 2.4 – Percentual bias (PBIAS, %) of precipitation for each bias correction method, raw model data, NorESM2-MM, ACCESS-ESM1-5, CanESM5, EC-Earth3, EC-Earth3-Veg-LR, INM-CM4-8, MPI-ESM1-2-LR, and NorESM2-LM models.

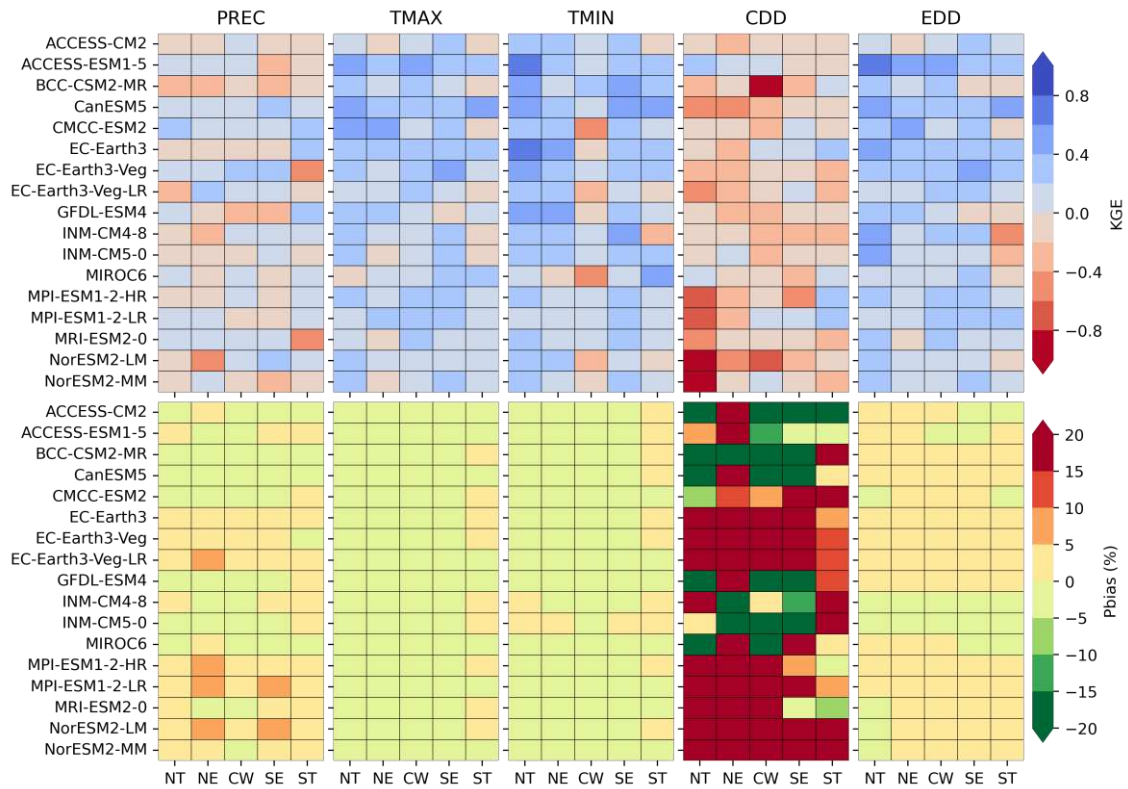


Figure 2.5 – KGE and PBIAS results for each variable (PREC, TMAX, TMIN, CDD and EDD), model and Brazilian region for QUANT method.

Broadly speaking, the QM methods performed better than LS in nearly all variables except for CDD. Moreover, models showed some issues in the representation of CDD, and the improvement was minimal with bias correction. In general, QM methods presented similar results when compared with each other, especially for EDD, TMIN, and TMAX. For PREC, there was a notable difference between the methods based on the parametric (PTF) and non-parametric (QUANT, RQUANT, and SSPLIN) approaches. The PTF method improved the performance of some models. However, the non-parametric methods performed better than PTF (Figures 2.5, S2.20, S2.21, and S2.22).

Considering QUANT as the best bias correction method, the models common to all five variables and were the best models: ACCESS-ESM1-5, EC-Earth3-Veg, CanESM5, EC-Earth3, and CMCC-ESM2 (Figure 2.6). I did not find a relationship between the horizontal spatial

resolution of the models and the best models selected for Brazil, since among the five best models we have the model with the lowest spatial resolution (CanESM5) and the models with the highest spatial resolution (EC-Earth3 and EC-Earth3-Veg).

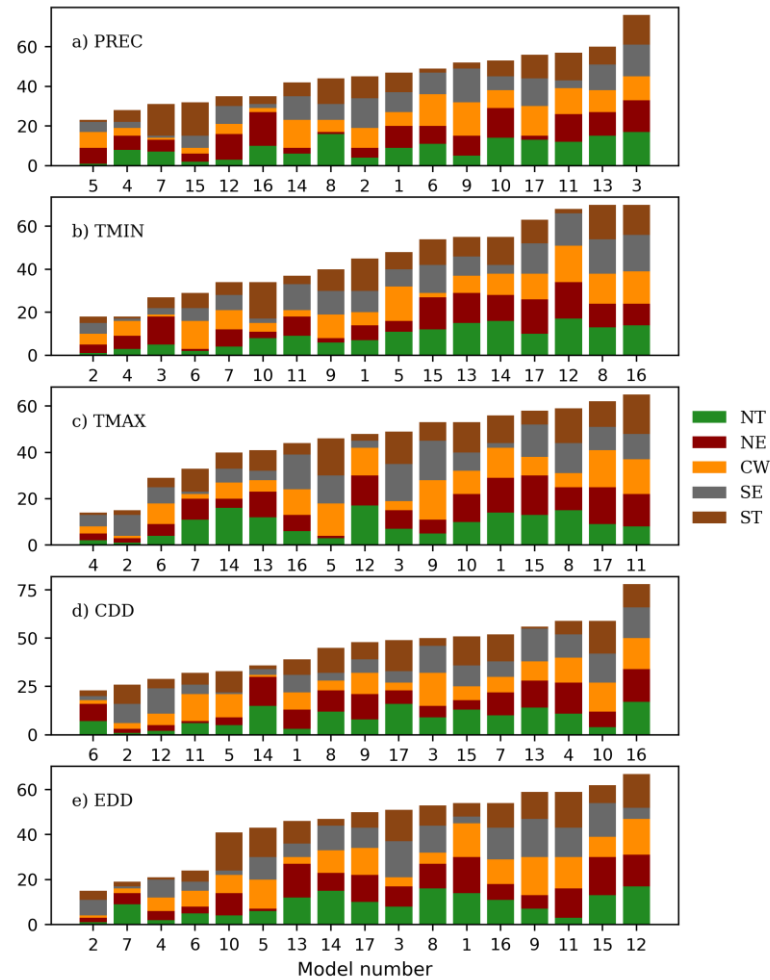


Figure 2.6 – Ranking of models' performance for a) PREC, b) TMIN, c) TMAX, d) CDD and e) EDD for NT, NE, CW, SE, and ST regions.

2.4 – Discussion

Our results demonstrate that all methods outperformed the original data in most models and that QM methods performed better than the LS method for almost all climate variables in Brazilian regions. LS worsened the performance of some models in NT when compared with the original data, for precipitation. Among QM methods, QUANT and RQUANT are the best performance bias-correction methods in virtually all models, regions, and variables. Correction of extreme climate indexes, such as CDD, was not as successful as for climate variables, although some models and regions corrected by LS showed a slightly better performance.

However, the performance increase of CDD after bias correction was minimal, because climate models do not represent this index well.

Despite a simple and widely adopted bias-correction method, LS showed inferior performance for all variables. This method aims to correct the bias of the mean and does not take into account variables' frequency distribution as in QM methods, which leads to inconsistencies in temporal variability (Themeßl *et al.*, 2011; Lafon *et al.*, 2013) and a poor representation of extreme climate indices that depend on daily values for calculation. Importantly, the LS method is the bias-correction method most commonly applied in many climate and hydrological impact studies in Brazil due to its simple implementation. Importantly, our results strongly indicate the need for a careful interpretation of the outcomes of studies that adopted Linear Scaling as their bias correction method, especially for precipitation, and suggest using more adequate methods in the future.

Among the QM methods, non-parametric methods performed better than parametric methods in almost all variables, regions, and models. The non-parametric methods are more flexible than those based on the parametric approach, mainly due to the absence of any predetermined functions, allowing good fits to any quantile-quantile relation (Gudmundsson *et al.*, 2012; Enayati *et al.*, 2021). The main differences in bias corrections between QM approaches were observed in precipitation (in all models) and CDD (in nearly all models). Other studies found the same behaviour for PREC in other countries (Gudmundsson *et al.*, 2012; Enayati *et al.*, 2021), with the QUANT and RQUANT methods standing out as better bias correction methods.

In climate models, more processes and parameters are involved in representing precipitation than for temperature, increasing the uncertainties in estimating these climate variables (Flato, 2011). Thus, precipitation is expected to show more biases than the minimum and maximum temperatures. Extreme climate indexes had a worse performance and greater error when compared with climate variables, especially CDD. The misrepresentation of CDD by CMIP6 models corroborates with the results of Medeiros *et al.*, (2022).

Dry spells are usually misrepresented in climate models due to a coarse resolution, which leads to the misrepresentation of topography and temporal variability (Maraun *et al.*, 2017). In addition, due to their low horizontal resolution, large-scale climate phenomena are better captured in models than regional and local climate phenomena. This results in the misrepresentation of extreme climate, which depend on climate phenomena that occur in a sub-

grid scale and are mostly parameterized in models (Flato, 2011; Iturbide *et al.*, 2022). Our results showed that most CMIP6 models overestimated the CDD index in most of the country territory, corroborating results found by Kim *et al.*, (2020) and Medeiros *et al.*,(2022). Statistical bias correction methods, such as those used in this study, slightly increased the performance of the CDD index of a few models in NT. However, major CDD improvements were not achieved because of the spatial resolution limit of the models (Maraun *et al.*, 2017).

Multiple models are recommended to reduce biases in climate prediction, (Flato, 2011; Ehret *et al.*, 2012). From the best bias correction method (QUANT), I could select the best models for each variable and Brazilian region (Figure 2.6), facilitating the ensemble construction. Although applying the bias correction method could introduce a degree of uncertainty (Laux *et al.*, 2021, Ehret *et al.*, 2012, Iturbide *et al.*, 2022), cautiously bias-corrected climate data models' ensemble improves the climate impact assessment. Bias correction is commonly used in hydrology and agricultural risk assessment, demonstrating to improve flow estimation and crop yield prediction (Ines and Hansen, 2006; Teutschbein and Seibert, 2012; Osuch *et al.*, 2017).

Considering that bias correction does not solve climate models' essential issues (Maraun *et al.*, 2017), but it could still improve water resources modeling and agricultural management (Laux *et al.*, 2021; Siqueira *et al.*, 2021), particularly when the best method is applied. Although the selection of the best bias correction during the current conditions does not guarantee a good performance under future changed conditions, it is more likely that this method will outperform other methods (that did not present good performance in the historical period) under future conditions (Teutschbein and Seibert, 2012).

Here I took the analyses further, comparing several bias correction methods for heterogeneous Brazilian regions and different models. This range of assessments creates a diverse and versatile model-choosing possibility that could increase climate representation in future studies.

2.5 – Conclusion

Climate models present some biases that could impact the future climate change adaptation assessment in studies in hydrology and agriculture. Therefore, there is a need to

correct existent bias to account for more realistic results. In this study, I assessed the performance of two bias correction methods: linear scaling and quantile mapping and the best models for climate and extreme variables in all Brazilian regions.

In general, all methods outperformed the raw model data. The non-parametric quantile mapping QUANT and RQUANT performed better for almost all variables and regions. The LS produced slightly better results for the CDD index, when compared with other methods, but the improvement of this index after bias correction was minimal. The models' performance varied according to the climate variable. However, the ACCESS-ESM1-5, EC-Earth3-Veg, CanESM5, EC-Earth3, and CMCC-ESM2 predominated among the best models for the variables studied here.

It was clear that CMIP6 models poorly represented relevant climate variables for Brazil. For future planning in the strategic sectors, the use of these models can be improved using our methods that brought the first detailed assessment of bias correction methods for the country, facilitating the choice of the best technique and models for each variable and Brazilian region to create an ensemble enhancing projection reliability. This approach can be particularly useful for climate studies, crop climate impact assessment, evaluation of extreme indices, and energy security.

2.6 - Supplementary material

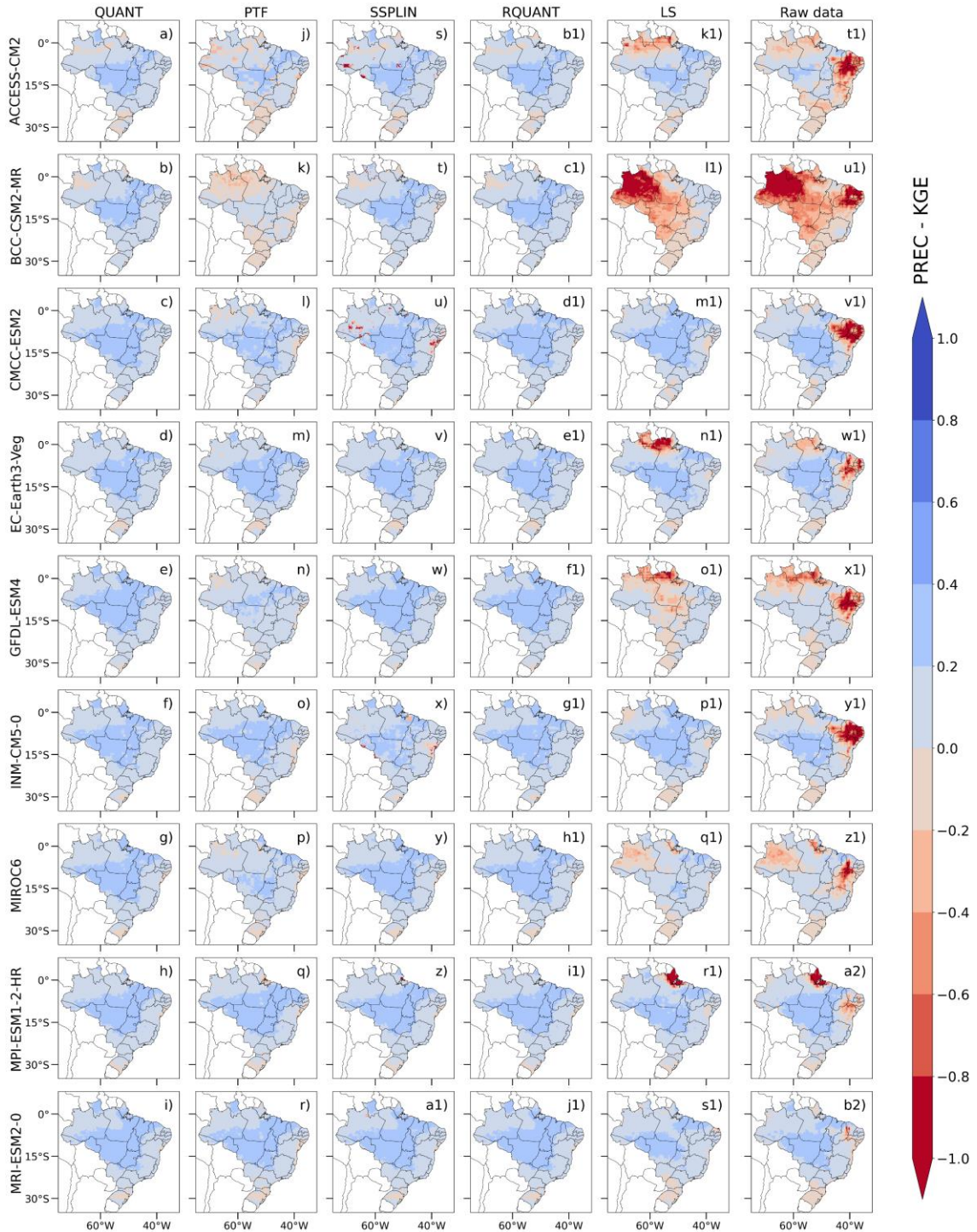


Figure S2.1 – KGE of precipitation for each bias correction method, raw model data, and ACCESS-CM2, BCC-ESM2-MR, CMCC-ESM2, EC-Earth3-Veg, GFDL-ESM4, INM-CM5-0, MIROC6, MPI-ESM1-2-HR, MRI-ESM2-0 models.

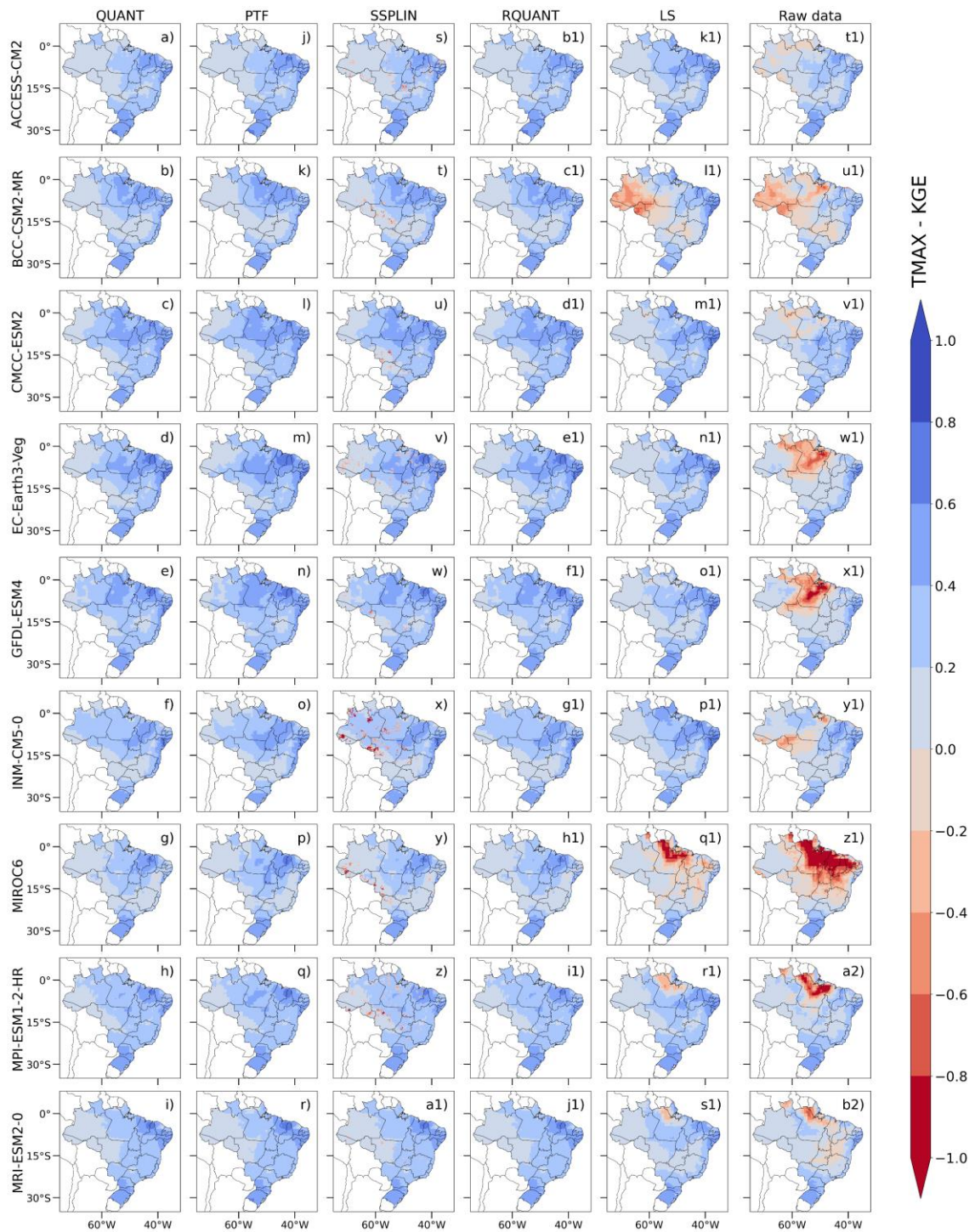


Figure S2.3 – KGE of maximum temperature for each bias correction method, raw model data, and ACCESS-CM2, BCC-ESM2-MR, CMCC-ESM2, EC-Earth3-Veg, GFDL-ESM4, INM-CM5-0, MIROC6, MPI-ESM1-2-HR, MRI-ESM2-0 models.

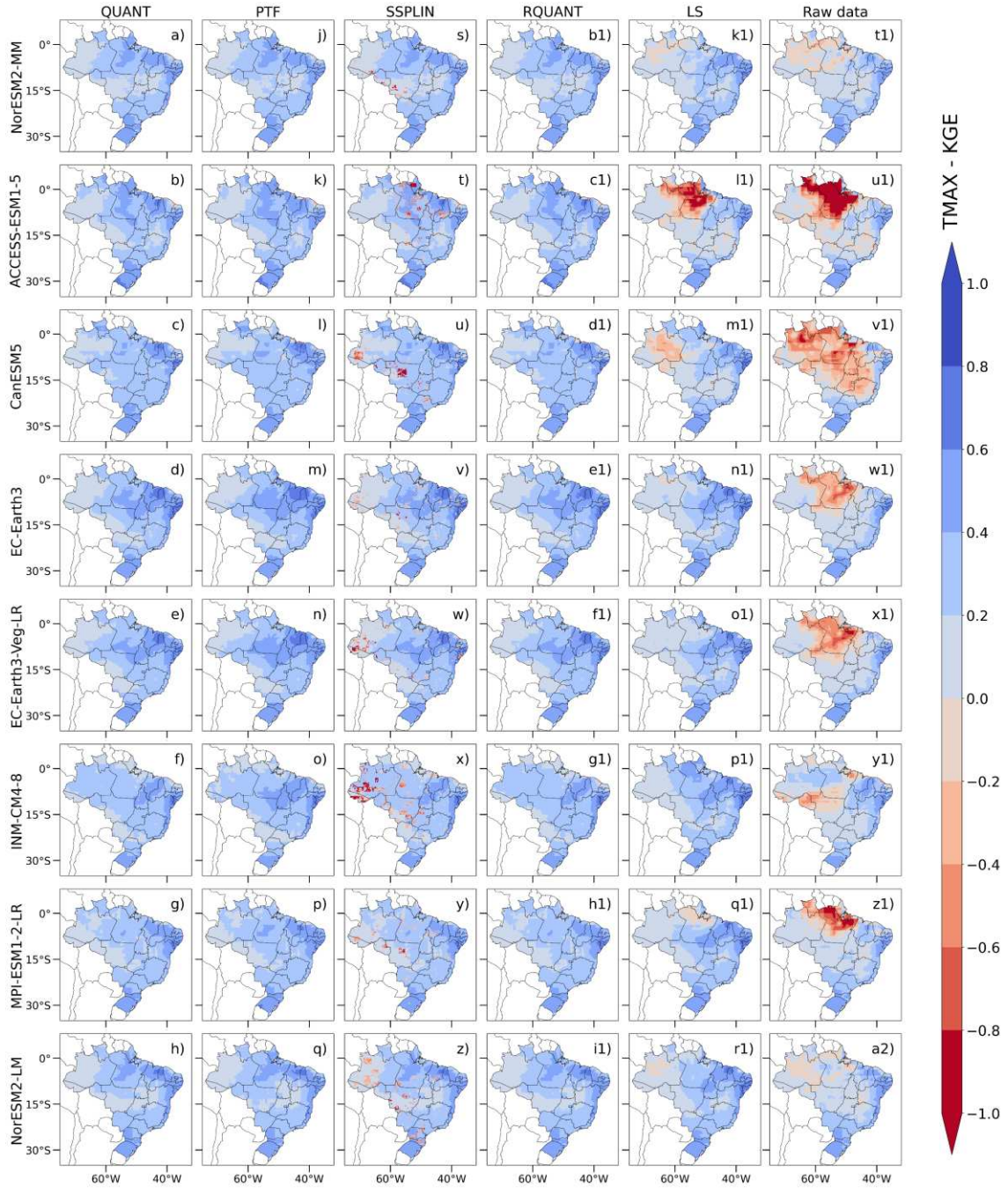


Figure S2.4 – KGE of maximum temperature for each bias correction method, raw model data, and NorESM2-MM, ACCESS-ESM1-5, CanESM5, EC-Earth3, EC-Earth3-Veg-LR, INM-CM4-8, MPI-ESM1-2-LR and NorESM2-LM models.

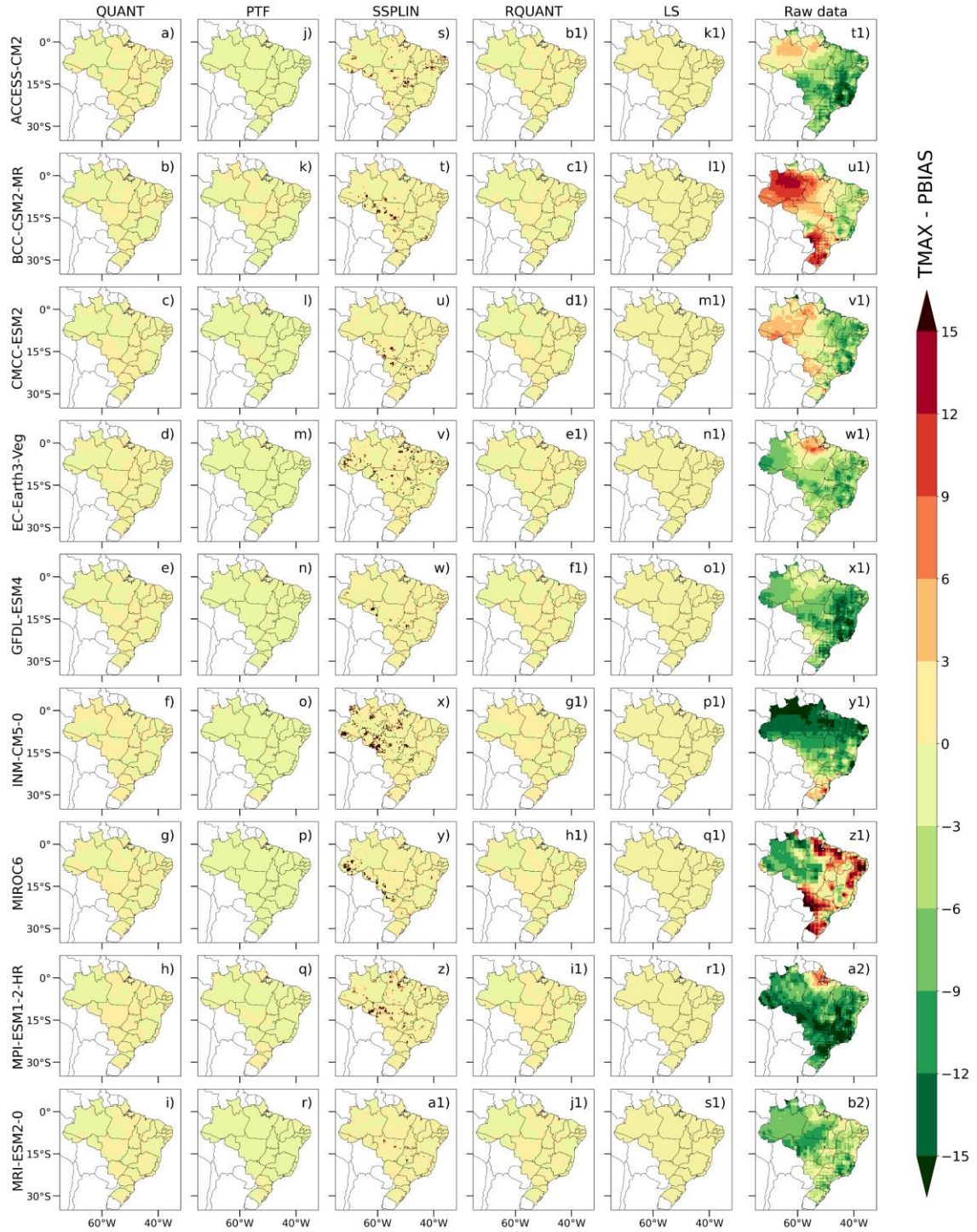


Figure S2.5 – Percentual bias (PBIAS) of maximum temperature for each bias correction method, raw model data, and ACCESS-CM2, BCC-ESM2-MR, CMCC-ESM2, EC-Earth3-Veg, GFDL-ESM4, INM-CM5-0, MIROC6, MPI-ESM1-2-HR, MRI-ESM2-0 models.

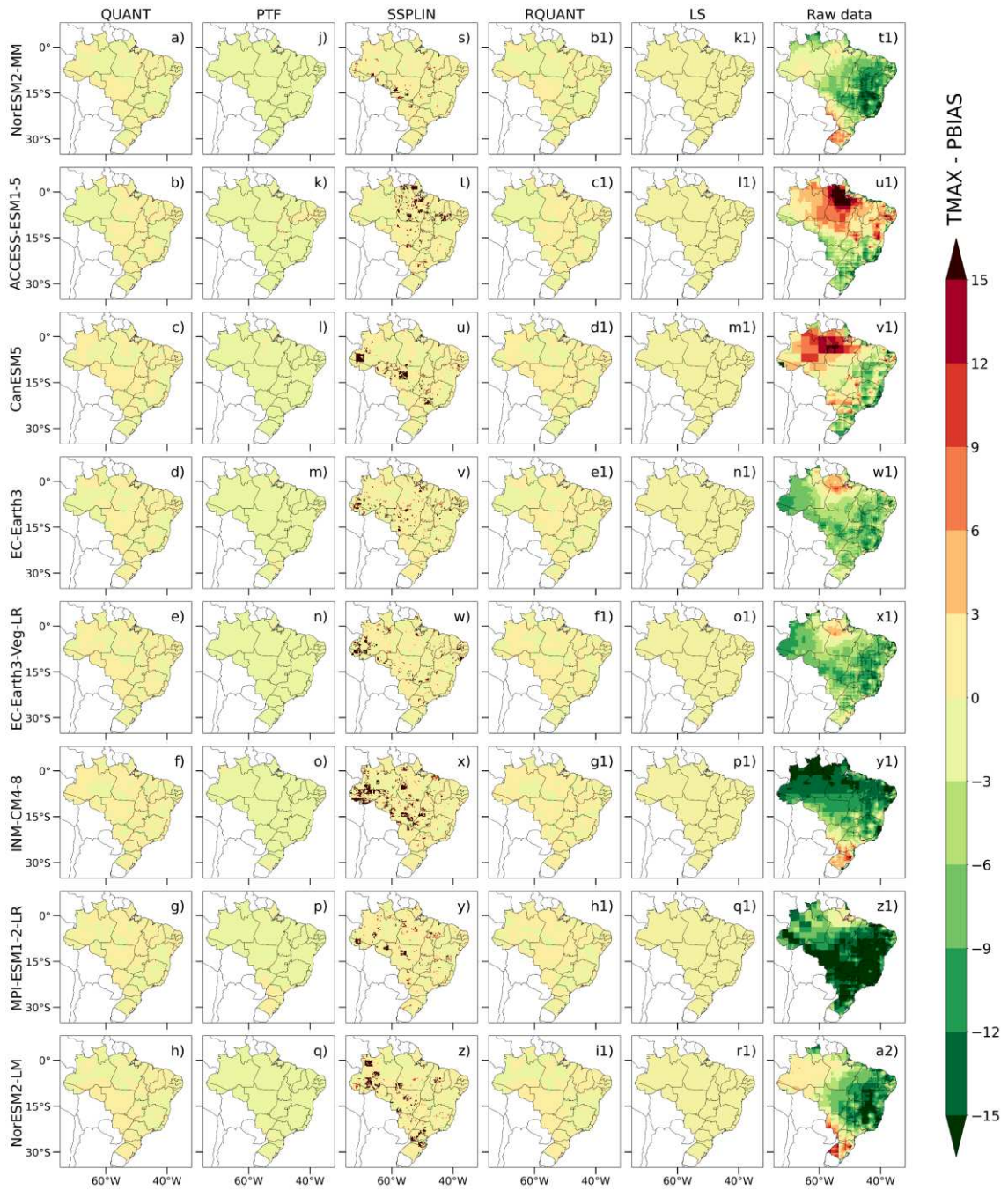


Figure S2.6 – Percentual bias (PBIAS) of maximum temperature for each bias correction method, raw model data, and NorESM2-MM, ACCESS-ESM1-5, CanESM5, EC-Earth3, EC-Earth3-Veg-LR, INM-CM4-8, MPI-ESM1-2-LR and NorESM2-LM models.

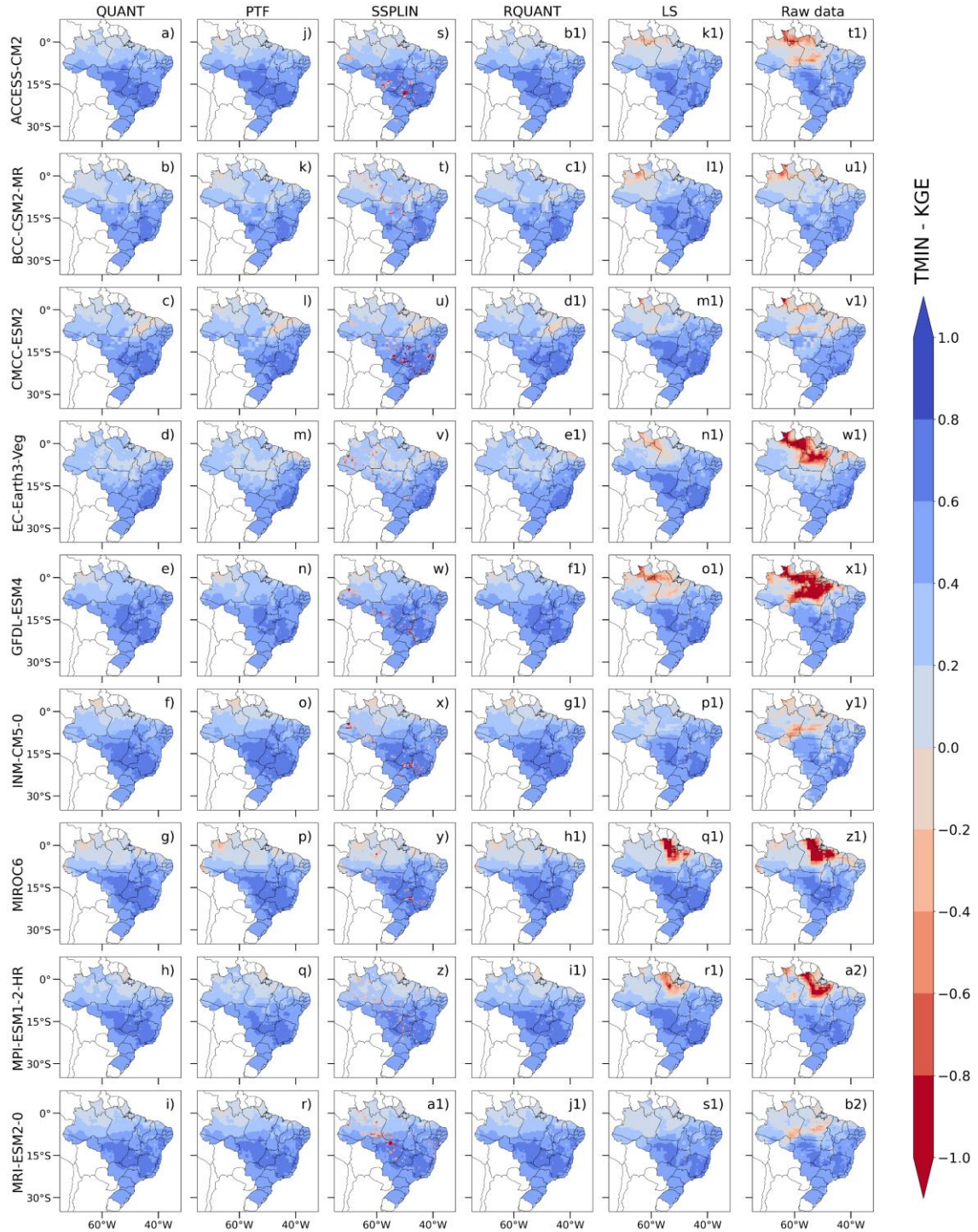


Figure S2.7 – KGE of minimum temperature for each bias correction method, raw model data, and ACCESS-CM2, BCC-ESM2-MR, CMCC-ESM2, EC-Earth3-Veg, GFDL-ESM4, INM-CM5-0, MIROC6, MPI-ESM1-2-HR, MRI-ESM2-0 models.

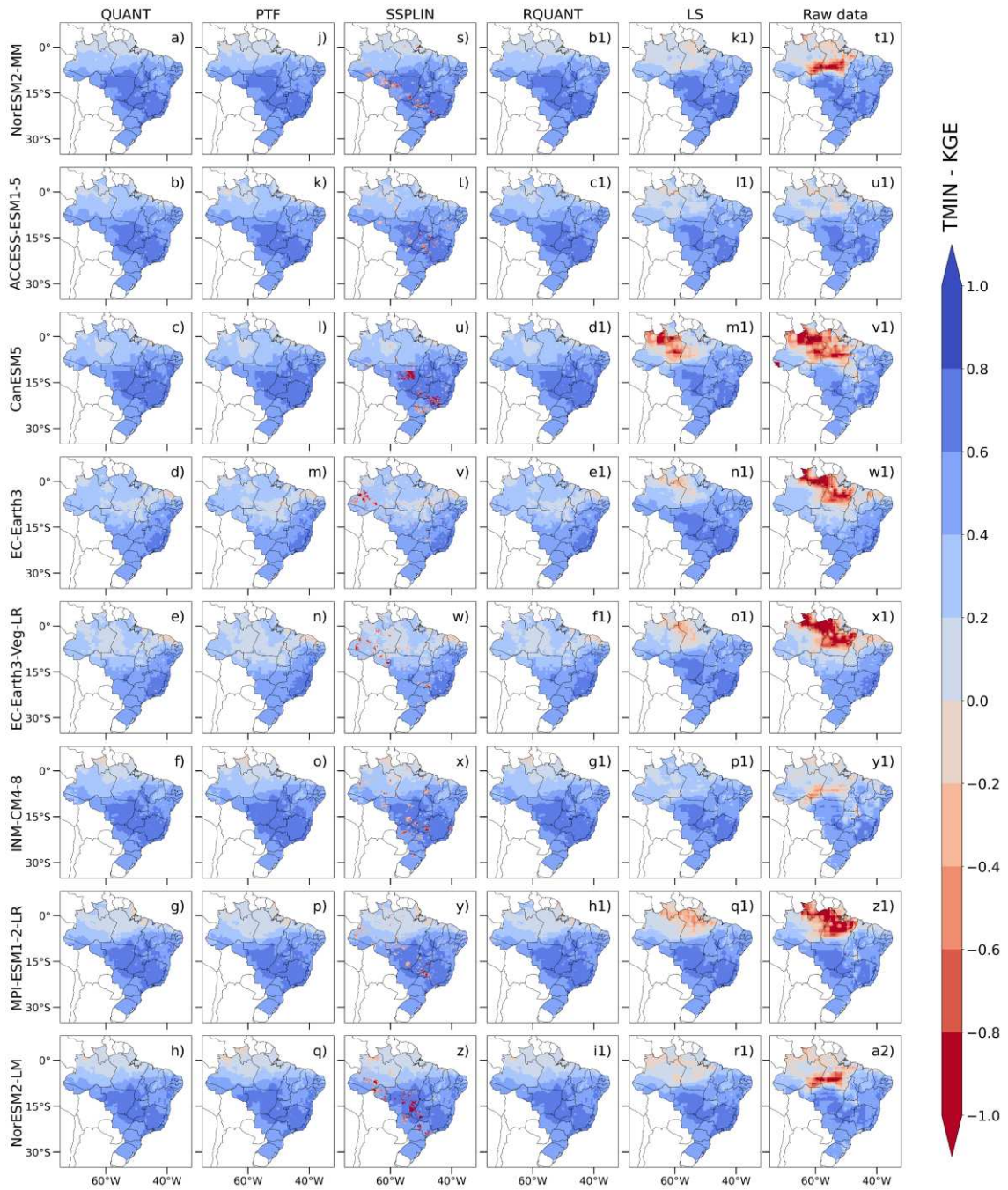


Figure S2.8 – KGE of minimum temperature for each bias correction method, raw model data, and NorESM2-MM, ACCESS-ESM1-5, CanESM5, EC-Earth3, EC-Earth3-Veg-LR, INM-CM4-8, MPI-ESM1-2-LR and NorESM2-LM models.

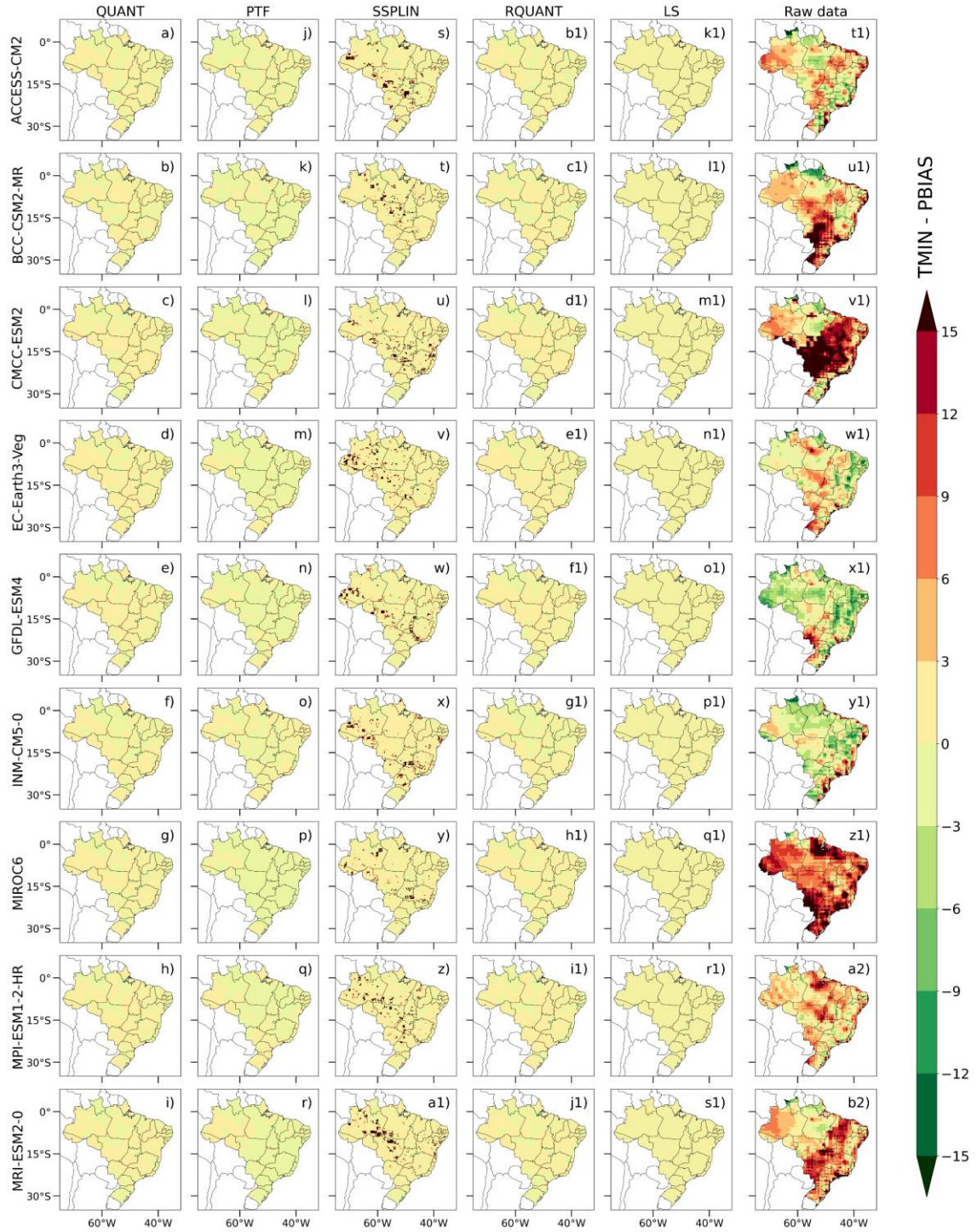


Figure S2.9 – Percentual bias (PBIAS) of minimum temperature for each bias correction method, raw model data, and ACCESS-CM2, BCC-ESM2-MR, CMCC-ESM2, EC-Earth3-Veg, GFDL-ESM4, INM-CM5-0, MIROC6, MPI-ESM1-2-HR, MRI-ESM2-0 models.

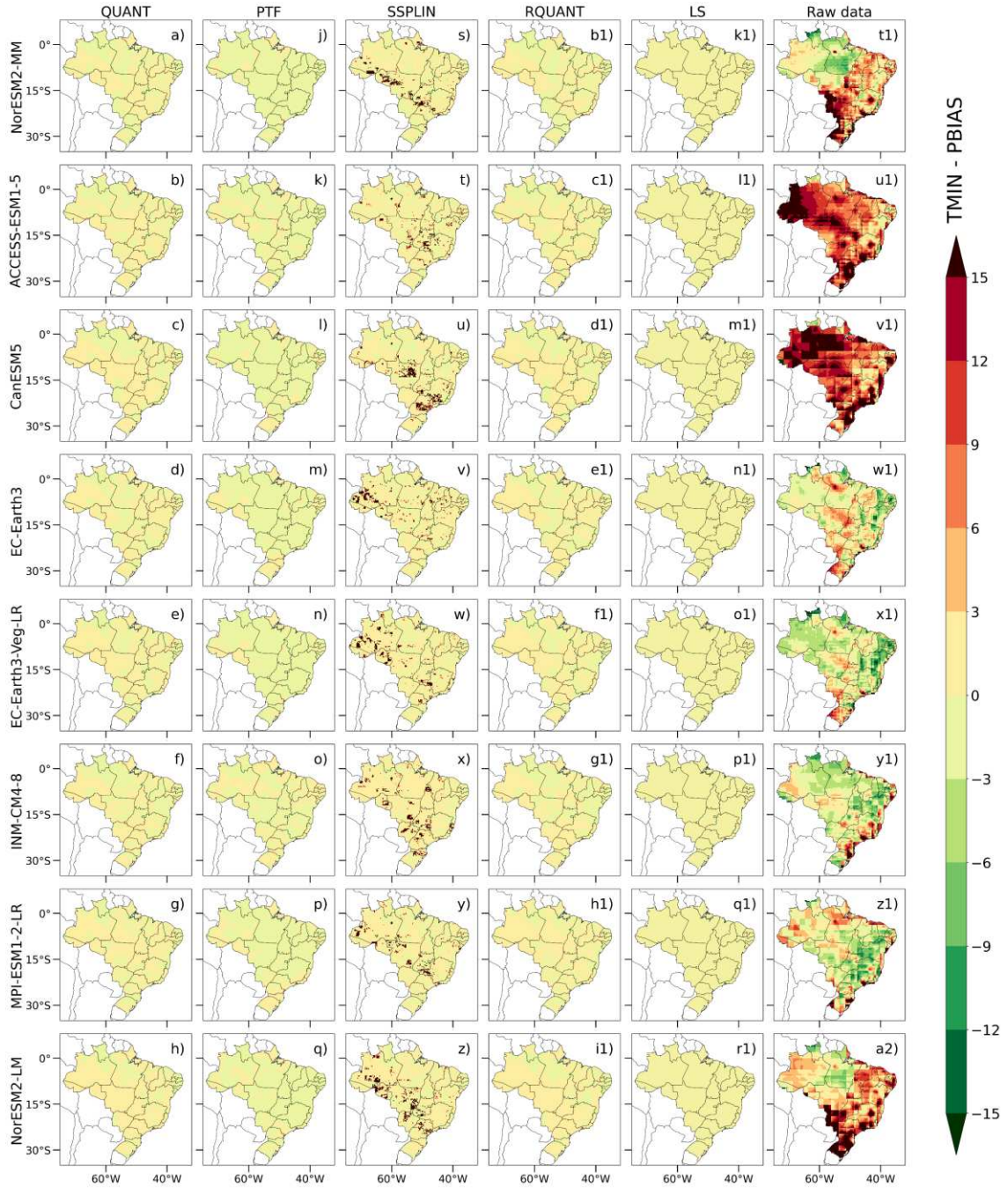


Figure S2.10 – Percentual bias (PBIAS) of minimum temperature for each bias correction method, raw model data, and NorESM2-MM, ACCESS-ESM1-5, CanESM5, EC-Earth3, EC-Earth3-Veg-LR, INM-CM4-8, MPI-ESM1-2-LR and NorESM2-LM models.

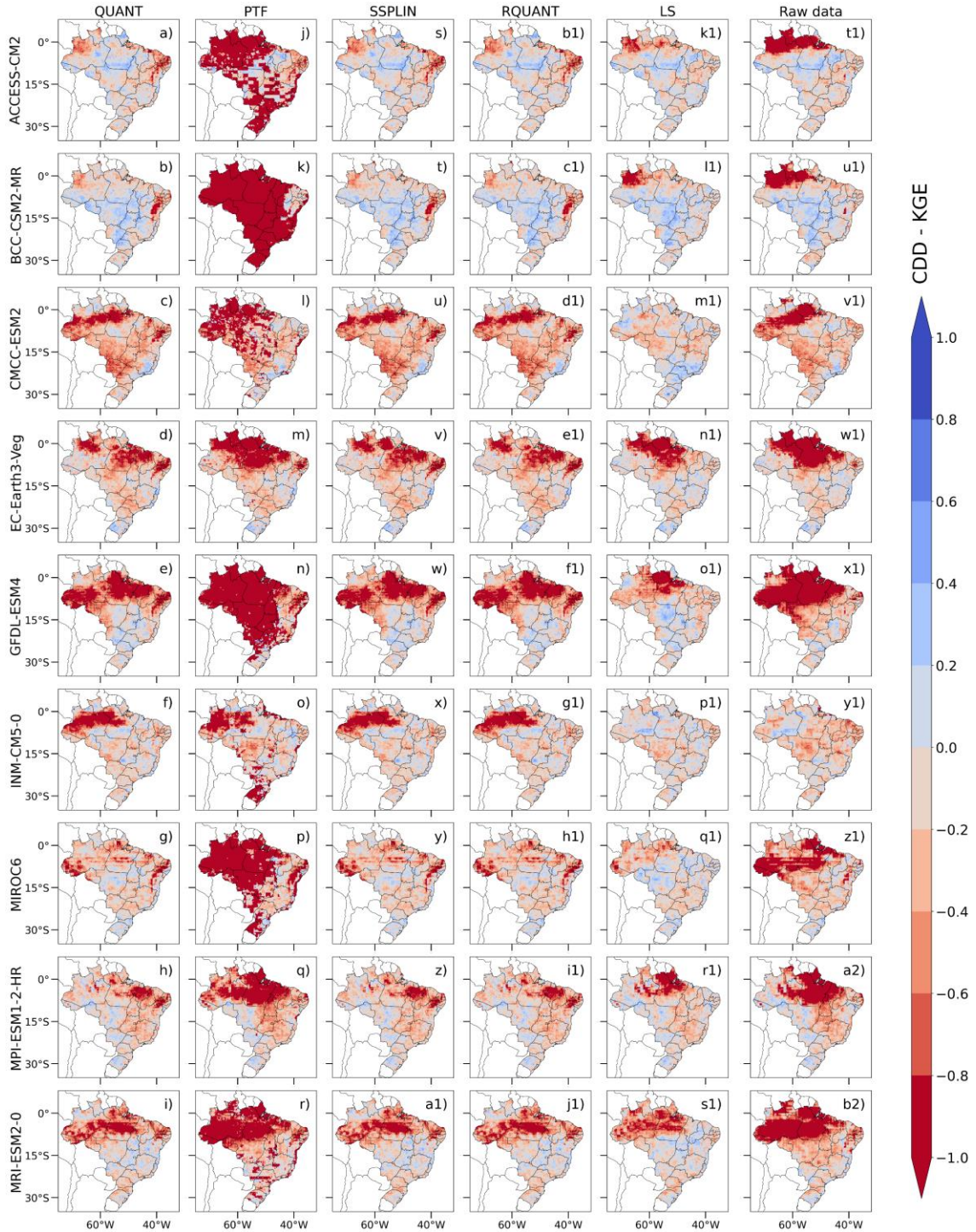


Figure S2.11 – KGE of CDD for each bias correction method, raw model data, and ACCESS-CM2, BCC-ESM2-MR, CMCC-ESM2, EC-Earth3-Veg, GFDL-ESM4, INM-CM5-0, MIROC6, MPI-ESM1-2-HR, MRI-ESM2-0 models.

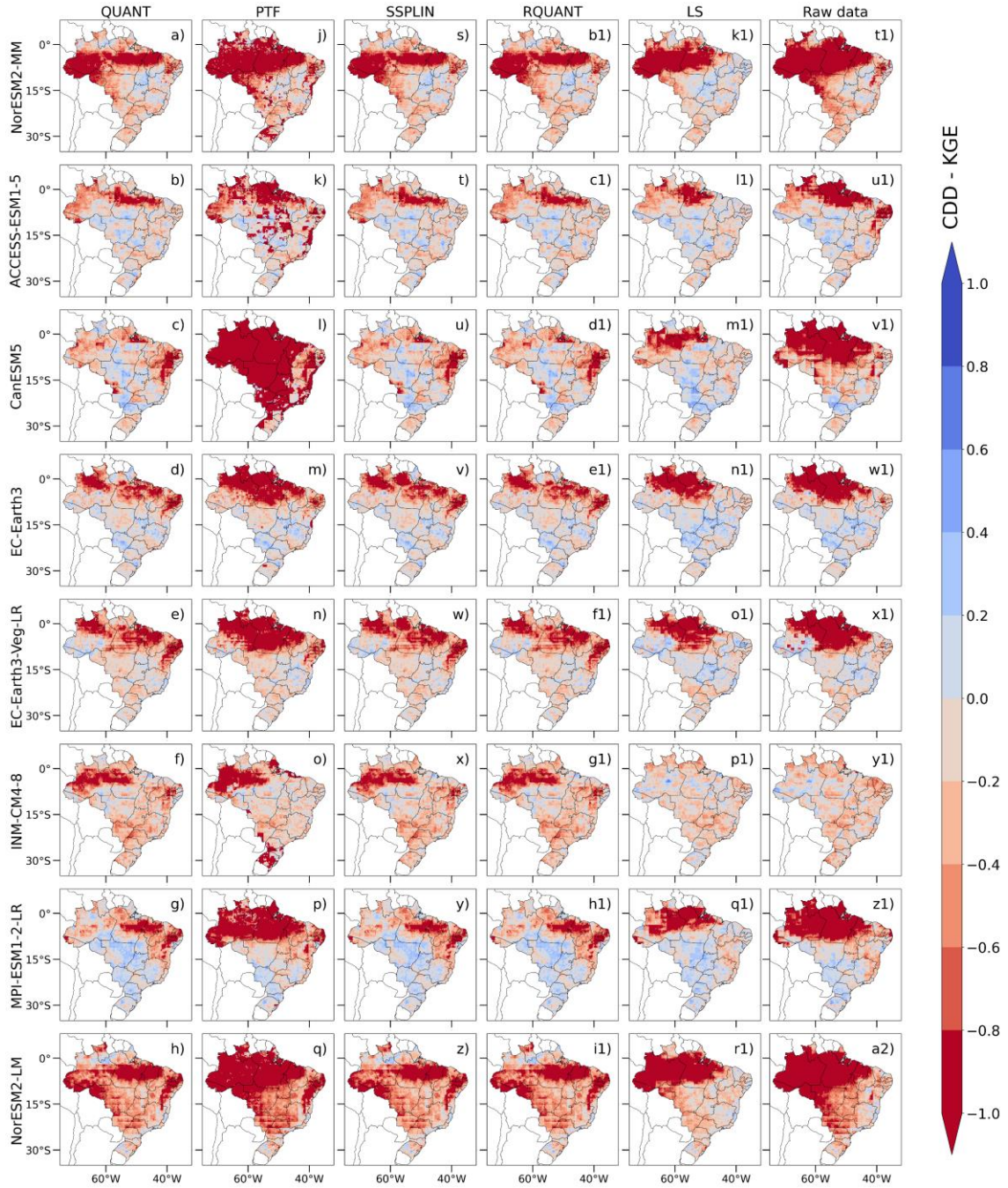


Figure S2.12 – KGE of CDD for each bias correction method, raw model data, and NorESM2-MM, ACCESS-ESM1-5, CanESM5, EC-Earth3, EC-Earth3-Veg-LR, INM-CM4-8, MPI-ESM1-2-LR and NorESM2-LM models.

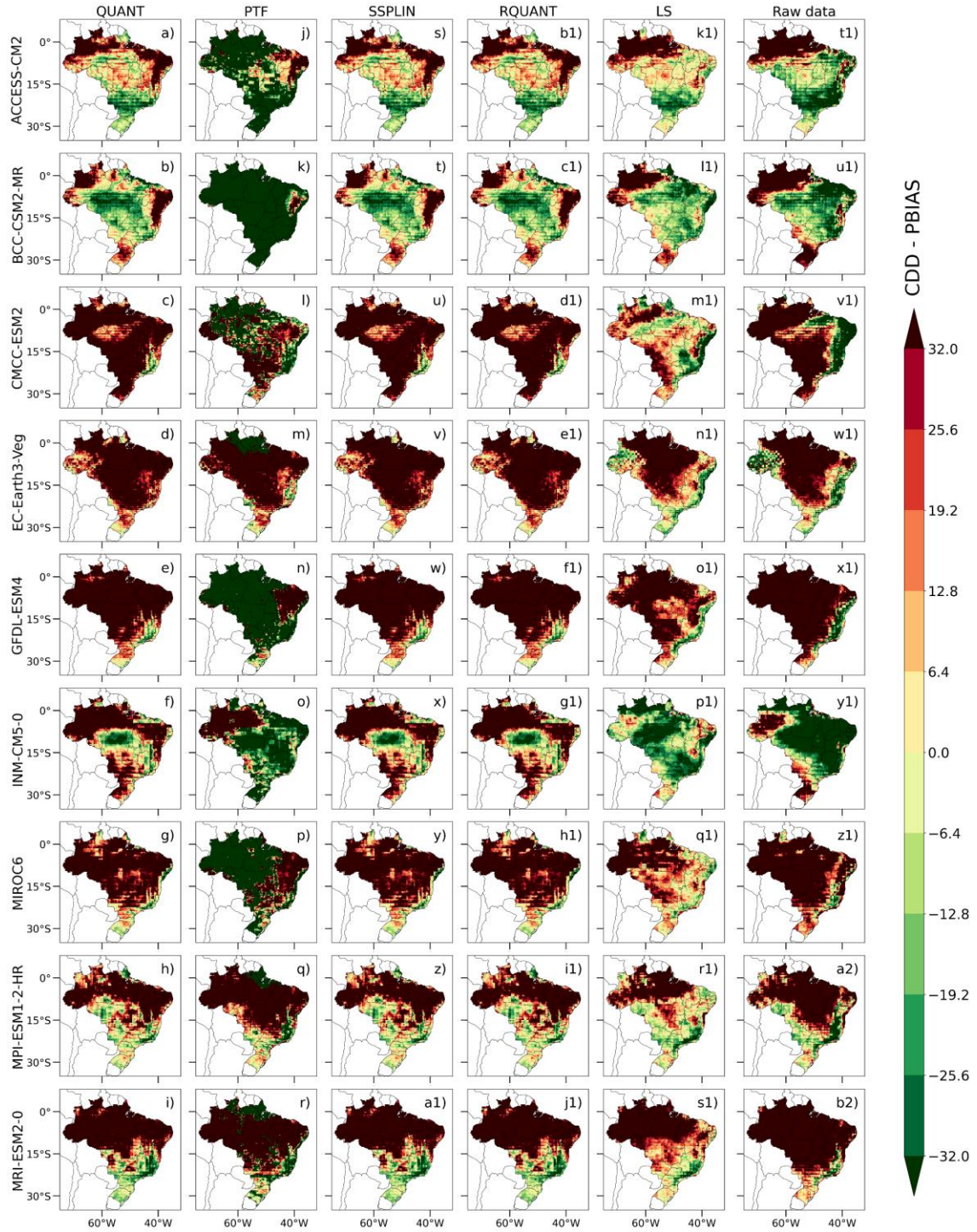


Figure S2.13 – Percentual bias (Pbias) of CDD for each bias correction method, raw model data, and ACCESS-CM2, BCC-ESM2-MR, CMCC-ESM2, EC-Earth3-Veg, GFDL-ESM4, INM-CM5-0, MIROC6, MPI-ESM1-2-HR, MRI-ESM2-0 models.

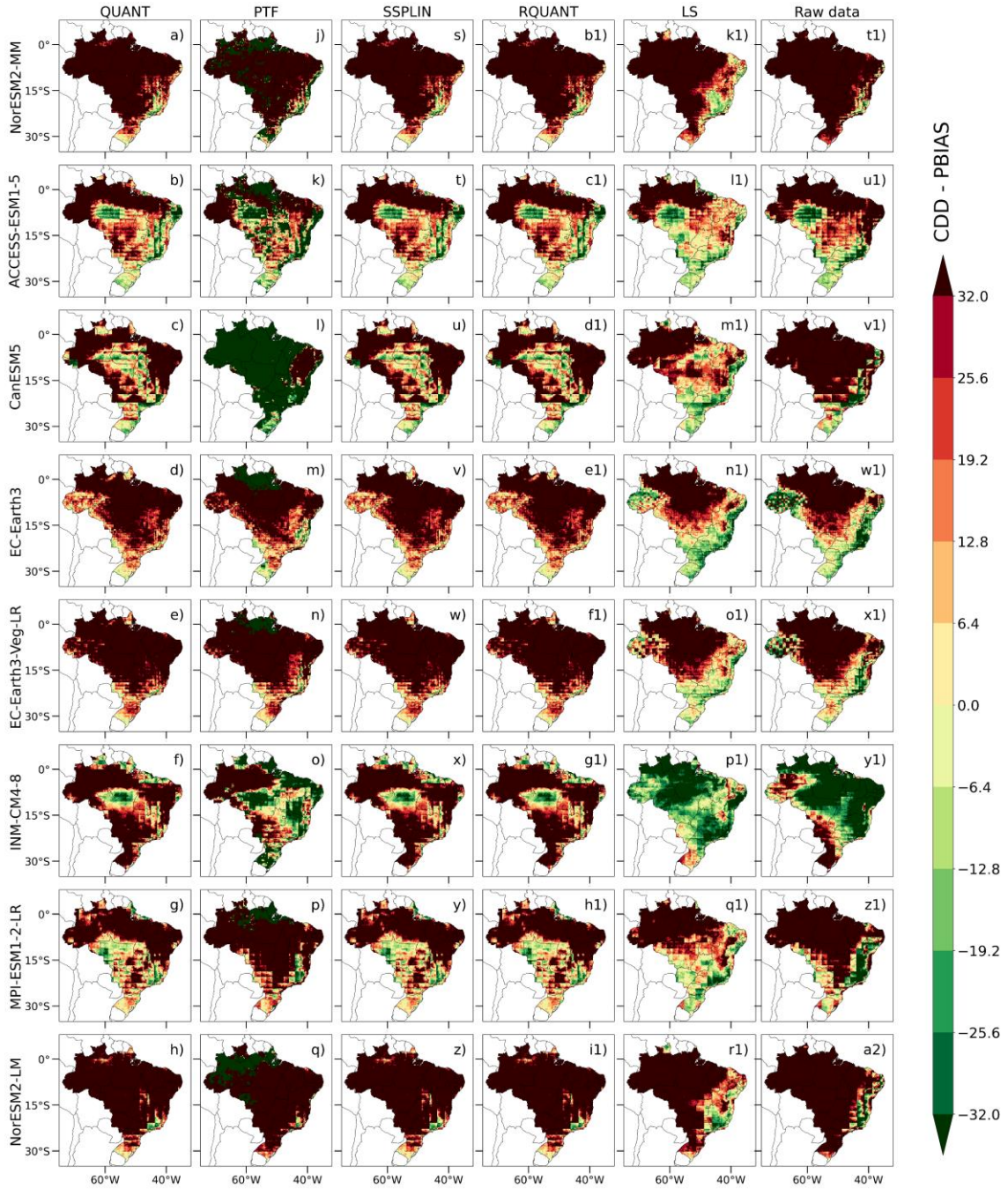


Figure S2.14 – Percentual bias (Pbias) of CDD for each bias correction method, raw model data, and NorESM2-MM, ACCESS-ESM1-5, CanESM5, EC-Earth3, EC-Earth3-Veg-LR, INM-CM4-8, MPI-ESM1-2-LR and NorESM2-LM models.

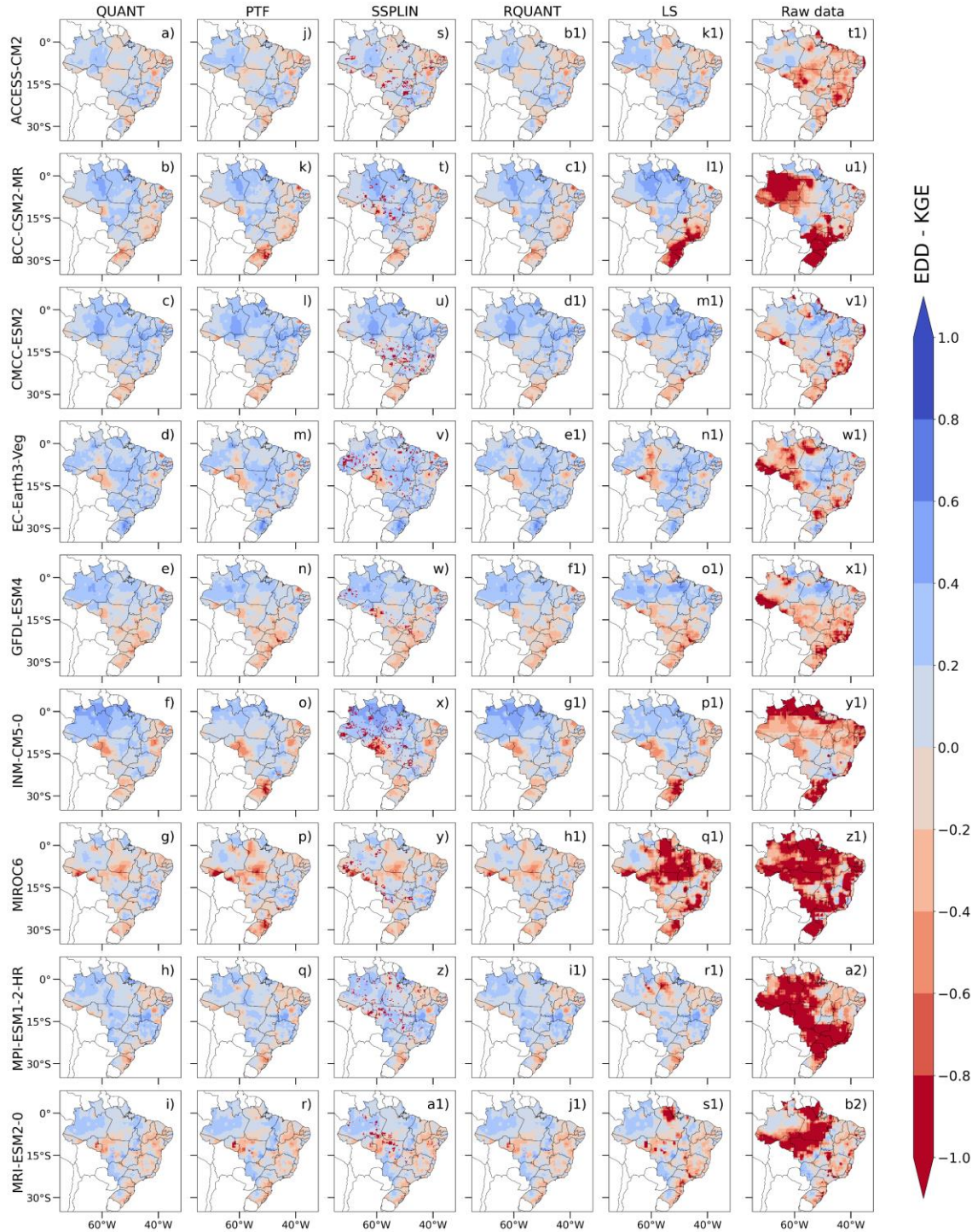


Figure S2.15 – KGE of EDD for each bias correction method, raw model data, and ACCESS-CM2, BCC-ESM2-MR, CMCC-ESM2, EC-Earth3-Veg, GFDL-ESM4, INM-CM5-0, MIROC6, MPI-ESM1-2-HR, MRI-ESM2-0 models.

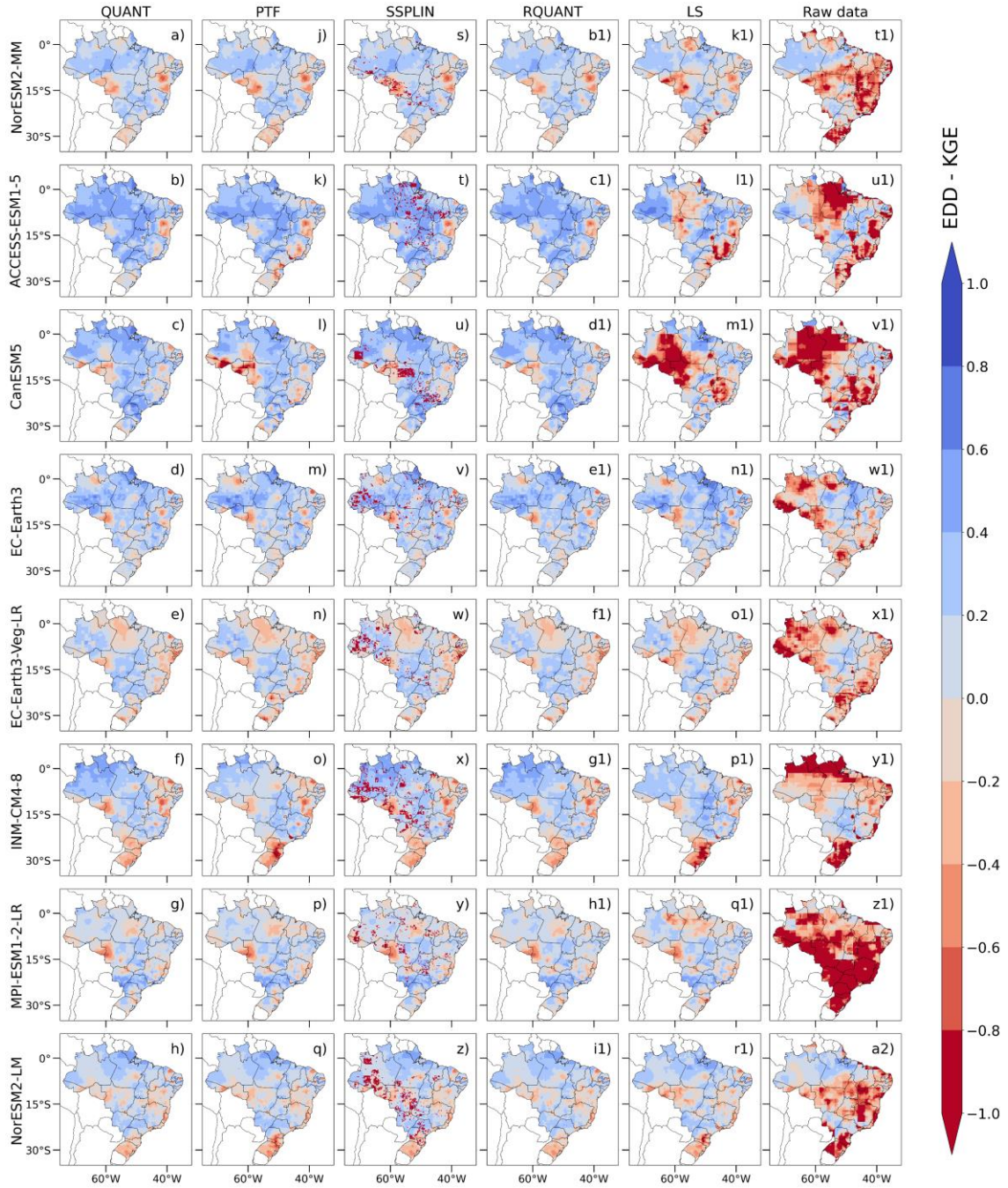


Figure S2.16 – KGE of EDD for each bias correction method, raw model data, and NorESM2-MM, ACCESS-ESM1-5, CanESM5, EC-Earth3, EC-Earth3-Veg-LR, INM-CM4-8, MPI-ESM1-2-LR and NorESM2-LM models.

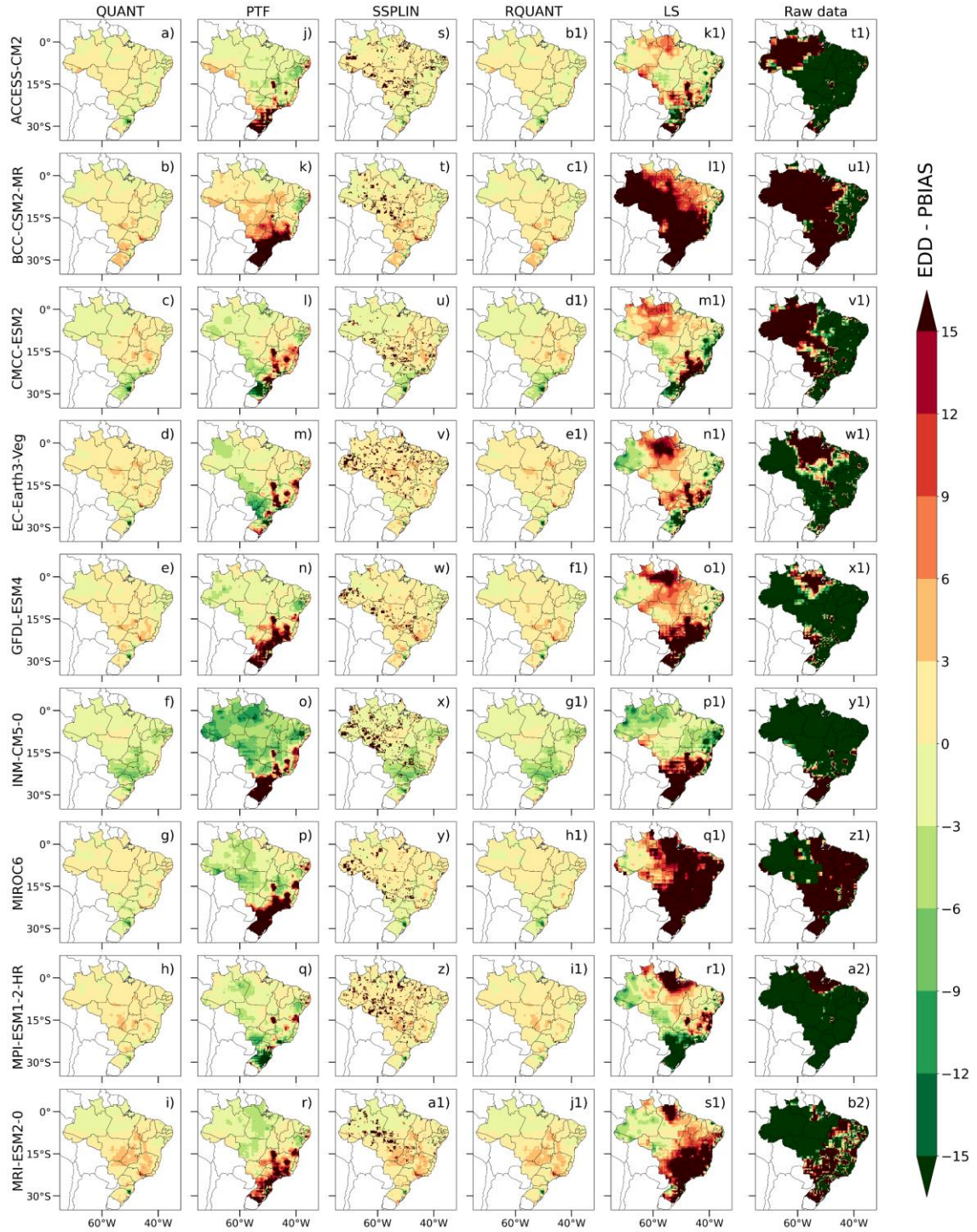


Figure S2.17 – Percentual bias (Pbias) of EDD for each bias correction method, raw model data, and ACCESS-CM2, BCC-ESM2-MR, CMCC-ESM2, EC-Earth3-Veg, GFDL-ESM4, INM-CM5-0, MIROC6, MPI-ESM1-2-HR, MRI-ESM2-0 models.

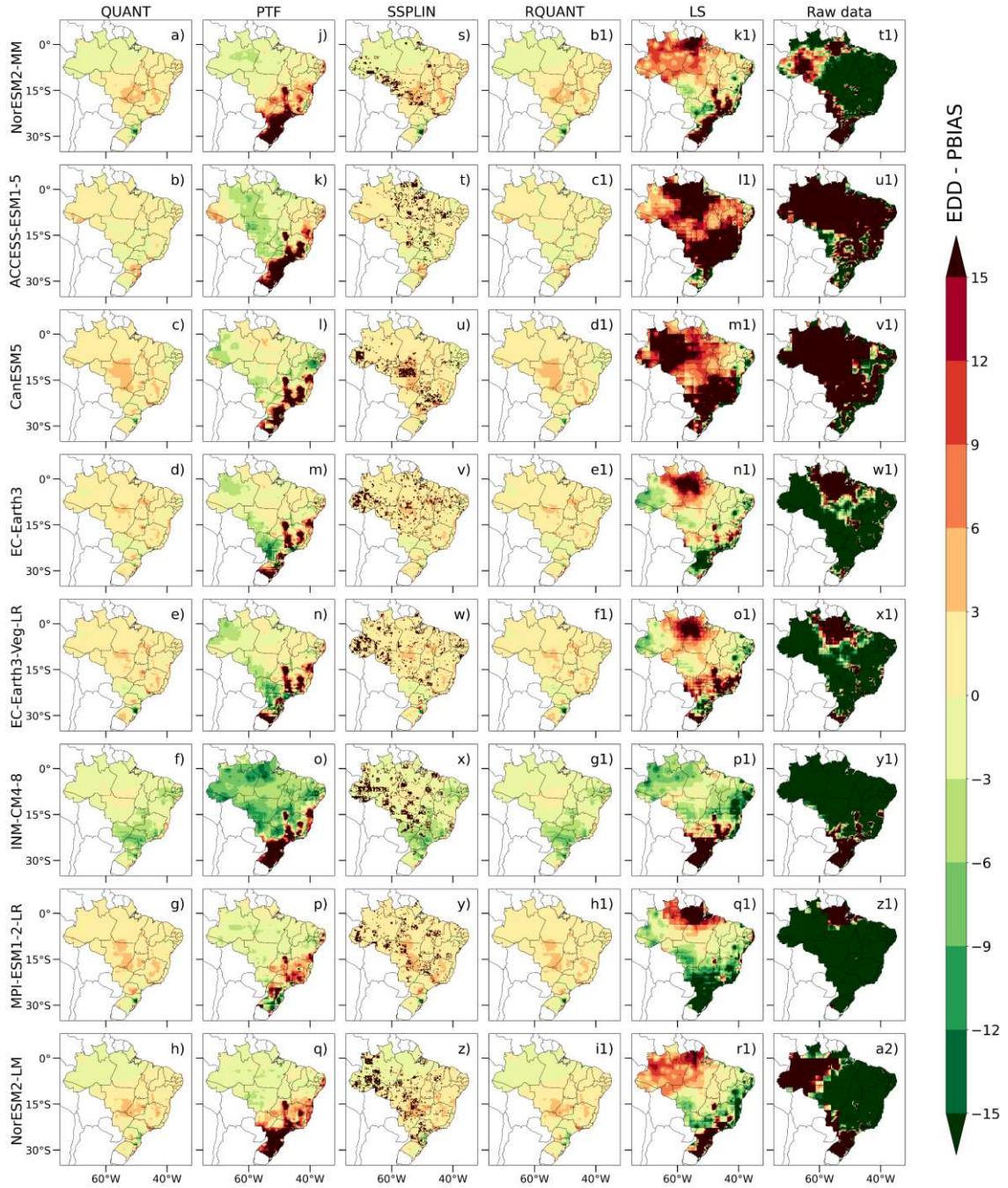


Figure S2.18 – Percentual bias (Pbias) of EDD for each bias correction method, raw model data, and NorESM2-MM, ACCESS-ESM1-5, CanESM5, EC-Earth3, EC-Earth3-Veg-LR, INM-CM4-8, MPI-ESM1-2-LR and NorESM2-LM models.

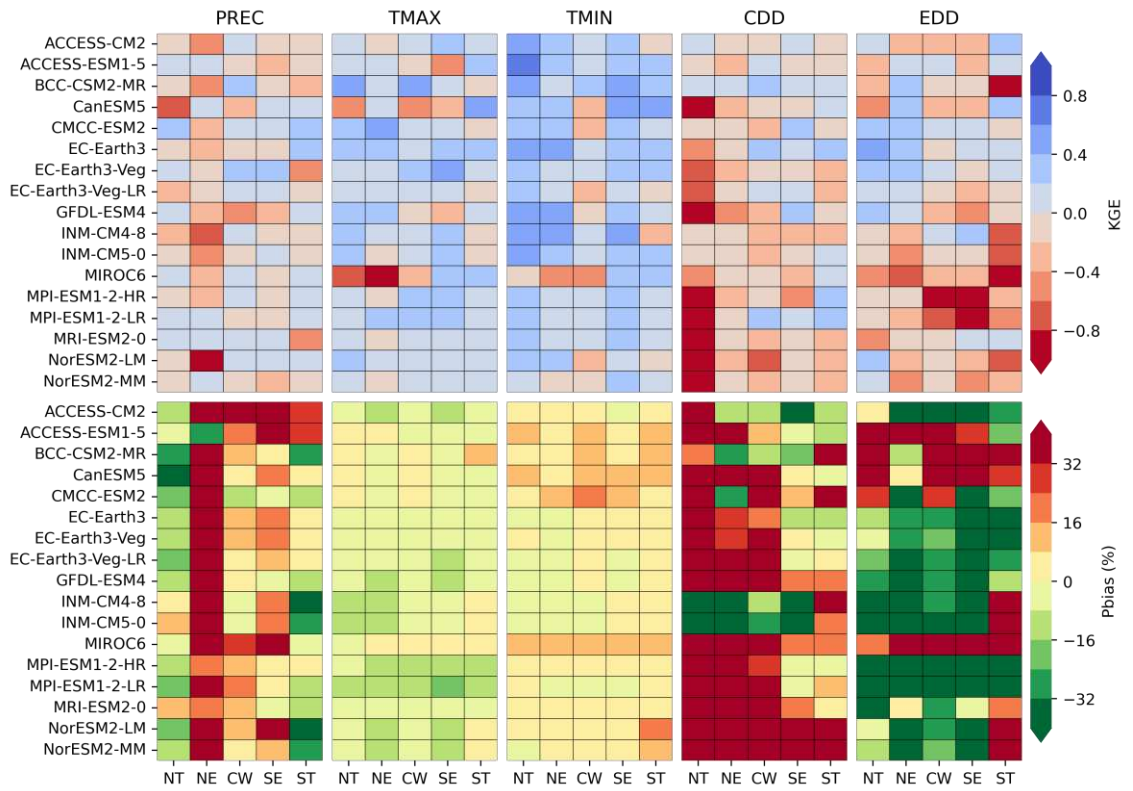


Figure S2.19 – KGE and PBIAS result for each variable (PREC, TMAX, TMIN, CDD and EDD), model and Brazilian region without bias correction.

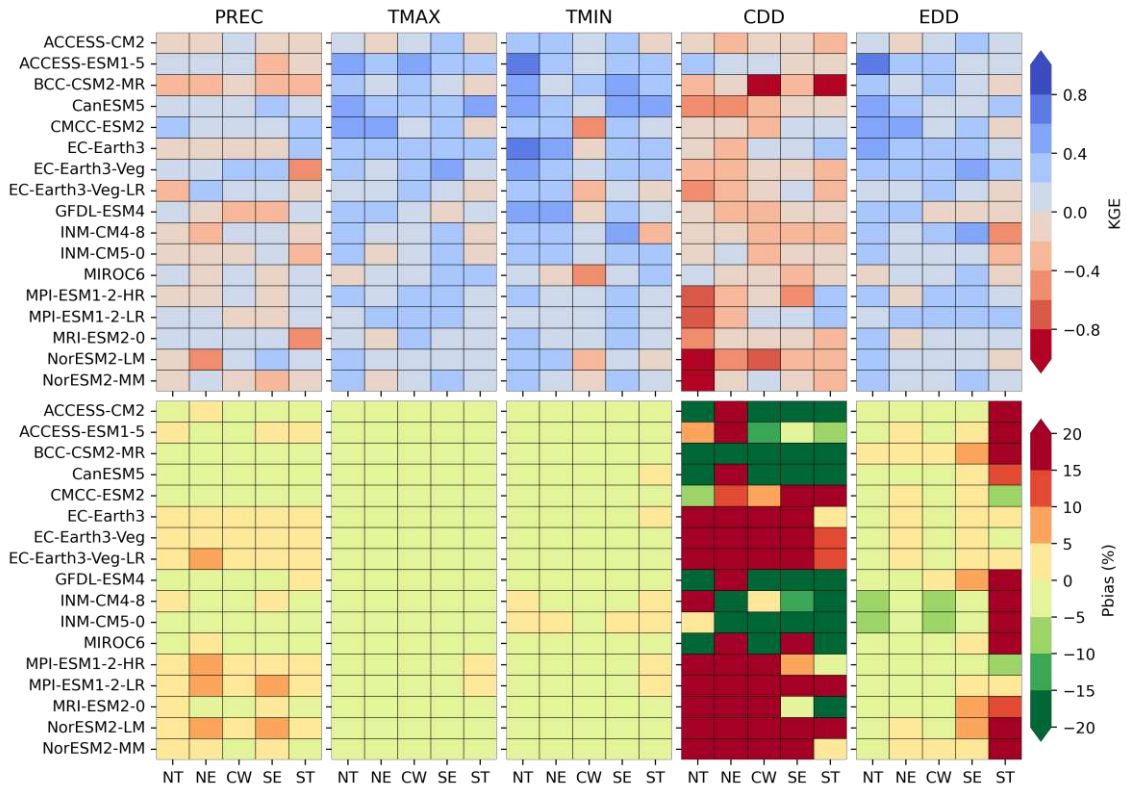


Figure S2.20 – KGE and PBIAS result for each variable (PREC, TMAX, TMIN, CDD and EDD), model and Brazilian region for PTF method.

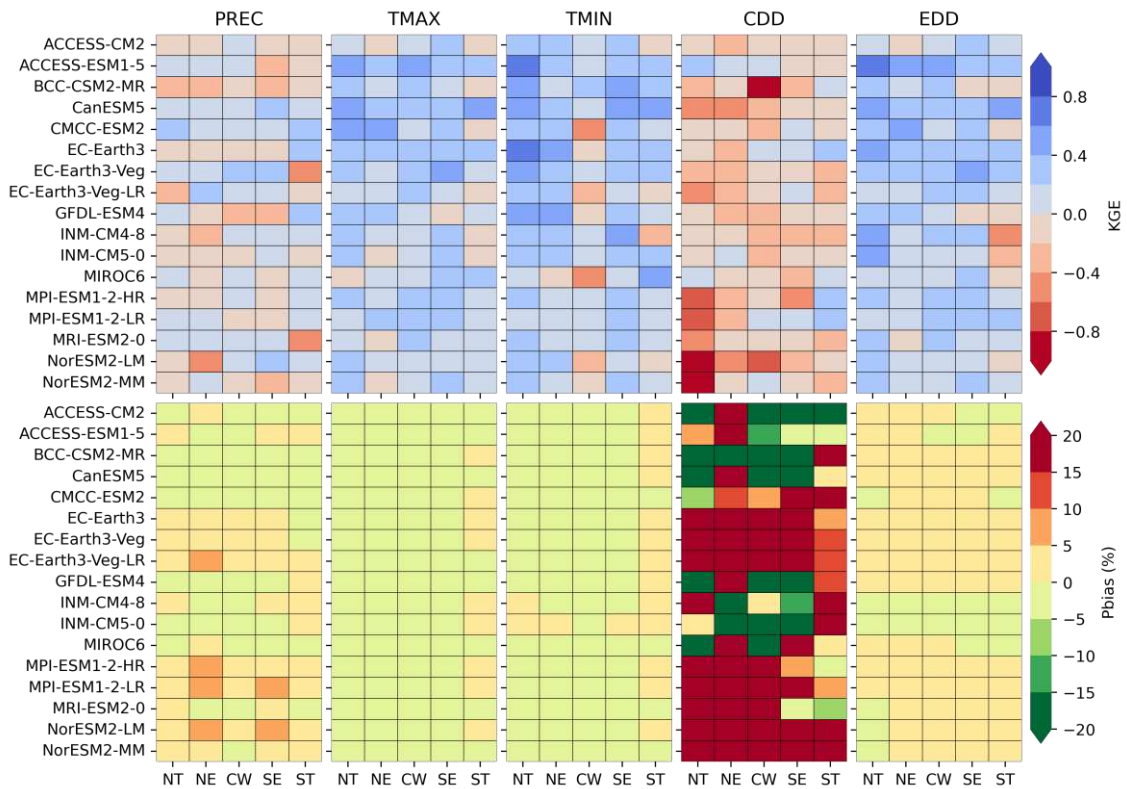


Figure S2.21 – KGE and Pbias result for each variable (PREC, TMAX, TMIN, CDD and EDD), model and Brazilian region for RQUANT method.

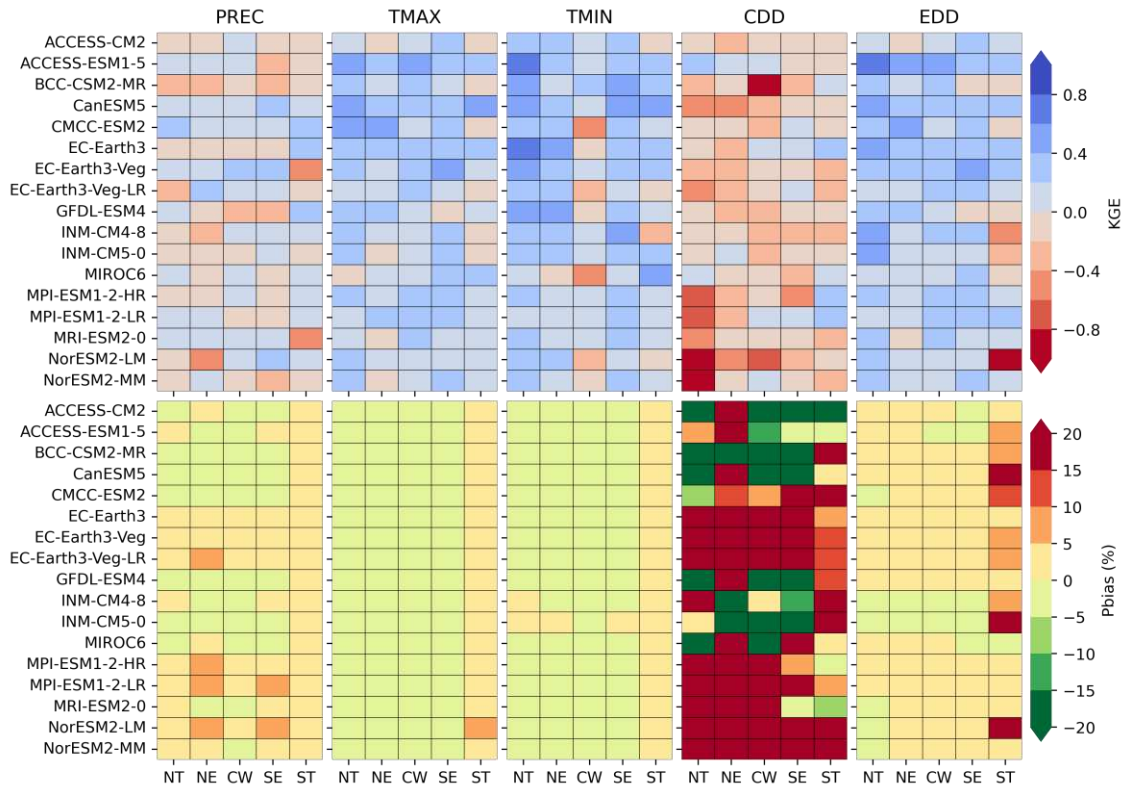


Figure S2.22 – KGE and Pbias result for each variable (PREC, TMAX, TMIN, CDD and EDD), model and Brazilian region for SSPLIN method.

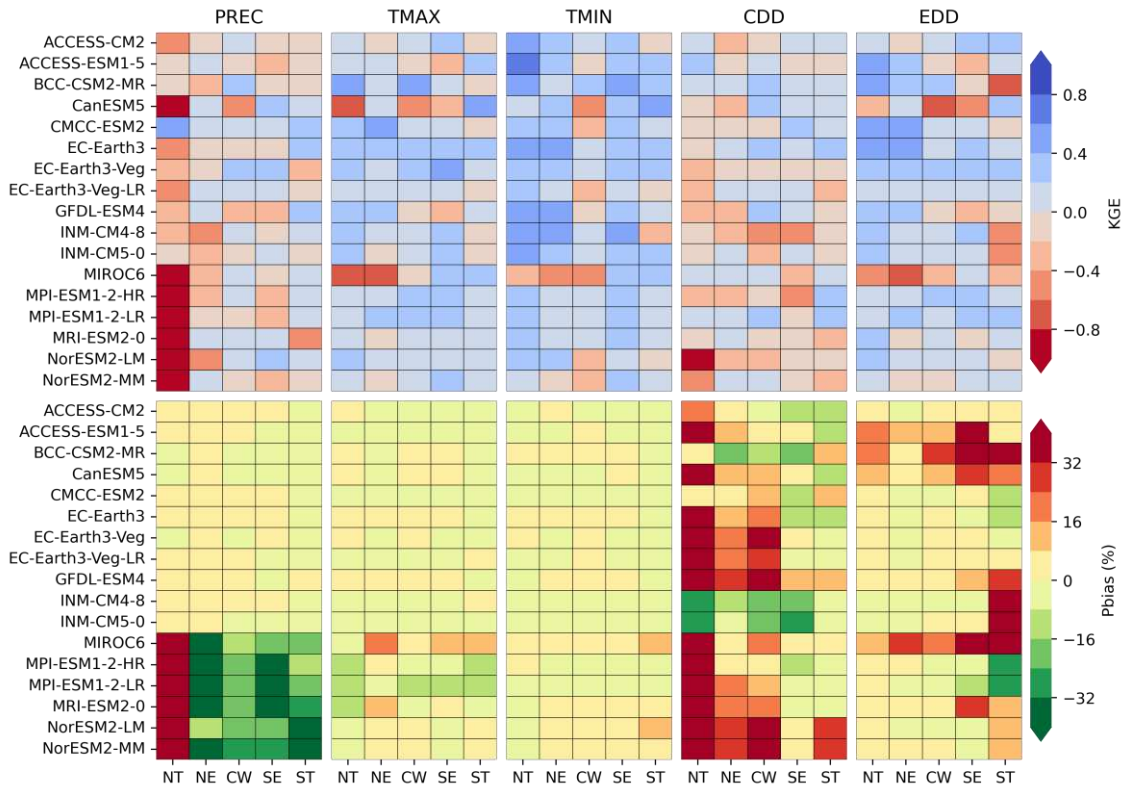


Figure S2.23 – KGE and Pbias result for each variable (PREC, TMAX, TMIN, CDD and EDD), model and Brazilian region for LS method.

Chapter 3: Future alternative pathways to Brazilian agriculture under climate change scenarios: contrasting semiarid family farmers and Mato Grosso and MATOPIBA commodity farmers.

Abstract

Climate change is directly related to extreme climate's increased frequency and intensity. These alterations can cause yield losses and impact the agricultural supply chain if no adaptation occurs. In this study, I aimed to assess how extreme climate indexes could change in this century and estimate their impacts on the main crops of semiarid family farming and central Brazil large-scale commodity agriculture. I calculated the significance of climate extreme trends and their magnitudes during crop growing season using Mann-Kendall and Theil-Sen tests for four climate scenarios of IPCC/CMIP6 (SSP1-2.6, SSP2-4.5, SSP3-7.0, and SSP5-8.5) and four bias corrected models (EC-Earth3, EC-Earth3-Veg, CanESM5, and CMCC-ESM2) and projected the crop yield changes for each municipality, model, and scenario using a fixed effect econometric model. Our results demonstrated increasing trends of hot and dry events during crop growing seasons of both agricultural types in most scenarios and periods, culminating in yield losses. In the near future, the extremes trends and the yield losses are similar among the scenarios for each crop; however, in the long-term period, the differences are clear, with greater yield losses in SSP5-8.5. Family farmers will experience a more extreme climate and greater yield losses than commodity farmers. Both agricultural systems must increase their resilience to deal with climate change, regardless of the scenario. However, more attention and immediate actions are needed for family farmers.

3.1 – Introduction

Climate change contributes to the intensification of extreme climate and increases the risk of economic activities that depend on climate, especially agriculture (IPCC, 2022). Many studies have shown that changes in rainfall patterns, temperature and extremes are occurring in agricultural areas of Brazil due to both land use and climate change (Salvador and de Brito, 2018; Leite-Filho *et al.*, 2019; Costa *et al.*, 2020; Rattis *et al.*, 2021; Marengo *et al.*, 2022b). Furthermore, predictions indicate that climate change will continue to increase and intensify in

the future, posing a threat to Brazilian agriculture (Costa *et al.*, 2019; Rattis *et al.*, 2021; Commar *et al.*, 2023).

In Brazil, two agriculture types stand out, supplying food for most of the international market. The first and of crucial importance for the national economy is large-scale commodity agriculture of Mato Grosso state (MT) and MATOPIBA region – an agricultural region formed by the municipalities of Maranhão, Tocantins, Piauí, and Bahia states – that produces mainly soybean and maize in double cropping systems. The second is family farming, which is responsible for supplying the internal market, while the greatest share of Brazilian family farmers are located in the semiarid region, cultivating a wide range of crops, but with a highlight to maize, bean, and cassava (Silva and Neto, 2019). These agricultural types play important roles in guaranteeing global and national food security.

Many studies evaluated the future climate change impacts on large-scale commodity agriculture in northern Brazil, predicting yield losses in soybean and maize 2nd season in the near future (Pires *et al.*, 2016; Brumatti *et al.*, 2020; Zilli *et al.*, 2020; Abrahão, 2021; Fernandes *et al.*, 2022) and in the long-term future (Fernandes *et al.*, 2022), mostly for intermediate (RCP 4.5) and pessimistic (RCP 8.5) scenarios. Fewer studies evaluated future climate change's impact on the main crops of family farming in semiarid or the northeast Brazilian region. Still, maize yield losses are predicted for the northeast in the future in intermediate (RCP 4.5) and pessimistic scenario (RCP 8.5) (Martins *et al.*, 2019). Reductions in the suitable area for cowpea bean cultivation in the northeast are predicted under future climate change scenarios (Silva *et al.*, 2010). Tanure *et al.* (2024) evaluated the climate change impacts on family farming and commodity crops in Brazil in 2021-2050. They found that maize, beans, and cassava of family farming agriculture of North and Northeast Brazilian regions could be negatively affected as well as corn and soybean of commodity agriculture in MATOPIBA. However, all these studies directly evaluated the impact of mean climate change on crop yield rather than extreme climate. Moreover, they do not use the most recent and up-to-date Shared Socioeconomic Pathways scenarios of IPCC and only focus on the northeast Brazilian region instead of the semiarid.

To minimize climate change impacts on agriculture it is essential to elaborate adaptation strategies for the future, especially for family farmers that are more exposed, vulnerable and impacted than commodity farmers (Brumatti *et al.*, *under review*). Here, I evaluate the trends in extreme climate in crop growing seasons considering two types of agriculture, and project yield losses using an econometric model in four climate scenarios of CMIP6 for the near-term and long-term future. Our work provides many pathways of the climate change impacts and the

adaptation for Brazilian agriculture since the decisions that we make now and in the near term affect the future adaptation, especially for the main crops of semiarid family farmers, where there is an alarming lack of studies. Although there is a fair number of studies about this theme in Brazilian commodity agriculture, our study provides the extreme climate impacts in a wide range of climate change scenarios with high resolution and periods. Finally, our work brings a complete assessment of climate change impacts on Brazilian agriculture, and the challenges that each agricultural system could face in the future.

3.2 – Data and methods

3.2.1 – Study areas

Our focus in this study is on two Brazilian agricultural types that stand out in the production of crops to supply the international and national markets: commodity and family farming agriculture, respectively.

The greatest share of the commodity production occurs in the Mato Grosso state and the MATOPIBA. In this agriculture type the main crops are soybean and maize, cultivated in a double cropping system, and most of these grains are for export contributing to the Brazilian economy. The production system is characterized by the utilization of high levels of technology as adapted cultivars, irrigation, expert labor, and machinery allowing the cultivation of multiple cropping in the same agricultural year and increasing the production.

On the other hand, the semiarid region of the country is home to the great share of family farmers in the country, and its production is aimed at subsistence and supplying the internal market. The semiarid region is formed by 1262 municipalities of the northeast Brazilian region and the northern part of Minas Gerais state (SUDENE, 2017), and the main crops cultivated by those family farmers are maize, bean, and cassava (Silva and Neto, 2019). The farmers in this region rely on family labor and limited technology for their production system. In recent years, they have been adversely affected by prolonged and intense droughts, environmental changes, and degradation, aggravating poverty and social inequality.

There are many differences between these two agricultural types: the geographical location, which influences the exposure of each crop to extreme climate; the technological level used in the production system and socioeconomic farmers' aspects, which influences the vulnerability; and the crops. However, both agricultural systems are important to the Brazilian

economy, and global food security, then it is crucial to estimate the extreme climate impacts on the yields of these crops, to create adaptation strategies for future climate change according to the particularities of each agricultural type.

3.2.2 – Climate data and scenarios

I used daily precipitation, relative humidity, and minimum and maximum temperatures from four models (CMCC-ESM2, EC-Earth3, EC-Earth3-Veg, and CanESM5) and five scenarios (historical, SSP1-2.6, SSP2-4.5, SSP3-7.0, and SSP5-8.5) of CMIP6/IPCC to calculate the extreme climate indexes. I applied the empirical quantiles (QUANT) to correct the bias of all these climate variables since this method performed better in our study areas and chose the four best models for them. The corrected climate variables from the QUANT method were available in $0.25^\circ \times 0.25^\circ$ (~27,5 km \times 27,5 km) spatial resolution. In this study, I evaluated the extreme climate impacts in the near-term (2021-2050, P1) and long-term (2071-2100, P2).

The climate change scenarios that I used are formed with the combination of socioeconomics (Shared Socioeconomic Pathways) and climate (Representative Concentration Pathways) scenarios that indicate possible socioeconomics, technological, and climate pathways to society at a global level (O'Neill *et al.*, 2014).

The SSP1-2.6 is the most optimistic among all scenarios studied here. Its socioeconomic narrative considers a world with increasing economic growth from adopting sustainable measures. The emissions over the century will reduce, and the combination with the negative emissions at the end of the century will lead to global warming of about 1.7 °C by 2100 (Gidden *et al.*, 2019). This scenario considers low socioeconomic challenges for mitigation and adaptation (O'Neill *et al.*, 2014).

The SSP2-4.5 is considered a middle-of-the-road scenario, then projects medium socioeconomic challenges to mitigation and adaptation (O'Neill *et al.*, 2014; Riahi *et al.*, 2017). In the SSP2 narrative, the trends in social, economic, and technological do not change markedly compared to the historical patterns (Riahi *et al.*, 2017). Besides that, it is expected an increase in the consumption of resource-intensive commodities and greenhouse gases emissions (at approximate rates as of today). In this way, global warming is about 2.6 °C until the end of the century in this scenario (Gidden *et al.*, 2019).

The SSP3-7.0 is considered a scenario with high socioeconomic challenges to mitigation and adaptation, due to moderate economic growth, an increase in population, and reduced technological advances in the energy sector (O'Neill *et al.*, 2014). Besides that, in this scenario, the world presents high inequality, lower investments in human capital, and weak international institutions resulting in the highest levels of pollutant and aerosol emissions, which contributes to these challenges (O'Neill *et al.*, 2014; Gidden *et al.*, 2019). All of this results in a radiative forcing of about 7 W.m^{-2} and a global warming about of $4.1 \text{ }^{\circ}\text{C}$ until 2100 (Gidden *et al.*, 2019).

The SSP5-8.5 is considered a scenario with high socioeconomic challenges for mitigation and low for adaptation. This is associated with high energy demand based on carbon-based fuels and lower investments in alternative energy technologies (O'Neill *et al.*, 2014). Although the challenges to mitigation, the adaptation challenges are reduced due to improved human capital and economic growth, which contributes to a less vulnerable world (O'Neill *et al.*, 2014). Considering this, the radiative forcing for this scenario is projected to reach 8.5 W.m^{-2} and a global warming of about $4.9 \text{ }^{\circ}\text{C}$ (Gidden *et al.*, 2019).

3.2.3 – Climate indexes and trend analysis

I calculated the extreme temperature and rainfall indexes for each crop growing season, scenario, and period. Crop growing seasons were defined as the possible maximum exposure time and were estimated using the sowing windows of the Climatic Risk Agricultural Zoning and the average crop cycles of each municipality.

The extreme temperature indexes that try to represent crop climate impacts used in this study were: extreme degree days (EDD), vapor pressure deficit (VPD), and the frequency of the VPD values critical to crop during growing season (VPD_lim). EDD calculates the impacts of higher temperatures that are harmful to crops and was calculated as in Schlenker and Roberts, (2009). The critical temperatures used to calculate EDD were: $30 \text{ }^{\circ}\text{C}$ (for cassava, cowpea bean, and soybean) (Hillocks *et al.*, 2001; Schlenker and Roberts, 2009; Silva *et al.*, 2010) and $29 \text{ }^{\circ}\text{C}$ (for maize) (Schlenker and Roberts, 2009).

VPD is the difference between saturated air vapor pressure and actual air vapor pressure and is a good indicator to associate the impact of combined dry and hot conditions on plants (Grossiord *et al.*, 2020). It was calculated using daily minimum and maximum temperatures,

and relative humidity following the methodology of (Allen *et al.*, 2006), and estimating the average for each crop growing season.

VPD_{lim} is defined as the number of days during the crop growing season when the daily VPD is above a limit value that leads crops to close the stomata and reduce transpiration, indicating water stress. This index was calculated using the daily VPD values and a critical VPD value for each crop. The critical VPD values considered for soybean and cassava were 2.0 kPa (El-Sharkawy, 1993; Fletcher *et al.*, 2007; Sinclair *et al.*, 2017), for maize was 1.7 kPa (Gholipoor *et al.*, 2013; Sinclair *et al.*, 2017), and cowpea bean was 2.2 kPa (Belko *et al.*, 2012; Sinclair *et al.*, 2017).

Finally, the extreme precipitation indexes that were used to capture the impacts on crops are: PRCPTOT and maximum consecutive dry days (CDD). I considered that PRCPTOT represents the total rainfall during the crop growing season and CDD is the maximum period of days under the crop growing season with daily rainfall below 1mm.day⁻¹.

After calculating the extreme climate indexes for each municipality, crop growing season, scenario, and period, I calculated the trends and their magnitude using Mann-Kendall (at a 5% and a 10% significance levels) and Theil-Sen tests, respectively. The Mann-Kendall and Theil-Sen tests were applied to the time series of each period (P1 or P2) constructed from the average of extreme climate index value for the municipalities that cultivates the crop in each year and region.

3.2.4 – Yield model and projections under climate change scenarios

I constructed fixed effect models using the anomalies of log(crops yield) and the extreme climate indices (CDD, EDD, PRCPTOT, VPD, and VPD_{lim}) for the period 2003-2019, to estimate the relationship of Yield and extreme climate in each municipality that cultivates the main crops of family farming of semiarid and commodity agriculture of the MT and MATOPIBA region.

To estimate the predicted values of yield changes in climate change scenarios, I followed the methodology of Abrahão, (2021). First, the anomalies of climate indexes (ΔW_i) were calculated from the difference between the average of the future period (2021-2050 or 2071-2100) and the average of the historical period (1981-2010) for each climate model, and

municipality. Then, the yield changes for each period, climate model and municipality (ΔY , %) were estimated using the following equation (Equation 1).

$$\Delta Y_i(\%) = 100 \times (e^{\sum \beta_w \Delta W_i} - 1) \quad \text{Equation 1}$$

The β_w represents the estimators of each climate index obtained from the fixed effect model (Tables S3.1-S3.5), that multiply the corresponding climate anomalies (ΔW_i). Finally, I applied an exponential function to estimate the yield changes, since the fixed effect model is logarithmic. An ensemble was constructed with the crops' yield changes of each climate model.

3.3 – Results

3.3.1 – Future trends in extreme climate indexes during crop growing season

In general, VPD, VPD_lim, EDD, and CDD are projected to increase during all crop growing seasons, while PRCPTOT presented reductions in most crop growing seasons. During the 2021-2050 period, the differences in index values among the scenarios are minimal, while during 2071-2100 the differences are clear between scenarios, and the models' variability increases. Even during 2021-2050, the greatest climate index trends were often observed in the most pessimistic scenarios: SSP3-7.0 and SSP5-8.5 (Figures 3.1-3.5, Table 3.1).

During the bean cycle, the ensemble shows an increase of VPD (Figure 3.1-b, Table 3.1), VPD_lim (Figure 3.2-b, Table 3.1), EDD (Figure 3.3-b, Table 3.1), and CDD (Figure 3.4-b, Table 3.1) and a reduction of PRCPTOT (Figure 3.5-b, Table 3.1). VPD and VPD_lim presented significant positive trends (at a 5% level) in most scenarios and periods, with exception of scenarios SSP1-2.6 and SSP2-4.5 during 2071-2100 (Table 3.1, Figures 3.1-b, 2-b). Similarly, EDD presented positive trends at a 5% significance level in almost all scenarios and periods, with exception of SSP1-2.6 during 2071-2100 (Table 3.1, Figure 3.3-b). CDD presented significant positive trends in almost all scenarios during 2021-2050, except in SSP2-4.5; and the same pattern was found for SSP2-4.5 and SSP3-7.0 during 2071-2100 (Table 3.1, Figure 3.4-b).

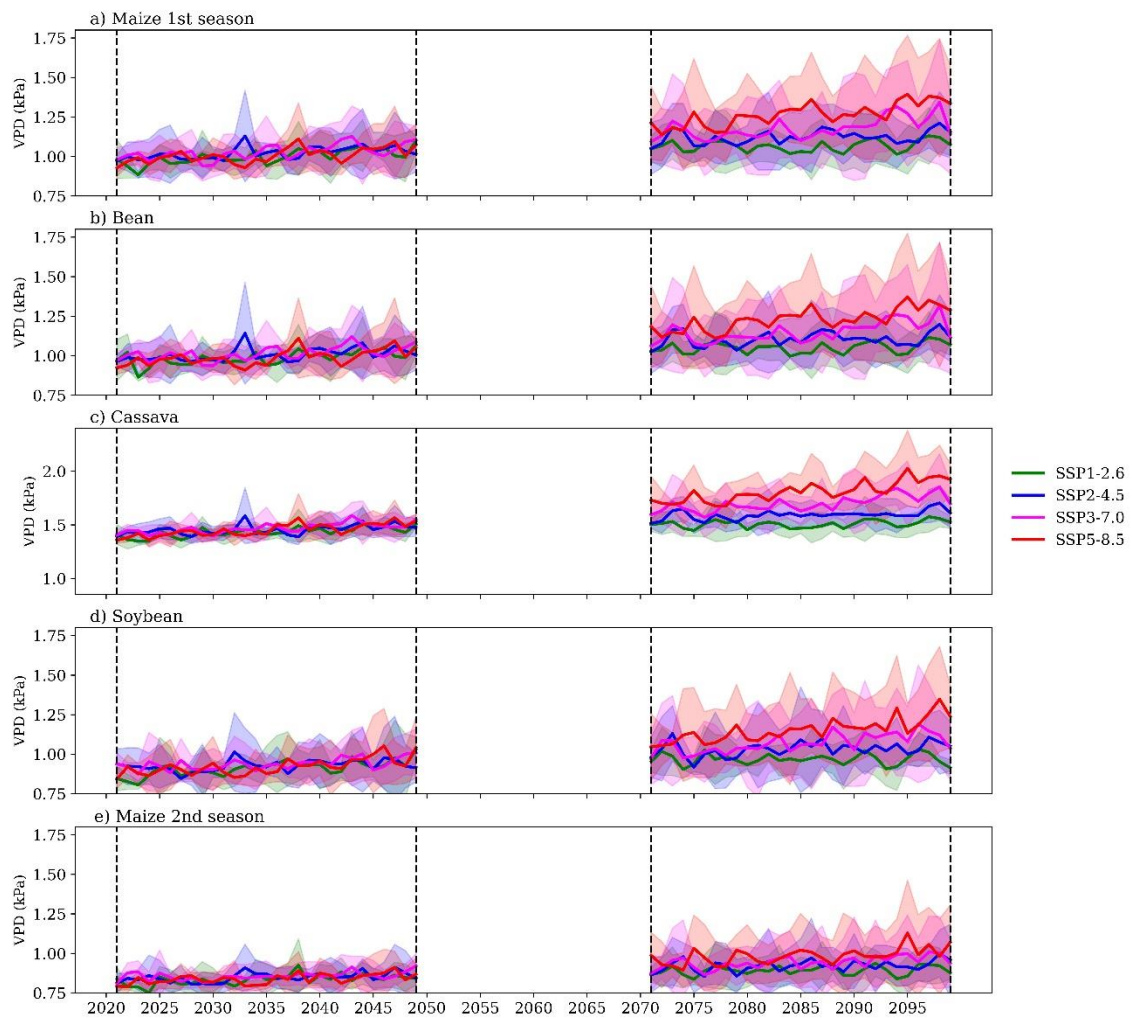


Figure 3.1 – VPD values during crop growing season, periods, and scenarios. The crops are represented in the lines: a) Maize 1st season, b) Bean, c) Cassava, d) Soybean, and e) Maize 2nd season. The vertical dashed lines represent the periods 2021-2050 and 2071-2100. The scenarios lines and the shadow on it represent the ensemble of the 4 models and their variability, respectively.

During Maize 1st season growing season, positive trends were found for CDD, EDD, VPD, and VPD_{lim}, while a reduction in the PRCPTOT was estimated without a significant trend in most scenarios (Table 3.1). All climate indexes do not present a significant trend during 2071-2100 in the SSP1-2.6, despite that, EDD, VPD, and VPD_{lim} presented a significant trend at a 5% level in all other scenarios and periods (Table 3.1, Figures 3.1-a, 3.2-a, 3.3-a).

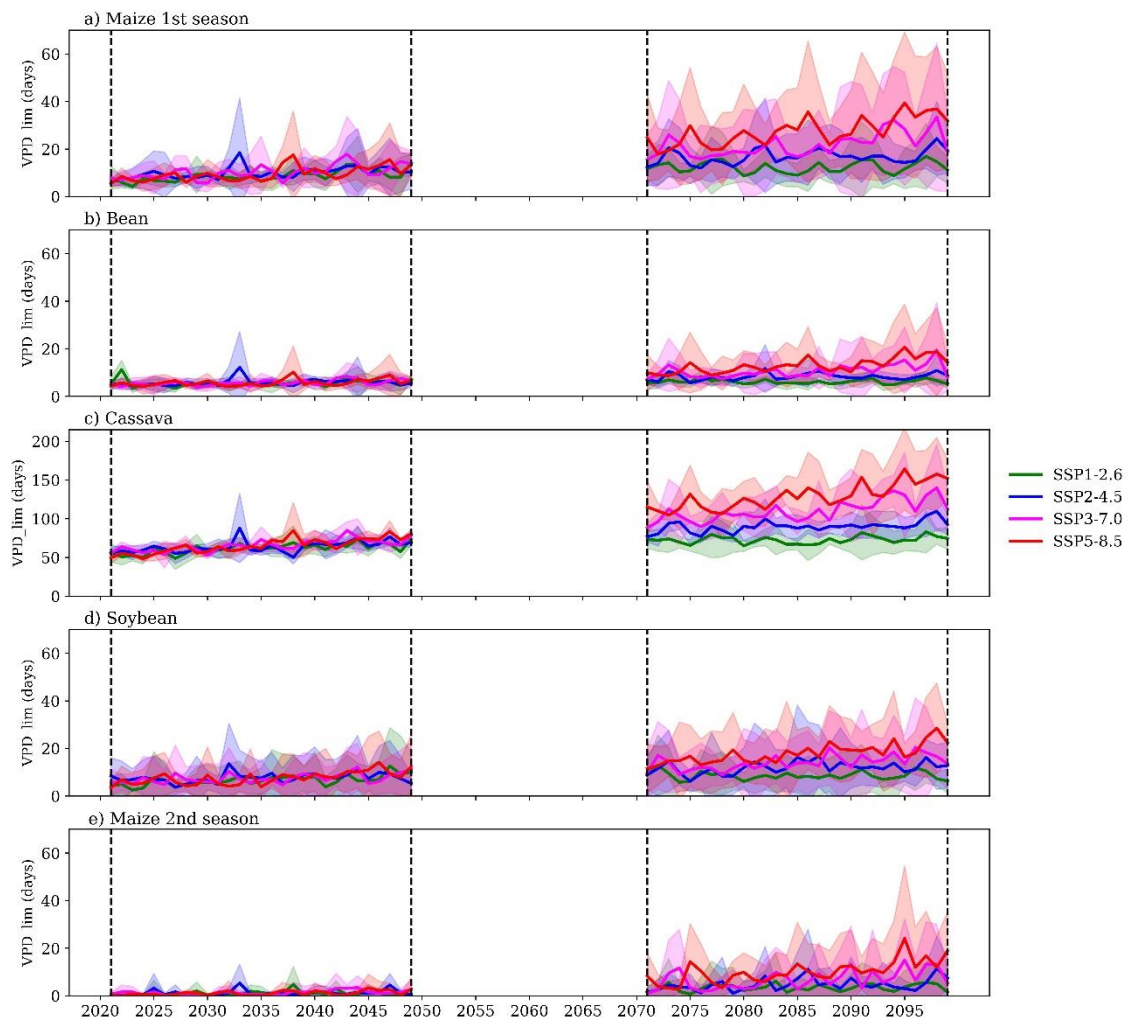


Figure 3.2 – VPD_lim values during crop growing season, periods, and scenarios. The crops are represented in the lines: a) Maize 1st season, b) Bean, c) Cassava, d) Soybean, and e) Maize 2nd season. The vertical dashed lines represent the periods 2021-2050 and 2071-2100. The scenarios lines and the shadow on it represent the ensemble of the 4 models and their variability, respectively.

During cassava growing season, CDD presented positive significant trends only in the SSP3-7.0 and SSP5-8.5 (Table 3.1, Figure 3.4-c). Positive significant trends were found in all scenarios and periods, except in the SSP1-2.6 during 2071-2100. Reductions in the PRCPTOT were observed in all scenarios and periods, but significant values were found only in SSP1-2.6 and SSP5-8.5 during 2021-2050 (Figure 3.5-c). VPD, VPD_lim, and EDD presented significant positive trends at a 5% level in all scenarios, with exception of SSP1-2.6 during 2071-2100 for EDD and VPD_lim (Table 3.1, Figures 3.1-c, 3.2-c, 3.3-c).

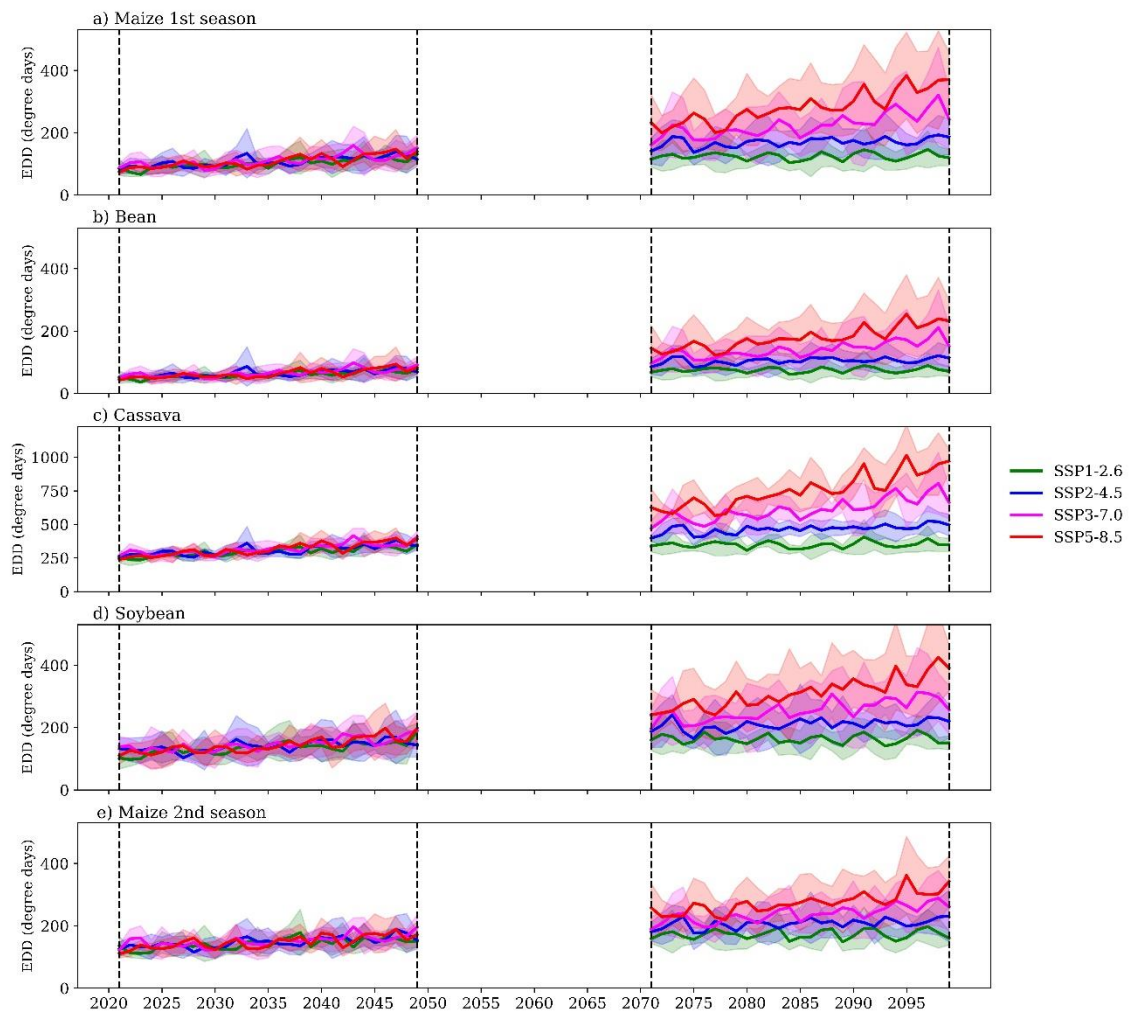


Figure 3.3 – EDD values during crop growing season, periods, and scenarios. The crops are represented in the lines: a) Maize 1st season, b) Bean, c) Cassava, d) Soybean, and e) Maize 2nd season. The vertical dashed lines represent the periods 2021-2050 and 2071-2100. The scenarios lines and the shadow on it represent the ensemble of the 4 models and their variability, respectively.

During the soybean growing season, a significant positive trend was found for CDD and VPD_lim in almost all scenarios and periods, except in P1 in SSP2-4.5 for CDD and in P2 in SSP1-2.6 for VPD_lim, where negative values were found without significance. EDD and VPD presented positive significant trends in all scenarios and periods, however negative values without trend significance were found for SSP1-2.6 during 2071-2100. For PRCPTOT, significant values were found only for SSP1-2.6 during 2021-2050.

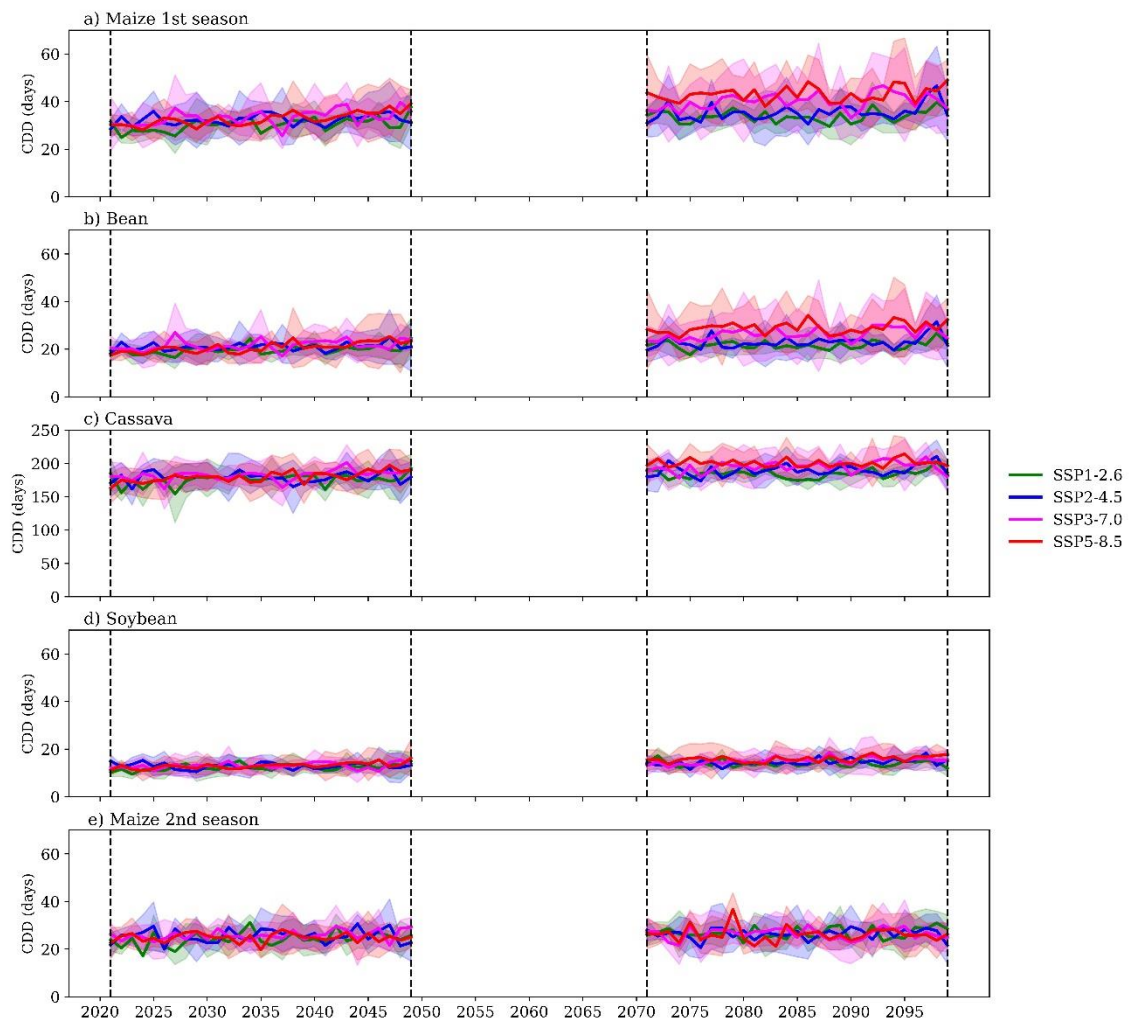


Figure 3.4 – CDD values during crop growing season, periods, and scenarios. The crops are represented in the lines: a) Maize 1st season, b) Bean, c) Cassava, d) Soybean, and e) Maize 2nd season. The vertical dashed lines represent the periods 2021-2050 and 2071-2100. The scenarios lines and the shadow on it represent the ensemble of the 4 models and their variability, respectively.

During the maize's 2nd season growing season, a significant positive trend of CDD was found only in SSP1-2.6 and SSP3-7.0 during 2021-2050. EDD and VPD presented significant positive trends in almost all scenarios and periods, except for the SSP1-2.6 and SSP2-4.5 during 2071-2100. No significant trend was detected for PRCPTOT. In both periods, there were significant positive trends were found for VPD_lim in the scenarios SSP2-4.5, SSP3-7.0, and SSP5-8.5.

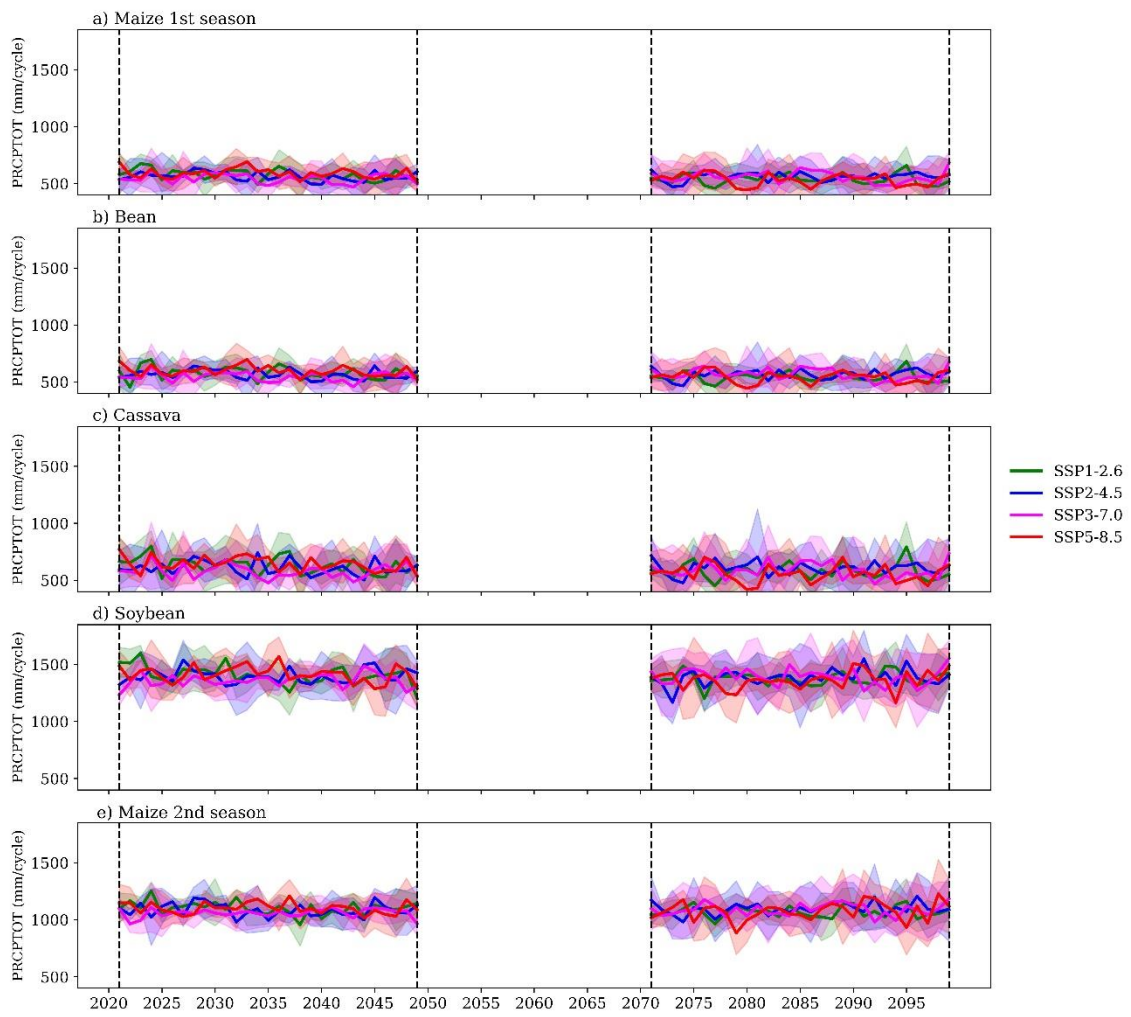


Figure 3.5 – PRCPTOT values during crop growing season, periods, and scenarios. The crops are represented in the lines: a) Maize 1st season, b) Bean, c) Cassava, d) Soybean, and e) Maize 2nd season. The vertical dashed lines represent the periods 2021-2050 and 2071-2100. The scenarios lines and the shadow on it represent the ensemble of the 4 models and their variability, respectively.

Table 3.1 – Trends of climate indexes for each crop, scenario, and period.

Crops	Scenarios	Periods	Climate Indexes					
			CDD (days/year)	EDD (degree days/year)	PRCPTOT (mm/year)	VPD (kPa/year)	VPD_lim (days/year)	
Bean	SSP1-2.6	P1	0.083**	0.892**	-2.025	0.003**	0.057**	
		P2	0.009	0.085	-0.941	0.001	-0.009	
	SSP2-4.5	P1	0.042	0.887**	-1.019	0.002**	0.042*	
		P2	0.085*	0.607**	0.795	0.001	0.041	
	SSP3-7.0	P1	0.112**	1.012**	-0.252	0.003**	0.068**	
		P2	0.145**	2.369**	-1.622	0.005**	0.196**	
	SSP5-8.5	P1	0.189**	1.263**	-1.759	0.003**	0.065**	
		P2	0.097	3.479**	-0.201	0.006**	0.268**	
	Maize 1 st Season	SSP1-2.6	P1	0.185**	1.436**	-2.771**	0.004**	0.160**
			P2	0.044	0.117	-1.108	0.001	0.024
SSP2-4.5		P1	0.082	1.456**	-1.047	0.002**	0.151**	
		P2	0.123*	0.946**	0.386	0.002*	0.145*	
SSP3-7.0		P1	0.192**	1.641**	-0.774	0.003**	0.212**	
		P2	0.169**	3.241**	-1.427	0.005**	0.354**	
SSP5-8.5		P1	0.249**	1.950**	-1.200	0.003**	0.196**	
		P2	0.099	5.355**	-0.817	0.006**	0.528**	
Cassava		SSP1-2.6	P1	0.235	3.023**	-3.558*	0.004**	0.595**
			P2	0.130	0.064	-1.119	0.001*	0.141
	SSP2-4.5	P1	-0.013	3.081**	-0.949	0.003**	0.458**	
		P2	0.269	2.716**	0.649	0.002**	0.391**	
	SSP3-7.0	P1	0.264**	3.553**	-0.723	0.004**	0.612**	
		P2	0.375**	7.519**	-1.354	0.006**	1.176**	
	SSP5-8.5	P1	0.651**	4.951**	-3.134*	0.005**	0.941**	
		P2	0.024	12.412**	-1.098	0.009**	1.566**	
	Soybean	SSP1-2.6	P1	0.085**	1.653**	-3.773*	0.004**	0.184**
			P2	0.009	-0.161	0.454	-0.000	-0.028
SSP2-4.5		P1	-0.001	1.202**	0.462	0.002**	0.057	
		P2	0.065**	1.091**	0.692	0.002**	0.107*	
SSP3-7.0		P1	0.053*	1.656**	2.156	0.003**	0.136**	
		P2	0.086**	3.422**	-1.395	0.005**	0.218**	
SSP5-8.5		P1	0.1003**	2.215**	-2.137	0.004**	0.222**	
		P2	0.059**	4.919**	1.076	0.007**	0.362**	
Maize 2 nd season		SSP1-2.6	P1	0.139**	1.309**	-1.384	0.002**	0.012
			P2	0.011	0.222	0.078	0.001	0.049
	SSP2-4.5	P1	0.025	1.440**	-0.607	0.002**	0.031**	
		P2	0.035	0.912**	0.931	0.001	0.105**	
	SSP3-7.0	P1	0.096**	1.387**	1.089	0.001**	0.043**	
		P2	-0.009	2.354**	1.119	0.003**	0.232**	
	SSP5-8.5	P1	-0.000	1.821**	-1.163	0.002**	0.061**	
		P2	0.000	2.846**	1.872	0.003**	0.369**	

**Significant at 5%, *Significant at 10%

3.3.2 – Future yield changes

Most municipalities cultivating the main family farming and commodity crops show yield losses in all scenarios and periods in the models' ensemble (Figures 3.6,3.7). The individual model's yield changes are presented in Figures S3.1-S3.8. The combination of the increase in extreme climate intensity and frequency (Figures 3.1-3.5) with the negative relationship between the extreme climate indexes and $\log(\text{Yield})$ in the fixed effect model (Tables S3.1-S3.5) contributed to the estimated impact.

3.3.2.1 – Family farming agriculture of the semiarid region

During 2021-2050, the differences between scenarios for each municipality and crop were minimal. In family farming agriculture, maize was the most affected crop with the greatest yield losses ranging from -10% to -50%, in all scenarios, with greater losses concentrated in the southwestern part of the semiarid region. Bean presented greater yield losses than cassava, with values ranging from -5% to -30% in all scenarios, while cassava yield losses were about -5% (Figure 3.6). Similarly to maize, the municipalities of the southwestern part of the semiarid region were the most affected during the bean growing season.

During 2071-2100 period, the differences between scenarios are evident, and the more pessimistic the scenario, the greater the yield losses (Figure 3.7). For maize 1st season, yield losses were greater than -50% and similar between SSP2-4.5, SSP3-7.0, and SSP5-8.5 (Figure 3.7-f,k,p). In SSP1-2.6, the yield losses were smaller than the other scenarios in some municipalities in the northern part of the semiarid region, with values ranging between -15% to -50% (Figure 3.7-a,f,k,p).

For beans, yield losses ranged from -15% to -30% and -15% to -40% in the northern semiarid region in SSP1-2.6 and SSP2-4.5, respectively (Figure 3.7-b,g). The losses in the southwestern part of the semiarid region increased compared with the 2021-2050 period, reaching values close to -40% in SSP1-2.6 and greater than -50% in other scenarios. The yield losses in the northern part of the semiarid region increased as the scenario became more pessimistic, with yield losses greater than -50% in some municipalities in the SSP5-8.5 (Figure 3.7-g,l,q).

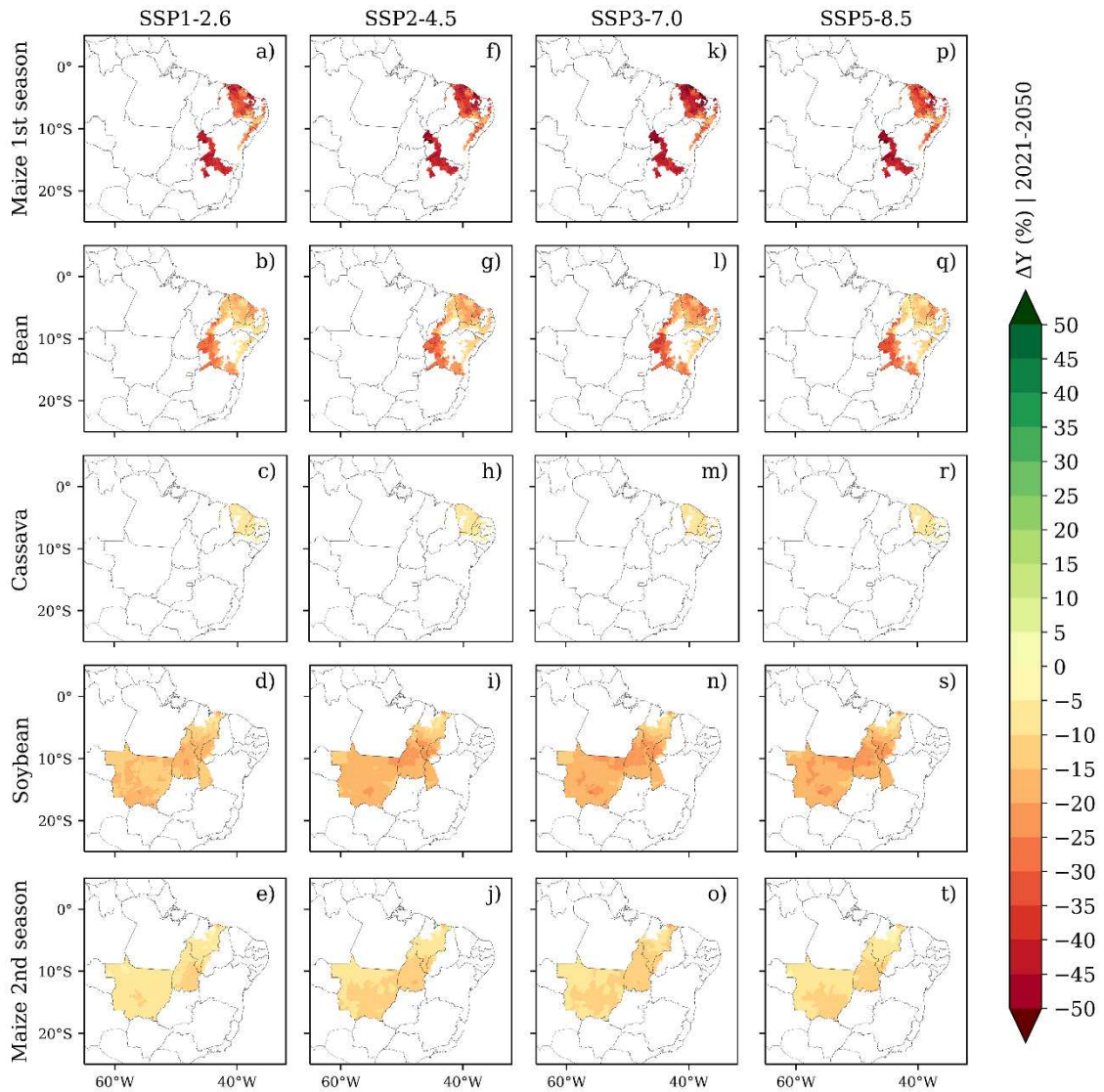


Figure 3.6 – Yield change from 2003-2019 to 2021-2050 for each crop, scenario and ensemble models.

The losses in cassava yield increased compared to the near-term period and over the scenarios (Figure 3.7-c,h,m,r). In the SSP1-2.6, the cassava yield losses were around -10% (Figure 3.7-c), while the yield losses were about -15%, -25%, and -35% in the SSP2-4.5, SSP3-7.0, and SSP5-8.5, respectively.

3.3.2.2 – Commodity agriculture of the MT and MATOPIBA

During 2021-2050, soybean presented greater yield losses (-5% to -15%) than maize 2nd season (-5% to -10%) in all scenarios, and the greatest yield losses were concentrated in the municipalities of the MATOPIBA region.

During 2071-2100, the differences in soybean yield losses are clear in most of the municipalities of MT and MATOPIBA among the scenarios (Figure 3.7-d,i,n,s), indicating that the scenario pathway will be crucial to soybean cultivation in these regions. In the SSP1-2.6, the yield losses ranged from -10% to -25%, while in the SSP2-4.5 the values ranged from -25% to -35% (Figure 3.7-d,i). In the SSP3-7.0, the yield losses are greater than -35% reaching values greater than -50% in some municipalities. In the SSP5-8.5, the majority of the municipalities had soybean yield losses greater than -50% (Figure 3.7-s).

The maize 2nd season yield losses were less intense than soybean, and the magnitude of yield losses increased subtly in the scenarios when compared with soybean (Figure 3.7-e,j,o,t). In the SSP1-2.6, the yield losses ranged from -5% to -20%, with the great values occurring in the southern region of MT and MATOPIBA. This portion of the MT and MATOPIBA were the most affected in the other scenarios too. The yield losses ranged from -10% to -30%, -15% to -30%, and -20% to -35% in SSP2-4.5, SSP3-7.0, and SSP5-8.5, respectively.

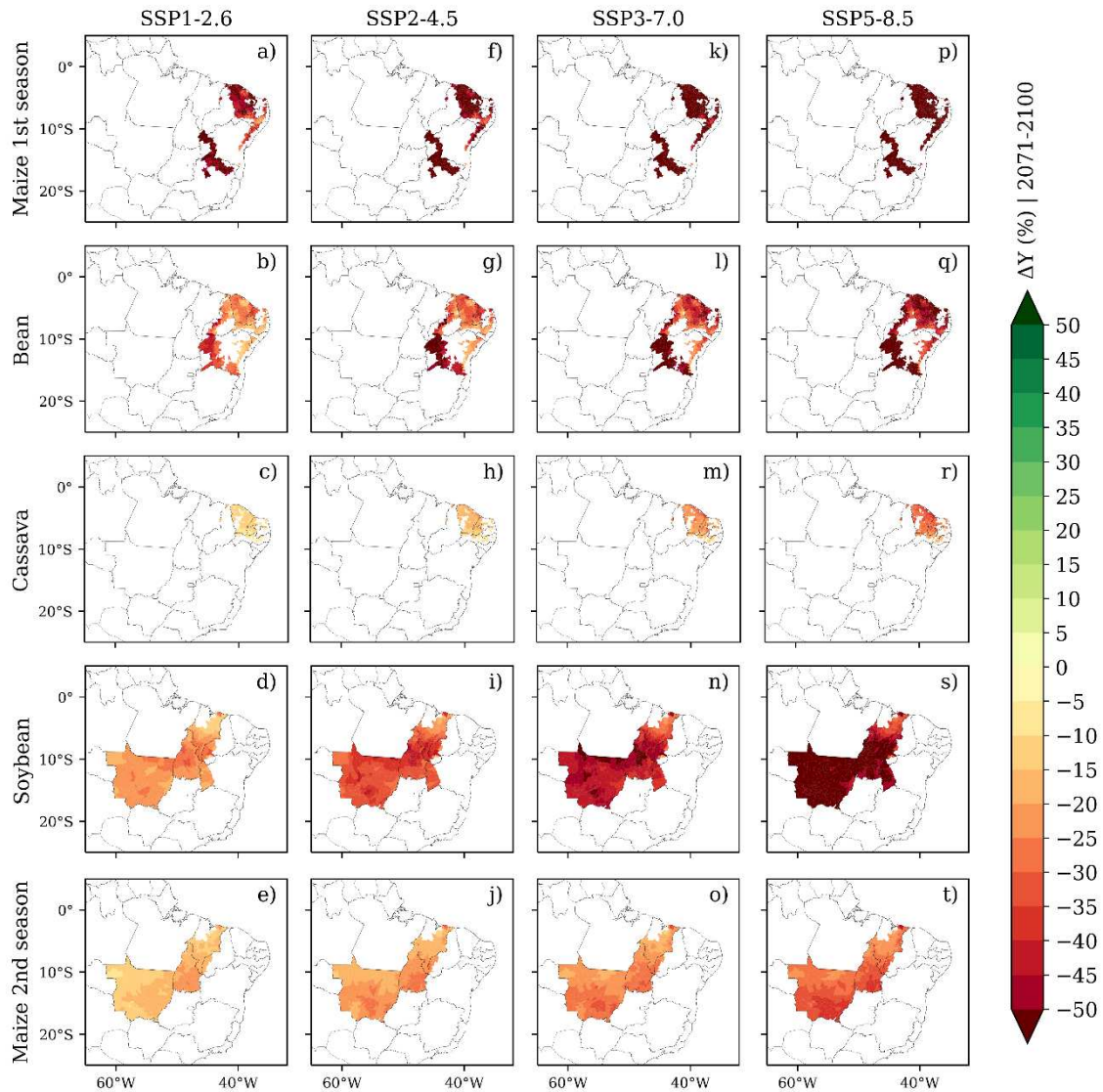


Figure 3.7 – Yield change from 2003-2019 to 2071-2100 for each crop, scenario, and ensemble models.

3.4 – Discussion

Our results showed an increase in the trends of extreme climate indexes that are harmful to crops (VPD, VPD_lim, EDD, and CDD), while reductions in PRCPTOT were observed in most scenarios, periods, and crop growing seasons. In both periods, the trends were greater, for most crops, in the pessimistic scenarios: SSP3-7.0 and SSP5-8.5, with larger differences in the long-term period. These results indicate an increase of hot and dry conditions in crop growing season in the future, regardless of the scenario in the near-term period, and reductions of the increase of these trends only in the SSP1-2.6 in the long-term period.

The projected hot and dry conditions in climate scenarios lead to yield losses in most of the municipalities that cultivated the main crops of family farming of the semiarid region and

large-scale commodity agriculture of the Brazilian northern region, regardless of the scenario. Yield loss differences were observed more clearly in the long-term period among the scenarios.

In the crop yield fixed effect models, the variables that more influenced the yield anomalies were VPD and EDD, with a negative relationship. These variables had greater and significant trend increases in most scenarios, especially in the long-term, contributing to crop yield losses. All other indexes also contribute to the results found for each crop, even with a smaller level of influence than VPD and EDD.

Our results for soybean of MT and MATOPIBA are similar to the results found by Abrahão (2021), that projected yield losses of these crops for SSP2-4.5 in 2035-2050 period, using a fixed effect model of VPD, EDD, GDD, and Total precipitation. Even with the differences in climate variables in the fixed effect model and the period, I found similar soybean yield changes, with values ranging from -5% to -10% in MT and MATOPIBA in SSP2-4.5.

I found similar results for soybean and maize 2nd season in studies that used different methodologies than ours. Pires *et al.*, (2016) and Brumatti *et al.*, (2020) used a mechanistic model to simulate the climate change impacts of soybean and maize 2nd season during 2011-2050 under CMIP5/RCP 8.5 in MT and MATOPIBA. These authors found soybean and maize 2nd season yield losses ranged from 11-40% and 10% in the study area, respectively. Zilli *et al.* (2020) also projected soybean and maize 2nd season yield losses in different scenarios until 2050, as well as Fernandes *et al.* (2022) projected soybean yield losses of about 23% in MATOPIBA during the 2040-2070 period under the RCP 8.5 scenario. However, these studies do not evaluate the impact of extreme climate directly as our study does, they consider changes in the average climate.

For family farming agriculture of the semiarid region the number of studies is reduced compared to the large-scale commodity agriculture; I found studies only for maize and cowpea bean. Martins *et al.* (2019) evaluated changes in maize yield in the northeast Brazilian region using the Aquacrop model and RCP 4.5 and RCP 8.5 scenarios of CMIP5 during the 2007-2040 and 2071-2099 periods. These authors found maize yield reduction greater than 60% under RCP 8.5 during the 2071-2099 period, corroborating our results of SSP5-8.5 in the long-term. Cowpea bean could also have reductions in production in the future under a pessimistic scenario, due to reductions in the suitable planted area for this crop in the Northeast Brazilian region (Silva *et al.*, 2010). To the best of our knowledge, I could not find studies that evaluate cowpea bean and cassava yield changes under climate change scenarios in northeast or semiarid

Brazilian regions. As well as in the studies about climate change impact on commodity crop' yield, these studies do not evaluate the impact of extreme climate directly as our study does, they consider changes in the average climate.

Our results showed that in all scenarios and periods, the main crops of large-scale commodity agriculture and family farming agriculture could present yield losses, bringing an alarming future for both agricultural systems. Even in the most optimistic scenario (SSP1-2.6) the projected yield losses are greater, especially on the crops of family farming agriculture and in the long-term period. Our results also showed that in the near-term period, the yield changes do not presented greater variations among scenarios, however, the differences are clear in the long-term period, which indicates the need and urgency to take actions to follow the pathway of the most optimistic scenario to achieve global warming below of 2 °C until the end of the century, to ensure reduced challenges of adaptation for the farmers of both agricultural systems.

In addition, more attention and actions need to be taken immediately to family farmers of the semiarid region, since production losses are already observed in the 2003-2019 period for the main crops (Brumatti et al., *under review*), to increase their adaptive capacity and prepare them for the future climate change intensification. Commodity farmers of the northern Brazilian region have demonstrated that they are adapting well to extreme climate events during the 2003-2019 period and increasing their yield (Brumatti et al., *under review*), however Rattis *et al.* (2021) showed that 28% of the current agricultural lands of northern Brazil are out of the optimal climate space to the cultivation of soybean and maize and that will be aggravated in the future, and could result in yield losses.

One way to reduce the projected impact of climate change and extremes in both agriculture types is to elaborate adaptation strategies to deal with climate change in the future. The capacity of farmers to adapt to climate change and extreme climate depends on several social, economic, financial, climatic, governmental, and institutional factors. These factors must be taken into account to identify and superpose the barriers to climate change adaptation to create adaptation plans for commodity and family farming agriculture. The barriers to climate change adaptation are greater to family farmers of the semiarid region than to commodity farmers of the MT and MATOPIBA, due to more vulnerable climatic, socioeconomic, and financial conditions. And the greater the combinations of these barriers, the smaller the range of adaptation options (IPCC, 2014).

Next, I will list several adaptation options for each agriculture type and their challenges and barriers to climate change adaptation. Nature-based adaptation strategies with reduced technological levels are the ones with the least barriers to climate change adaptation and are easier to be adopted by farmers of both agriculture types, especially family farmers. The conservation of the biomes inserted in the MT and MATOPIBA and the semiarid of Brazil (Cerrado, Amazônia, and Caatinga) brings some ecosystem services that benefit these agricultural regions (Pires *et al.*, 2016; Strand *et al.*, 2018; Angelotti and Giongo, 2019; Brumatti *et al.*, 2020; Commar *et al.*, 2023). Agroforestry, livestock system, and intercropping systems are viable options with several agroecological benefits and low carbon emissions levels (Angelotti and Giongo, 2019).

Soil and water conservation techniques also provide a low-technological approach to adaptation. Examples include the construction of *barraginhas* (small dams that promote water infiltration and reduce erosion), which is commonly used by family farmers (Marengo *et al.*, 2022a); no-tillage and mulching are techniques that reduce evaporation and increase soil moisture (Marengo *et al.*, 2022a) and could be adopted by both types of farmers. In fact, He and Rosa (2023) showed the benefits of the adoption of these strategies that conserve soil moisture in the future under 3.0 °C and 1.5 °C of warming, with area reductions on croplands facing green water scarcity (water scarcity related to soil moisture and plant). However, Angelotti and Giongo (2019) point out that the no-tillage practice could be difficult to adopt by family farmers of the semiarid region because crop residues are traditionally used for animal feed during dry periods.

Other adaptation strategies that could be applied in both agriculture types are changes in the crop planting dates (Pires *et al.*, 2016; Angelotti and Giongo, 2019), adoptions of short-cycle cultivars (Abrahão and Costa, 2018; Brumatti *et al.*, 2020); adoption of cultivars more tolerant to heat and drought conditions and diseases (Lybbert and Sumner, 2012; Angelotti and Giongo, 2019; Hampf *et al.*, 2020); development and adoption of the forecast system (Marengo *et al.*, 2022a). However, compared with the strategies mentioned in the previous paragraphs, I considered these strategies as medium challenges to adoption, especially for family farmers. Although the existence of adapted cultivars of maize, bean, and cassava for the semiarid region, access to these cultivars could be limited when compared to commodity farmers. Moreover, the development of new drought tolerant cultivars takes time and is dependent on investments in research. On the other hand, some family farmers opt to produce their seeds storing a part for the next season, which contributes to the selection of more adapted grains (Angelotti and

Giongo, 2019). Family farmers could opt for other crops more adapted to the semiarid region as agave, and sorghum (Marengo *et al.*, 2022a). The development of a forecast system demands investment in research and the utilization of this tool could be limited by farmers' lower level of education and inexistent or reduced technical assistance. Additionally, training users can be expensive and time demanding.

The adaptation strategy that I consider with more challenges to adoption by family farmers is irrigation. Irrigation is an efficient adaptation practice to agriculture; however, it is dependent on water availability, infrastructure, technical assistance, and financial resources, that are limited to family farmers of the semiarid region. Nowadays, family farmers of the semiarid region make use of wells, weirs, and cisterns to mitigate the impact of droughts, being the wells and weirs more efficient for agricultural production (Marengo *et al.*, 2022a). Commodity farmers of MT and MATOPIBA have adapted through irrigation practice, and these regions encompass large irrigation poles for the production of grains, as western Bahia, Alto Rio das Mortes, and Alto Teles Pires (ANA, 2021). However, with future climate change, even these farmers could have challenges to continue to adapt through this practice.

The projected increase in dry and hot events during the crop growing season reduces the soil moisture and increases the water demand by the plant and consequently, the irrigated depth, putting the actual existent irrigated areas in a possible water conflict in the future and making it very difficult for farmers to adapt through this practice in some regions, as semiarid, where water uses are more competitive due to lower water availability. The adoption and expansion of the irrigation practice need to be done from the evaluation of cautions water management in each region in the future, to guarantee all the water uses.

Adaptation challenges vary according to the future scenario of climate change that the world will follow, and a combination of strategies will likely be needed to adapt these two agriculture types in the future as the climate and socioeconomic scenario become more pessimistic. Then, investment in adaptation strategies need to be done considering the particularities of commodity and family farming agriculture. Interestingly, some adaptation measures listed above can also serve as effective practices for mitigating climate change, with agriculture potentially playing a key role in reducing emissions.

All these future climate and adaptation challenges put in risk future national and international food security and underscore the need for careful consideration of the current measures being taken now to address future climate change and support farmers' adaptation

efforts, particularly those of family farming. To facilitate the adaptation of farmers and the entire food chain to climate change, it is necessary to develop institutional measures at the global, regional, and local levels (IPCC, 2019).

3.5 – Conclusion

Our results showed an alarming and worrying situation to the future of the family farming of the semiarid and the large-scale commodity agriculture. Although our results had demonstrated that all scenarios predicted yield losses for the main crops of these agricultural types, we need to move efforts to follow the pathway of the SSP1-2.6 scenario and achieve a global warming below of 2 °C until the end of the century. The yield losses in this scenario occurred in lower magnitude level than other scenarios, especially in the long-term period and the challenges to the farmers adaptation are reduced.

Even if the world follows the SSP1-2.6 pathways, our results demonstrate that the challenges to family farmers will be greater than commodity farmers, and the measures to enhance the resilience of them need to be taken immediately. Moreover, our results demonstrate the need to increase the resilience of both agricultural systems in the future, regardless of the climate change scenario.

3.6 - Supplementary Material

Table S3.1 – Fixed effect model estimators of Maize 1st season.

<i>Predictors</i>	<i>Estimates</i>	anomy		<i>p</i>
		<i>CI</i>		
anomedd	-0.0063	-0.0074 – -0.0053		6.329e-34
anompr	0.0011	0.0009 – 0.0012		4.215e-51
anomvpd	-0.8888	-1.1385 – -0.6391		3.211e-12
anomcdd	0.0012	-0.0020 – 0.0044		4.537e-01
anomvpdlim	0.0033	0.0004 – 0.0062		2.663e-02
year	-0.0186	-0.0233 – -0.0140		5.504e-15
Observations	10196			
R ² / R ² adjusted	0.230 / 0.175			

Table S3.2 – Fixed effect model estimators of bean.

<i>Predictors</i>	<i>Estimates</i>	anomy		<i>p</i>
		<i>CI</i>		
anomedd	-0.0041	-0.0051 – -0.0031		2.081e-16
anompr	0.0008	0.0007 – 0.0009		4.668e-51
anomvpd	-0.3782	-0.5346 – -0.2218		2.173e-06
anomcdd	-0.0034	-0.0061 – -0.0007		1.367e-02
anomvpdlim	0.0031	-0.0000 – 0.0061		5.081e-02
year	-0.0270	-0.0304 – -0.0236		7.483e-54
Observations	12432			
R ² / R ² adjusted	0.153 / 0.094			

Table S3.3 – Fixed effect model estimators of cassava.

<i>Predictors</i>	<i>Estimates</i>	anomy	
		<i>CI</i>	<i>p</i>
anomedd	-0.0004	-0.0009 – 0.0001	1.013e-01
anompr	0.0001	0.0001 – 0.0002	1.263e-03
anomvpd	-0.2012	-0.3947 – -0.0078	4.147e-02
anomcdd	0.0010	0.0003 – 0.0016	4.031e-03
anomvpdlim	-0.0000	-0.0011 – 0.0010	9.274e-01
year	-0.0142	-0.0175 – -0.0109	2.816e-17
Observations	4718		
R ² / R ² adjusted	0.072 / -0.003		

Table S3.4 – Fixed effect model estimators of soybean.

<i>Predictors</i>	<i>Estimates</i>	anomy	
		<i>CI</i>	<i>p</i>
anomedd	-0.0029	-0.0031 – -0.0027	3.964e-122
anompr	-0.0001	-0.0001 – -0.0000	5.141e-04
anomvpd	0.0472	-0.0309 – 0.1252	2.362e-01
anomcdd	0.0030	0.0018 – 0.0042	1.452e-06
anomvpdlim	-0.0080	-0.0093 – -0.0066	2.403e-30
year	0.0146	0.0135 – 0.0157	7.594e-135
Observations	3881		
R ² / R ² adjusted	0.299 / 0.235		

Table S3.5 – Fixed effect model estimators of maize 2nd season.

<i>Predictors</i>	<i>Estimates</i>	anomy	
		<i>CI</i>	<i>p</i>
anomedd	-0.0007	-0.0017 – 0.0002	1.464e-01
anompr	-0.0000	-0.0001 – 0.0001	9.144e-01
anomvpd	-1.0344	-1.3973 – -0.6716	2.614e-08
anomcdd	-0.0033	-0.0055 – -0.0011	3.331e-03
anomvpdlim	-0.0038	-0.0083 – 0.0006	9.158e-02
year	0.0485	0.0455 – 0.0515	4.073e-174
Observations	2013		
R ² / R ² adjusted	0.426 / 0.347		

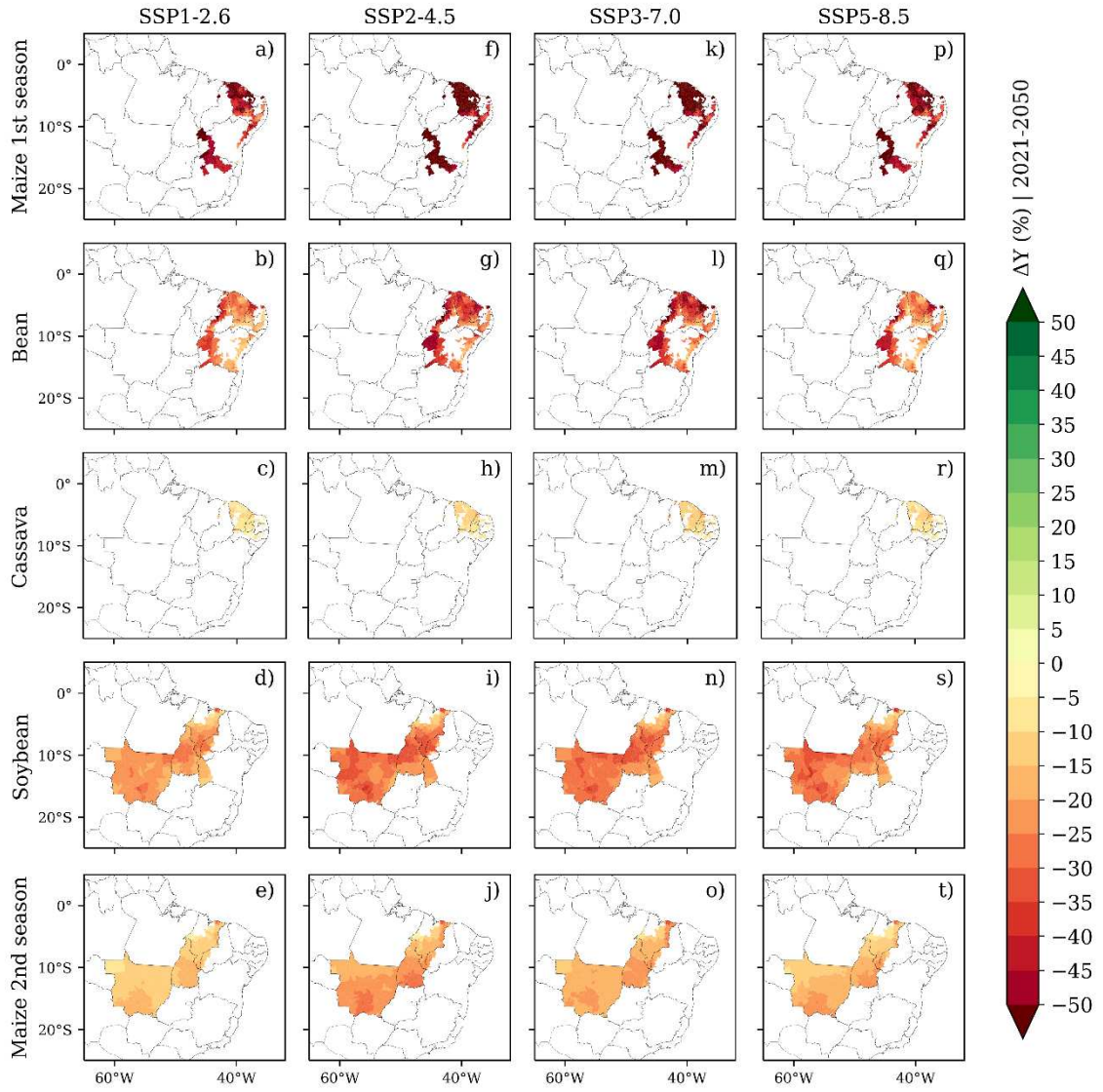


Figure S3.1 – Yield change CanESM5 (2021-2050).

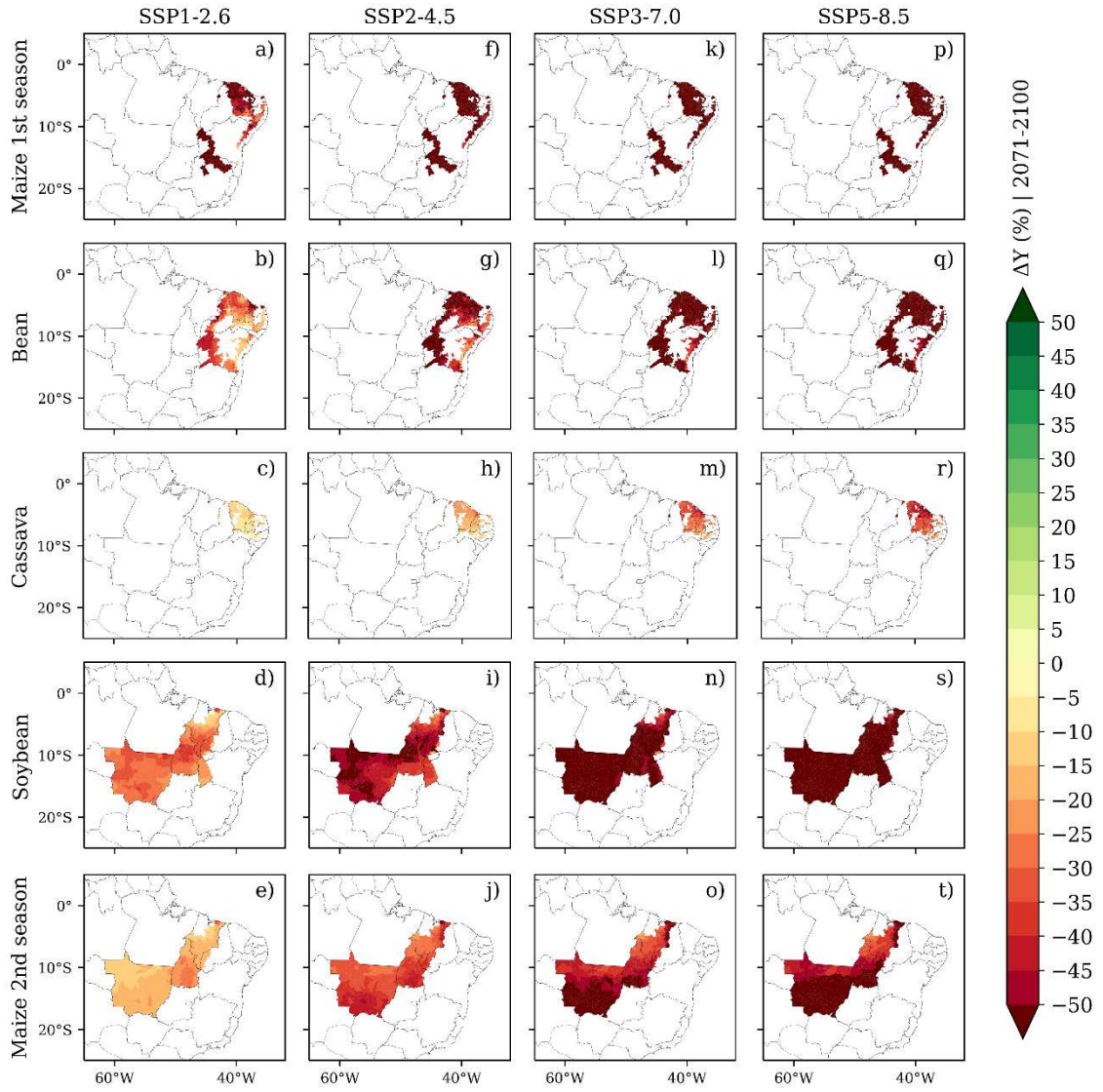


Figure S3.2 – Yield change CanESM5 (2071-2100).

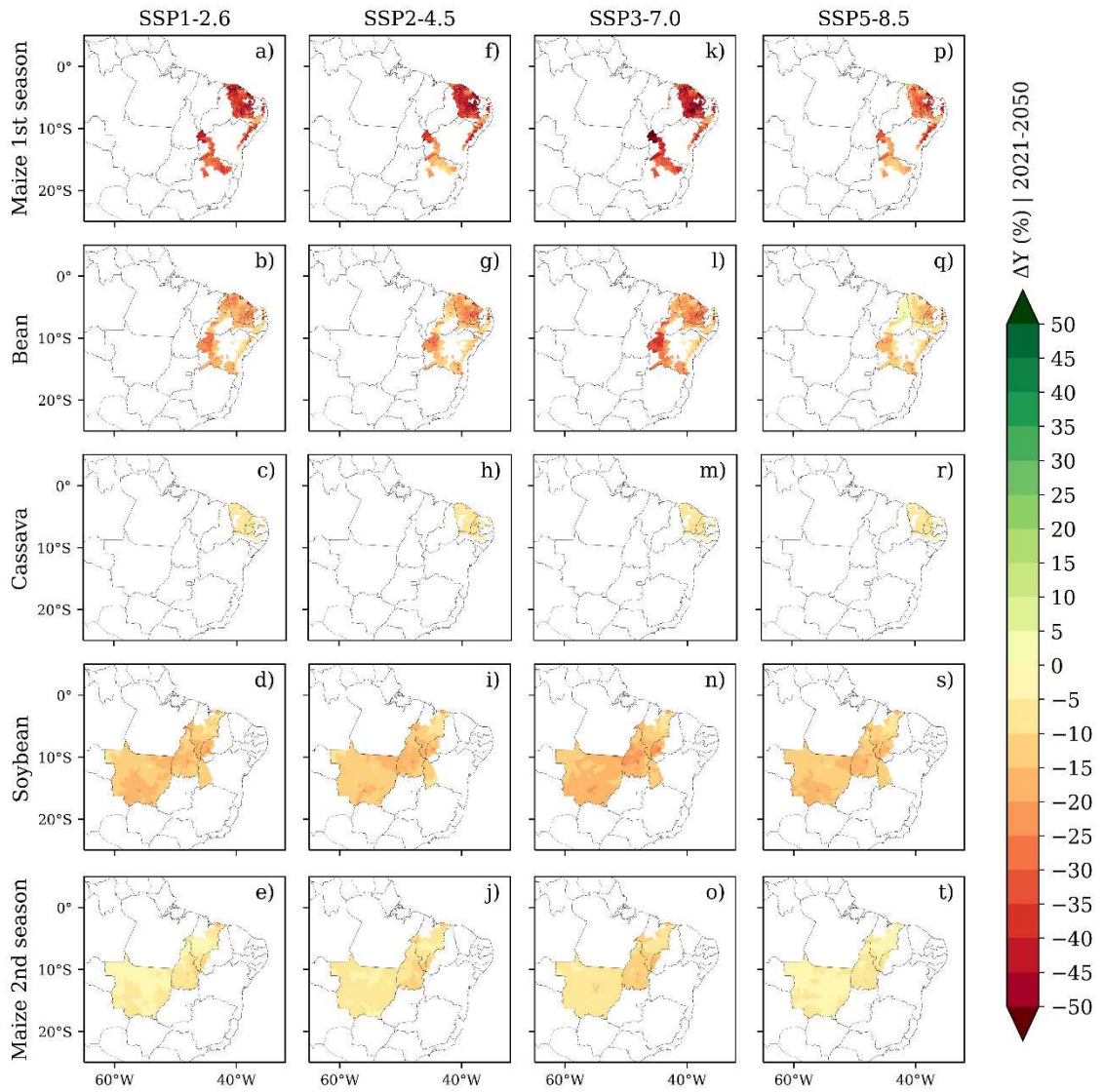


Figure S3.3 – Yield change CMCC-ESM2 (2021-2050).

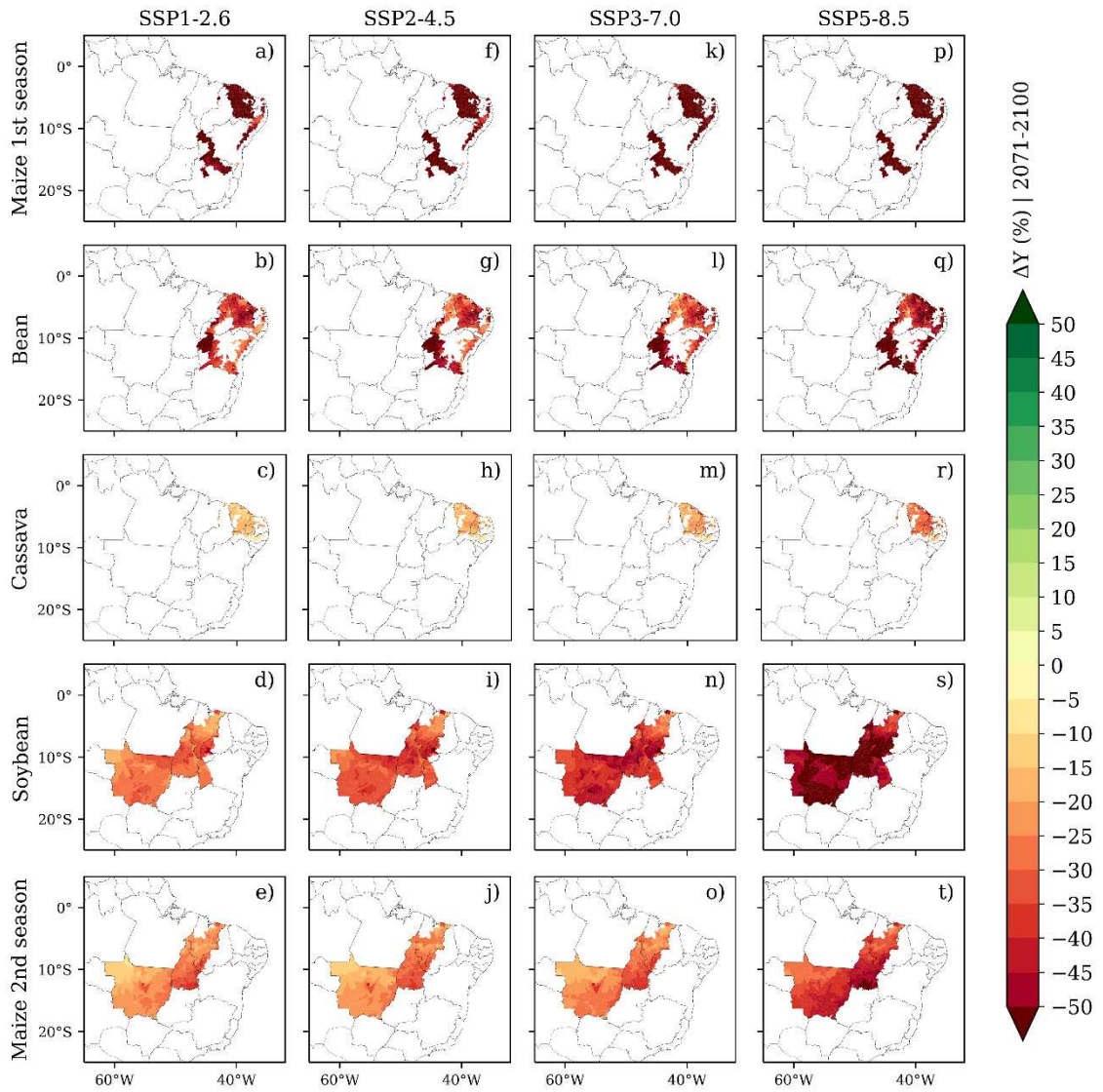


Figure S3.4 – Yield change CMCC-ESM2 (2071-2100).

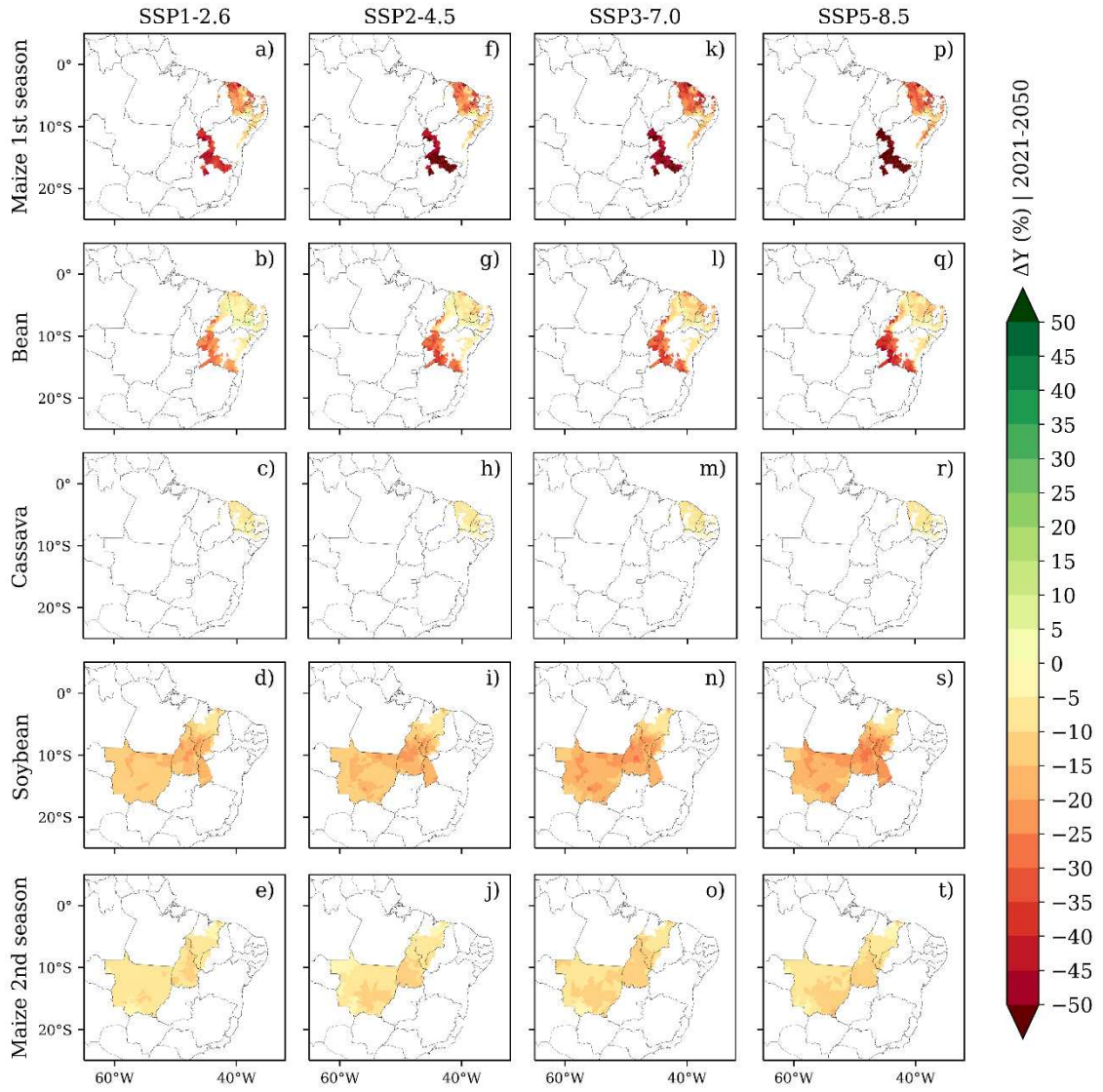


Figure S3.5 – Yield change EC-Earth3 (2021-2050).

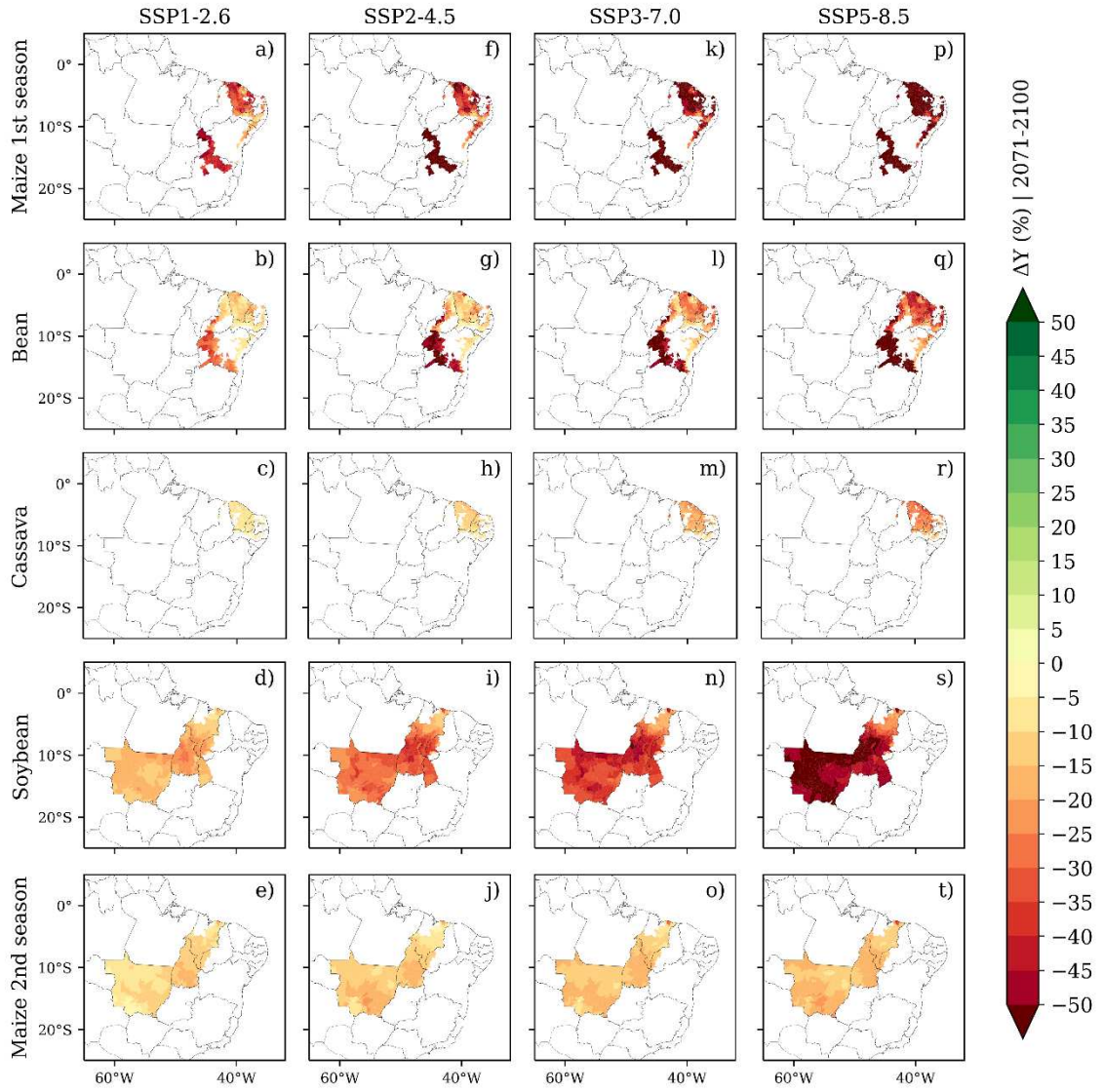


Figure S3.6 – Yield change EC-Earth3 (2071-2100).

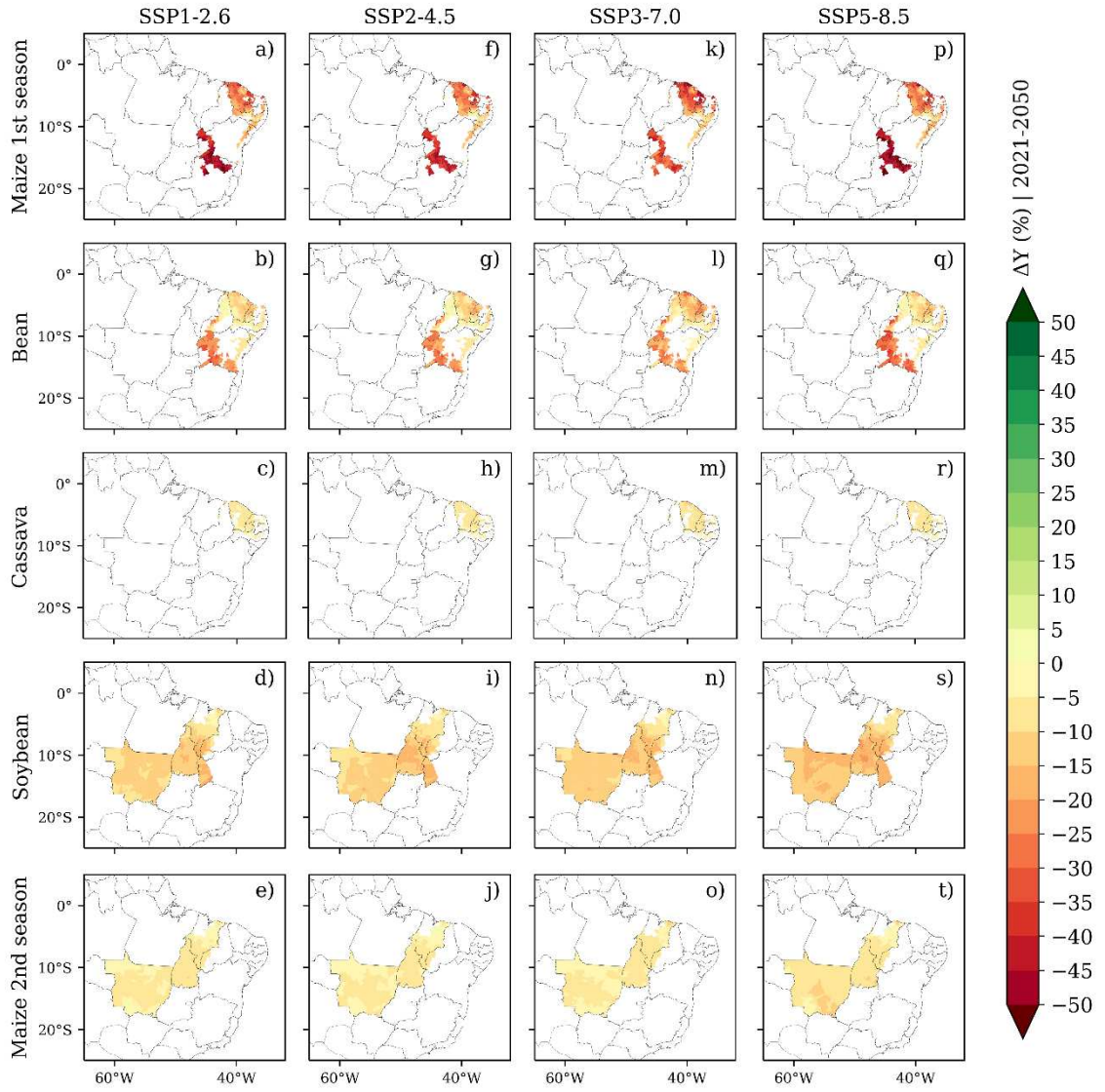


Figure S3.7 – Yield change EC-Earth3-Veg (2021-2050).

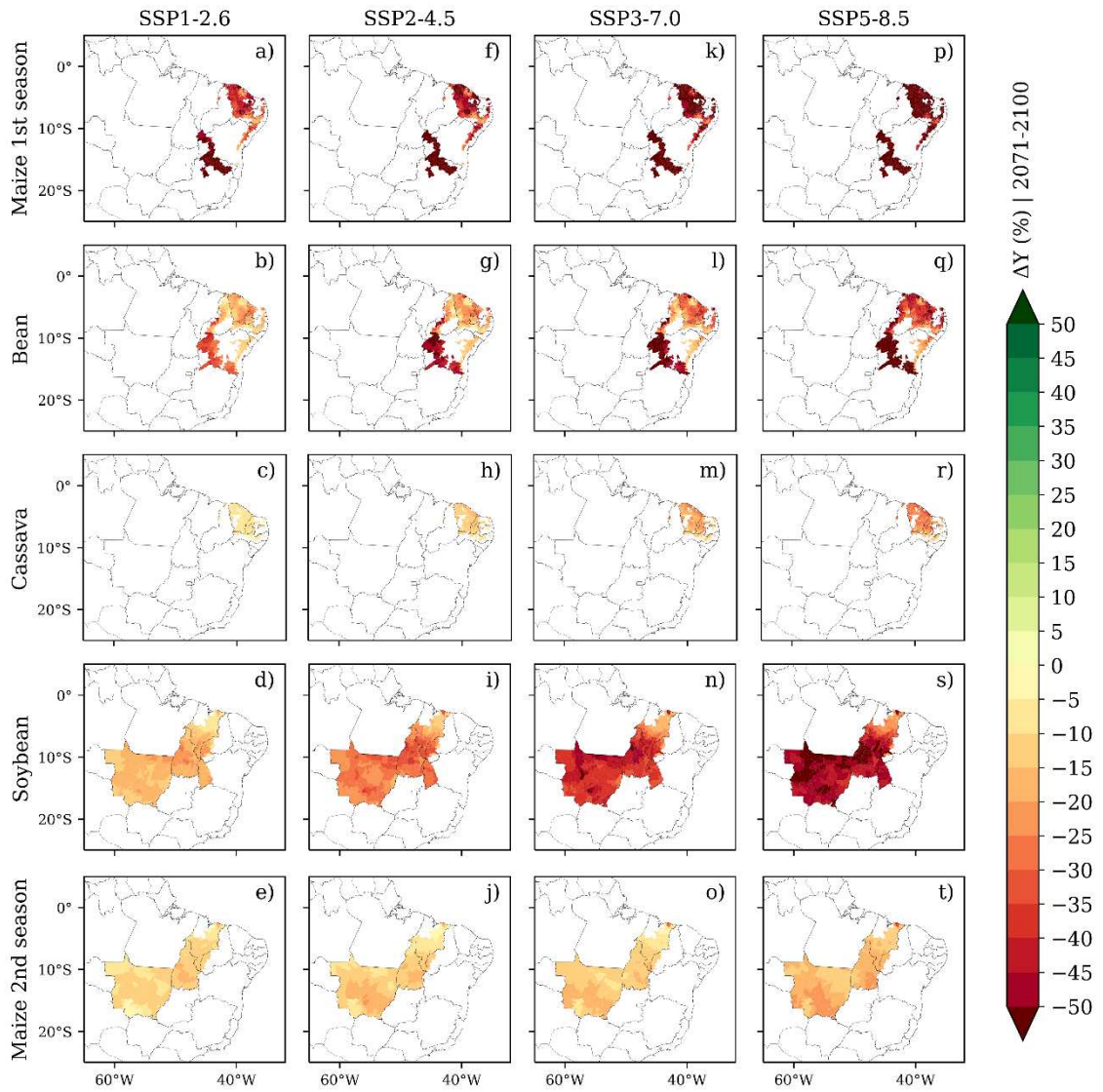


Figure S3.8 – Yield change EC-Earth3-Veg (2071-2100).

General Conclusions

Family farming of the semiarid region and large-scale commodity agriculture of the MT and MATOPIBA are two distinct Brazilian agriculture types, with great importance level for the country. Since these agriculture types are predominantly rainfed in these regions, both systems were and could be affected by the climate. This thesis analyzed how family farmers of the Brazilian semiarid and commodity farmers of MT and MATOPIBA were affected by climate extremes in the past, showing the vulnerability of each system to those events, and how these agricultural types could be affected in the future in four climate change scenarios. Besides that, this thesis brings an evaluation of the best bias correction method and the selection of the best IPCC/CMIP6 models for climate and climate extreme variables to improve the future climate assessment in Brazil.

In Chapter 1, I evaluated how climate extremes affected the main crops of commodity and family farming agriculture calculating five climate extremes indexes for both agricultural types and three additional indexes, to represent the limitations of the rainy season, for commodity agriculture. These indexes were used to construct fixed effect models to evaluate the relationship between extremes and $\log(\text{Yield})$ of each crop. I concluded that the family farmers of the semiarid region were more exposed to and affected by dry and hot events than commodity farmers of the MT and MATOPIBA during 2003-2019. Maize was the crop most affected in both agriculture types. Family farming crops presented negative trends of $\log(\text{Yield})$ and harvested-planted area ratio during 2003-2019, while commodity crops presented increases in $\log(\text{Yield})$. All these results indicate that family farmers are more vulnerable than commodity farmers to climate extremes, presenting negative trends in agricultural outputs during 2003-2019.

In Chapter 2, I evaluated what is the best bias correction method and the best models of IPCC/CMIP6 to climate (PREC, TMIN, and TMAX) and climate extremes variables (CDD and EDD) in Brazil. The application of the bias correction method contributes to a better climate assessment in agriculture and hydrology. I evaluated two bias correction methods commonly used in the literature: linear scaling and quantile mapping. For almost all climate and extreme climate variables the non-parametric quantile mapping (QUANT and RQUANT) were the best bias correction method. Models had difficulty in the representation of the CDD index presenting poor performance even with the application of bias correction, and slightly improve was

achieved with linear scaling in some regions and models. After the selection of the best bias correction method, I evaluated the best models for the construction of the ensemble for each climate and climate extreme variable, and ACCESS-ESM1-5, EC-Earth3, EC-Earth3-Veg, CanESM5, and CMCC-ESM2 were the models that predominated in the ranking models for all Brazilian regions and variables. This chapter provides insights to guide researchers to achieve better results in climate assessment studies.

In Chapter 3, I evaluated how climate extremes could change in the future (2021-2050 and 2071-2100) using four bias corrected models in four climate change scenarios (SSP1-2.6, SSP2-4.5, SSP3-7.0, and SSP5-8.5) during the growing season of the main commodity and family farming crops, and how these changes will impact the yield of these crops. The results showed that dry and hot events will increase in the future in all scenarios and especially in the long-term period, which could cause yield losses in all crops. Even in the most optimistic scenario (SSP1-2.6), crops presented yield losses, however, with lower magnitude than the other scenarios. This brings attention to the vulnerability of Brazilian agriculture to future climate change, and the need to increase the resilience of both agriculture types, especially family farming which presented greater yield losses than commodity agriculture.

This thesis presented a complete assessment of the climate extreme impacts on commodity and family farming agriculture, showing the vulnerability of each agriculture type and the future challenges and impacts of climate change. Among the two agriculture types, family farming was negatively affected by climate extremes during the 2003-2019 period and could be more strongly affected by climate change in the future. Measures need to be taken immediately to increase the resilience of these farmers to deal with climate change and guarantee food security. Despite the results of Chapter 1 demonstrating that commodity farmers adapted well and increase yield during 2003-2019, these farmers will face drier and hotter climate during the crop growing season that threatens food production and will need to increase their resilience to deal with climate change too.

Future research efforts to increase resilience and promote adaptation in Brazilian agriculture should focus on:

- Modeling of adaptation strategies to family farmers of the semiarid region in future climate change scenarios;
- Improvement of climate models' spatial resolution to achieve better results in climate risk assessment;

- Estimate the vulnerability of each agriculture type considering climate and socio-economic aspects.

REFERENCES

- Abrahão GM. 2021. Interactions between deforestation and atmospheric composition on the climate of Amazônia and Cerrado and their consequences to agriculture. Federal University of Viçosa.
- Abrahão GM, Costa MH. 2018. Evolution of rain and photoperiod limitations on the soybean growing season in Brazil: The rise (and possible fall) of double-cropping systems. *Agricultural and Forest Meteorology*. Elsevier, 256–257(April 2017): 32–45. <https://doi.org/10.1016/j.agrformet.2018.02.031>.
- Allen RG, Pereira LS, Raes D, Smith M. 2006. *Crop evapotranspiration: Guidelines for computing crop requirements*. Irrigation and Drainage paper No. 56, FAO.
- Althoff D, Rodrigues LN. 2021. Goodness-of-fit criteria for hydrological models: Model calibration and performance assessment. *Journal of Hydrology*. Elsevier B.V., 600(July): 126674. <https://doi.org/10.1016/j.jhydrol.2021.126674>.
- Alvalá RCDS, Cunha APMA, Brito SSB, Seluchi ME, Marengo JA, Moraes OLL, Carvalho MA. 2017. Drought monitoring in the Brazilian semiarid region. *Anais da Academia Brasileira de Ciências*, 91: 1–15. <https://doi.org/10.1590/0001-3765201720170209>.
- Alvarez MS, Vera CS, Kiladis GN, Liebmann B. 2016. Influence of the Madden Julian Oscillation on precipitation and surface air temperature in South America. *Climate Dynamics*. Springer Berlin Heidelberg, 46(1–2): 245–262. <https://doi.org/10.1007/s00382-015-2581-6>.
- ANA. 2021. *ATLAS IRRIGAÇÃO USO DA ÁGUA NA AGRICULTURA IRRIGADA*. Brasília-DF.
- Andrade CWL, Montenegro SMGL, Montenegro AAA, Lima JR d. S, Srinivasan R, Jones CA. 2021. Climate change impact assessment on water resources under RCP scenarios: A case study in Mundaú River Basin, Northeastern Brazil. *International Journal of Climatology*, 41(S1): E1045–E1061. <https://doi.org/10.1002/joc.6751>.
- Andrea MC da S, Dallacort R, Barbieri JD, Tieppo RC. 2019. Impacts of Future Climate Predictions on Second Season Maize in an Agrosystem on a Biome Transition Region in Mato Grosso State. *Revista Brasileira de Meteorologia*, 34(2): 335–347. <https://doi.org/10.1590/0102-77863340241>.
- Angelotti F, Giongo V. 2019. Ações de mitigação e adaptação frente às mudanças climáticas. In: Freire de Melo, R. & Voltolini, T. V. (Eds.) *Agricultura Familiar Dependente de Chuva No Semiárido*. Brasília.
- Arias ME, Farinosi F, Lee E, Livino A, Briscoe J, Moorcroft PR. 2020. Impacts of climate change and deforestation on hydropower planning in the Brazilian Amazon. *Nature Sustainability*. Springer US, 3(6): 430–436. <https://doi.org/10.1038/s41893-020-0492-y>.
- Arvor D, Dubreuil V, Ronchail J, Simões M, Funatsu BM. 2014. Spatial patterns of rainfall regimes related to levels of double cropping agriculture systems in Mato Grosso (Brazil). *International Journal of Climatology*, 34(8): 2622–2633. <https://doi.org/10.1002/joc.3863>.
- Avila-Diaz A, Benezoli V, Justino F, Torres R, Wilson A. 2020. Assessing current and future trends of climate extremes across Brazil based on reanalyses and earth system model projections. *Climate Dynamics*. Springer Berlin Heidelberg, 55(5–6): 1403–1426. <https://doi.org/10.1007/s00382-020-05333-z>.
- Avila-Diaz A, Torres RR, Zuluaga CF, Cerón WL, Oliveira L, Benezoli V, Rivera IA, Marengo JA, Wilson AB, Medeiros F. 2023. *Current and Future Climate Extremes Over Latin America and Caribbean: Assessing Earth System Models from High Resolution Model Intercomparison Project (HighResMIP)*. *Earth Systems and Environment*. Springer International Publishing.

- Ballarin AS, Sone JS, Gesualdo GC, Schwamback D, Reis A, Almagro A, Wendland EC. 2023. CLIMBra - Climate Change Dataset for Brazil. *Scientific Data*, 10(1): 1–16. <https://doi.org/10.1038/s41597-023-01956-z>.
- Belko N, Zaman-allah M, Cisse N, Diop NN, Zombre G, Ehlers JD, Vadez V. 2012. Lower soil moisture threshold for transpiration decline under water deficit correlates with lower canopy conductance and higher transpiration efficiency in drought-tolerant cowpea. *Functional Plant Biology*, 39: 306–322. <https://doi.org/http://dx.doi.org/10.1071/FP11282>.
- Bezerra BG, Silva LL, Santos e Silva CM, de Carvalho GG. 2019. Changes of precipitation extremes indices in São Francisco River Basin, Brazil from 1947 to 2012. *Theoretical and Applied Climatology*. *Theoretical and Applied Climatology*, 135(1–2): 565–576. <https://doi.org/10.1007/s00704-018-2396-6>.
- Brito SSB, Cunha APMA, Cunningham CC, Alvalá RC, Marengo JA, Carvalho MA. 2018. Frequency, duration and severity of drought in the Semiarid Northeast Brazil region. *International Journal of Climatology*, 38(2): 517–529. <https://doi.org/10.1002/joc.5225>.
- Brumatti LM, Pires GF, Santos AB. 2020. Challenges to the adaptation of double cropping agricultural systems in Brazil under changes in climate and land cover. *Atmosphere*, 11(12): 1–15. <https://doi.org/10.3390/atmos11121310>.
- Cai W, McPhaden MJ, Grimm AM, Rodrigues RR, Taschetto AS, Garreaud RD, Dewitte B, Poveda G, Ham Y-G, Santoso A, Ng B, Anderson W, Wang G, Geng T, Jo H-S, Marengo JA, Alves LM, Osman M, Li S, Wu L, Karamperidou C, Takahashi K, Vera C. 2020. Climate impacts of the El Niño–Southern Oscillation on South America. *Nature Reviews Earth & Environment*. Springer US, 1(4): 215–231. <https://doi.org/10.1038/s43017-020-0040-3>.
- Castro NR, Spolador HFS, Marin FR. 2019. Assessing the economy–climate relationships for Brazilian agriculture. *Empirical Economics*. Springer Berlin Heidelberg. <https://doi.org/10.1007/s00181-019-01711-7>.
- CEPEA. 2023. *PIB do agronegócio 2022*. .
- Cohn AS, Vanwey LK, Spera SA, Mustard JF. 2016. Cropping frequency and area response to climate variability can exceed yield response. *Nature Climate Change*, 6(6): 601–604. <https://doi.org/10.1038/nclimate2934>.
- Commar LFS, Abrahão GM, Costa MH. 2023. A possible deforestation-induced synoptic-scale circulation that delays the rainy season onset in Amazonia. *Environmental Research Letters*, 18(4): 044041. <https://doi.org/10.1088/1748-9326/acc95f>.
- Cortez BN, Pires GF, Avila-Diaz A, Fonseca HP, Oliveira LR. 2022. Nonstationary extreme precipitation in Brazil. *Hydrological Sciences Journal*. Taylor & Francis, 67(9): 1372–1383. <https://doi.org/10.1080/02626667.2022.2075267>.
- Costa MH, Fleck LC, Cohn AS, Abrahão GM, Brando PM, Coe MT, Fu R, Lawrence D, Pires GF, Pousa R, Soares-Filho BS. 2019. Climate risks to Amazon agriculture suggest a rationale to conserve local ecosystems. *Frontiers in Ecology and the Environment*, 584–590. <https://doi.org/10.1002/fee.2124>.
- Costa RL, Macedo de Mello Baptista G, Gomes HB, Daniel dos Santos Silva F, Lins da Rocha Júnior R, de Araújo Salvador M, Herdies DL. 2020. Analysis of climate extremes indices over northeast Brazil from 1961 to 2014. *Weather and Climate Extremes*, 28. <https://doi.org/10.1016/j.wace.2020.100254>.
- Cunha APMA, Zeri M, Leal KD, Costa L, Cuartas LA, Marengo JA, Tomasella J, Vieira RM, Barbosa AA, Cunningham C, Cal Garcia JV, Broedel E, Alvalá R, Ribeiro-Neto G. 2019. Extreme drought events over Brazil from 2011 to 2019. *Atmosphere*, 10(11). <https://doi.org/10.3390/atmos10110642>.

- da Silva RFB, Batistella M, Dou Y, Moran E, Torres SMM, Liu J. 2017. The Sino-Brazilian telecoupled soybean system and cascading effects for the exporting country. *Land*, 6(3): 1–19. <https://doi.org/10.3390/land6030053>.
- Delazeri LMM, Da Cunha DA, Oliveira LR. 2022. Climate change and rural–urban migration in the Brazilian Northeast region. *GeoJournal*, 87(3): 2159–2179. <https://doi.org/10.1007/s10708-020-10349-3>.
- dos Reis LC, Silva CMS e., Bezerra BG, Mutti PR, Spyrides MHC, da Silva PE. 2020. Analysis of Climate Extreme Indices in the MATOPIBA Region, Brazil. *Pure and Applied Geophysics*, 177(9): 4457–4478. <https://doi.org/10.1007/s00024-020-02474-4>.
- Ehret U, Zehe E, Wulfmeyer V, Liebert J. 2012. HESS Opinions “ Should we apply bias correction to global and regional climate model data ?” , 3391–3404. <https://doi.org/10.5194/hess-16-3391-2012>.
- El-Sharkawy MA. 1993. Drought-tolerant cassava for Africa, Asia, and Latin America: breeding projects work to stabilize productivity without increasing pressures on limited natural resources. *BioScience*, 43(7): 441–451. <https://doi.org/https://doi.org/10.2307/1311903>.
- Enayati M, Bozorg-Haddad O, Bazrafshan J, Hejabi S, Chu X. 2021. Bias correction capabilities of quantile mapping methods for rainfall and temperature variables. *Journal of Water and Climate Change*, 12(2): 401–419. <https://doi.org/10.2166/wcc.2020.261>.
- Fernandes RDM, de Melo DM, Elli EF, Battisti R. 2022. Climate change impacts on rainfed and irrigated soybean yield in Brazil’s new agricultural frontier. *Theoretical and Applied Climatology*. Springer Vienna, 147(1–2): 803–816. <https://doi.org/10.1007/s00704-021-03865-w>.
- Flach R, Abrahão G, Bryant B, Scarabello M, Soterroni AC, Ramos FM, Valin H, Obersteiner M, Cohn AS. 2021. Conserving the Cerrado and Amazon biomes of Brazil protects the soy economy from damaging warming. *World Development*. The Author(s), 146(July): 105582. <https://doi.org/10.1016/j.worlddev.2021.105582>.
- Flato GM. 2011. Earth system models: An overview. *Wiley Interdisciplinary Reviews: Climate Change*, 2(6): 783–800. <https://doi.org/10.1002/wcc.148>.
- Fletcher AL, Sinclair TR, Allen LH. 2007. Transpiration responses to vapor pressure deficit in well watered ‘ slow-wilting ’ and commercial soybean. , 61: 145–151. <https://doi.org/10.1016/j.envexpbot.2007.05.004>.
- Fonseca HP, Pires GF, Brumatti LM. 2022. Spatial and Temporal Evolution of Sowing and the Onset of the Rainy Season in a Region of Large Agricultural Expansion in Brazil. *Agronomy*, 12(7). <https://doi.org/10.3390/agronomy12071679>.
- Funk C, Peterson P, Landsfeld M, Pedreros D, Verdin J, Shukla S, Husak G, Rowland J, Harrison L, Hoell A, Michaelsen J. 2015. The climate hazards infrared precipitation with stations - A new environmental record for monitoring extremes. *Scientific Data*, 2: 1–21. <https://doi.org/10.1038/sdata.2015.66>.
- Gbegbelegbe S, Chung U, Shiferaw B, Msangi S, Tesfaye K. 2014. Quantifying the impact of weather extremes on global food security: A spatial bio-economic approach. *Weather and Climate Extremes*. Elsevier, 4: 96–108. <https://doi.org/10.1016/j.wace.2014.05.005>.
- Gholipoor M, Choudhary S, Sinclair TR, Messina CD, Cooper M. 2013. Transpiration response of maize hybrids to atmospheric vapour pressure deficit. *Journal of Agronomy and Crop Science*, 199(3): 155–160. <https://doi.org/10.1111/jac.12010>.
- Gidden MJ, Riahi K, Smith SJ, Fujimori S, Luderer G, Kriegler E, Van Vuuren DP, Van Den Berg M, Feng L, Klein D, Calvin K, Doelman JC, Frank S, Fricko O, Harmsen M, Hasegawa T, Havlik P, Hilaire J, Hoesly R, Horing J, Popp A, Stehfest E, Takahashi K. 2019. Global emissions pathways under different socioeconomic scenarios for use in CMIP6: A dataset of harmonized emissions

trajectories through the end of the century. *Geoscientific Model Development*, 12(4): 1443–1475. <https://doi.org/10.5194/gmd-12-1443-2019>.

Grossiord C, Buckley TN, Cernusak LA, Novick KA, Poulter B, Siegwolf RTW, Sperry JS, McDowell NG. 2020. Plant responses to rising vapor pressure deficit. *New Phytologist*, 226(6): 1550–1566. <https://doi.org/10.1111/nph.16485>.

Gudmundsson L, Bremnes JB, Haugen JE, Engen-Skaugen T. 2012. Technical Note: Downscaling RCM precipitation to the station scale using statistical transformations – A comparison of methods. *Hydrology and Earth System Sciences*, 16(9): 3383–3390. <https://doi.org/10.5194/hess-16-3383-2012>.

Gupta H V., Kling H, Yilmaz KK, Martinez GF. 2009. Decomposition of the mean squared error and NSE performance criteria: Implications for improving hydrological modelling. *Journal of Hydrology*. Elsevier B.V., 377(1–2): 80–91. <https://doi.org/10.1016/j.jhydrol.2009.08.003>.

Hampf AC, Stella T, Berg-Mohnicke M, Kawohl T, Kilian M, Nendel C. 2020. Future yields of double-cropping systems in the Southern Amazon, Brazil, under climate change and technological development. *Agricultural Systems*, 177(September 2019). <https://doi.org/10.1016/j.agry.2019.102707>.

Hatfield JL, Prueger JH. 2015. Temperature extremes: Effect on plant growth and development. *Weather and Climate Extremes*, 10: 4–10. <https://doi.org/10.1016/j.wace.2015.08.001>.

He L, Rosa L. 2023. Solutions to agricultural green water scarcity under. *PNAS Nexus*. Oxford University Press, 2(4): 1–11. <https://doi.org/10.1093/pnasnexus/pgad117>.

Hillocks RJ, Thresh JM, Belotti AC. 2001. *Cassava: Biology, Production and Utilization*. .

IBGE. 2021. *SIDRA - Sistema IBGE de recuperação automática. Tabela 1612 - Área plantada, área colhida, quantidade produzida, rendimento médio e valor da produção das lavouras temporárias*. .

IBGE. 2022. *SIDRA - Sistema de Recuperação Automática. Tabela 839: Área plantada, área colhida, quantidade produzida e rendimento médio de milho, 1ª e 2ª safras*, www.sidra.ibge.gov.br.

IBGE - Instituto Brasileiro de Geografia e Estatística. 2017. *Censo Agropecuário 2017*. .

Ines AVM, Hansen JW. 2006. Bias correction of daily GCM rainfall for crop simulation studies. *Agricultural and Forest Meteorology*, 138(1–4): 44–53. <https://doi.org/10.1016/j.agrformet.2006.03.009>.

IPCC. 2012. *Managing the Risks of Extreme Events and Disasters to Advance Climate Change Adaptation. A Special Report of Working Groups I and II of the Intergovernmental Panel on Climate Change*.

IPCC. 2014. *Climate Change 2014: Impacts, Adaptation, and Vulnerability. Part A: Global and Sectoral Aspects. Contribution of Working Group II to the Fifth Assessment Report of the Intergovernmental Panel on Climate Change [Field, C.B., V.R. Barros, 2156 D.J. Dokken, . .*

IPCC. 2019. *Summary for Policymakers. In: Climate Change and Land: an IPCC special report on climate change, desertification, land degradation, sustainable land management, food security, and greenhouse gas fluxes in terrestrial ecosystems*. .

IPCC. 2022. *Climate Change 2022: Impacts, Adaptation and Vulnerability. Working Group II Contribution to the IPCC Sixth Assessment Report [H.-O. Pörtner, D.C. Roberts, M. Tignor, E.S. Poloczanska, K. Mintenbeck, A. Alegria, M. Craig, S. Langsdorf, S. Löschke, V. Möll. .*

IPCC -Intergovernmental Panel on Climate Change. 2022. *Climate change 2022: Impacts, adaptation and vulnerability*. .

Iturbide M, Casanueva A, Bedia J, Herrera S, Milovac J, Gutiérrez JM. 2022. On the need of bias

adjustment for more plausible climate change projections of extreme heat. *Atmospheric Science Letters*, 23(2): 1–10. <https://doi.org/10.1002/asl.1072>.

Jakob Themeßl M, Gobiet A, Leuprecht A. 2011. Empirical-statistical downscaling and error correction of daily precipitation from regional climate models. *International Journal of Climatology*, 31(10): 1530–1544. <https://doi.org/10.1002/joc.2168>.

Jeferson de Medeiros F, Prestrelo de Oliveira C, Avila-Diaz A. 2022. Evaluation of extreme precipitation climate indices and their projected changes for Brazil: From CMIP3 to CMIP6. *Weather and Climate Extremes*. Elsevier B.V., 38(September): 100511. <https://doi.org/10.1016/j.wace.2022.100511>.

Jiménez-Muñoz JC, Mattar C, Barichivich J, Santamaría-Artigas A, Takahashi K, Malhi Y, Sobrino JA, Schrier G Van Der. 2016. Record-breaking warming and extreme drought in the Amazon rainforest during the course of El Niño 2015-2016. *Scientific Reports*. Nature Publishing Group, 6(August): 1–7. <https://doi.org/10.1038/srep33130>.

Kim YH, Min SK, Zhang X, Sillmann J, Sandstad M. 2020. Evaluation of the CMIP6 multi-model ensemble for climate extreme indices. *Weather and Climate Extremes*. Elsevier B.V., 29: 100269. <https://doi.org/10.1016/j.wace.2020.100269>.

Kling H, Fuchs M, Paulin M. 2012. Runoff conditions in the upper Danube basin under an ensemble of climate change scenarios. *Journal of Hydrology*. Elsevier B.V., 424–425: 264–277. <https://doi.org/10.1016/j.jhydrol.2012.01.011>.

Lafon T, Dadson S, Buys G, Prudhomme C. 2013. Bias correction of daily precipitation simulated by a regional climate model: A comparison of methods. *International Journal of Climatology*, 33(6): 1367–1381. <https://doi.org/10.1002/joc.3518>.

Laux P, Rötter RP, Webber H, Dieng D, Rahimi J, Wei J, Faye B, Srivastava AK, Bliefernicht J, Adeyeri O, Arnault J, Kunstmann H. 2021. To bias correct or not to bias correct? An agricultural impact modelers' perspective on regional climate model data. *Agricultural and Forest Meteorology*, 304–305(September 2020). <https://doi.org/10.1016/j.agrformet.2021.108406>.

Leite-Filho AT, Pontes VY de S, Costa MH. 2019. Effects of deforestation on the onset of the rainy season and the duration of dry spells in southern Amazonia. *Journal of Geophysical Research: Atmospheres*, 2018JD029537. <https://doi.org/10.1029/2018JD029537>.

Lenderink G, Buishand A, Van Deursen W. 2007. Estimates of future discharges of the river Rhine using two scenario methodologies: Direct versus delta approach. *Hydrology and Earth System Sciences*, 11(3): 1145–1159. <https://doi.org/10.5194/hess-11-1145-2007>.

Lesk C, Rowhani P, Ramankutty N. 2016. Influence of extreme weather disasters on global crop production. *Nature*. Nature Publishing Group, 529(7584): 84–87. <https://doi.org/10.1038/nature16467>.

Li Y, Guan K, Schnitkey GD, DeLucia E, Peng B. 2019. Excessive rainfall leads to maize yield loss of a comparable magnitude to extreme drought in the United States. *Global Change Biology*, 25(7): 2325–2337. <https://doi.org/10.1111/gcb.14628>.

Lybbert TJ, Sumner DA. 2012. Agricultural technologies for climate change in developing countries: Policy options for innovation and technology diffusion. *Food Policy*. Elsevier Ltd, 37(1): 114–123. <https://doi.org/10.1016/j.foodpol.2011.11.001>.

Maraun D, Shepherd TG, Widmann M, Zappa G, Walton D, Gutiérrez JM, Hagemann S, Richter I, Soares PMM, Hall A, Mearns LO. 2017. Towards process-informed bias correction of climate change simulations. *Nature Climate Change*, 7(11): 764–773. <https://doi.org/10.1038/nclimate3418>.

Marengo JA, Cunha AP, Alvala RCS, Galdos M V, Challinor A, Marin FR, Moraes OL. 2022a. Drought in Northeast Brazil : A review of agricultural and policy adaptation options for food security. *Climate Resilience and Sustainability*, (January 2021): 1–20. <https://doi.org/10.1002/cli2.17>.

- Marengo JA, Jimenez JC, Espinoza JC, Cunha AP, Aragão LEO. 2022b. Increased climate pressure on the agricultural frontier in the Eastern Amazonia–Cerrado transition zone. *Scientific Reports*. Nature Publishing Group UK, 12(1): 1–10. <https://doi.org/10.1038/s41598-021-04241-4>.
- Marengo JA, Torres RR, Alves LM. 2017. Drought in Northeast Brazil—past, present, and future. *Theoretical and Applied Climatology*. Theoretical and Applied Climatology, 129(3–4): 1189–1200. <https://doi.org/10.1007/s00704-016-1840-8>.
- Martins MA, Tomasella J, Dias CG. 2019. Maize yield under a changing climate in the Brazilian Northeast: Impacts and adaptation. *Agricultural Water Management*. Elsevier, 216(February): 339–350. <https://doi.org/10.1016/j.agwat.2019.02.011>.
- Matiu M, Ankerst DP, Menzel A. 2017. Interactions between temperature and drought in global and regional crop yield variability during 1961–2014. *PLoS ONE*, 12(5): 1–23. <https://doi.org/10.1371/journal.pone.0178339>.
- Melo RF, Voltolini TV. 2019. *Agricultura Familiar Dependente de Chuva no Semiárido*. Embrapa: Brasília, DF.
- Nóia Júnior R de S, Sentelhas PC. 2019. Soybean-maize succession in Brazil: Impacts of sowing dates on climate variability, yields and economic profitability. *European Journal of Agronomy*. Elsevier, 103(August 2018): 140–151. <https://doi.org/10.1016/j.eja.2018.12.008>.
- O'Neill BC, Krieger E, Riahi K, Ebi KL, Hallegatte S, Carter TR, Mathur R, van Vuuren DP. 2014. A new scenario framework for climate change research: The concept of shared socioeconomic pathways. *Climatic Change*, 122(3): 387–400. <https://doi.org/10.1007/s10584-013-0905-2>.
- Osuch M, Lawrence D, Meresa HK, Napiorkowski JJ, Romanowicz RJ. 2017. Projected changes in flood indices in selected catchments in Poland in the 21st century. *Stochastic Environmental Research and Risk Assessment*. Springer Berlin Heidelberg, 31(9): 2435–2457. <https://doi.org/10.1007/s00477-016-1296-5>.
- Pierce DW, Cayan DR, Maurer EP, Abatzoglou JT, Hegewisch KC. 2015. Improved bias correction techniques for hydrological simulations of climate change. *Journal of Hydrometeorology*, 16(6): 2421–2442. <https://doi.org/10.1175/JHM-D-14-0236.1>.
- Pires GF, Abrahão GM, Brumatti LM, Oliveira LJC, Costa MH, Liddicoat S, Kato E, Ladle RJ. 2016. Increased climate risk in Brazilian double cropping agriculture systems: Implications for land use in Northern Brazil. *Agricultural and Forest Meteorology*. Elsevier B.V., 228–229: 286–298. <https://doi.org/10.1016/j.agrformet.2016.07.005>.
- Powell JP, Reinhard S. 2015. Measuring the effects of extreme weather events on yields. *Weather and Climate Extremes*. Elsevier, 12: 69–79. <https://doi.org/10.1016/j.wace.2016.02.003>.
- Pushpalatha R, Gangadharan B. 2020. Is Cassava (*Manihot esculenta* Crantz) a Climate “Smart” Crop? A Review in the Context of Bridging Future Food Demand Gap. *Tropical Plant Biology*. Tropical Plant Biology, 13(3): 201–211. <https://doi.org/10.1007/s12042-020-09255-2>.
- Qian W, Chang HH. 2021. Projecting health impacts of future temperature: A comparison of quantile-mapping bias-correction methods. *International Journal of Environmental Research and Public Health*, 18(4): 1–12. <https://doi.org/10.3390/ijerph18041992>.
- Rattis L, Brando PM, Macedo MN, Spera SA, Castanho ADA, Marques EQ, Costa NQ, Silverio D V., Coe MT. 2021. Climatic limit for agriculture in Brazil. *Nature Climate Change*. Springer US, 11(12): 1098–1104. <https://doi.org/10.1038/s41558-021-01214-3>.
- Reboita MS, da Rocha RP, Souza CA de, Baldoni TC, Silva PLL da S, Ferreira GWS. 2022. Future Projections of Extreme Precipitation Climate Indices over South America Based on CORDEX-CORE Multimodel Ensemble. *Atmosphere*, 13(9). <https://doi.org/10.3390/atmos13091463>.

Riahi K, van Vuuren DP, Kriegler E, Edmonds J, O'Neill BC, Fujimori S, Bauer N, Calvin K, Dellink R, Fricko O, Lutz W, Popp A, Cuaresma JC, KC S, Leimbach M, Jiang L, Kram T, Rao S, Emmerling J, Ebi K, Hasegawa T, Havlik P, Humpenöder F, Da Silva LA, Smith S, Stehfest E, Bosetti V, Eom J, Gernaat D, Masui T, Rogelj J, Strefler J, Drouet L, Krey V, Luderer G, Harmsen M, Takahashi K, Baumstark L, Doelman JC, Kainuma M, Klimont Z, Marangoni G, Lotze-Campen H, Obersteiner M, Tabeau A, Tavoni M. 2017. The Shared Socioeconomic Pathways and their energy, land use, and greenhouse gas emissions implications: An overview. *Global Environmental Change*, 42: 153–168. <https://doi.org/10.1016/j.gloenvcha.2016.05.009>.

Rodrigues RR, McPhaden MJ. 2014. Why did the 2011–2012 La Niña cause a severe drought in the Brazilian Northeast? *Geophysical Research Letters*, 1012–1018. <https://doi.org/10.1002/2013GL058703>. Received.

Rosenzweig C, Iglesias A, Yang XB, Epstein PR, Chivian E. 2001. Implications for food production, plant diseases, and pests. *Global Change and Human Health*, 2(2): 90–104. <https://doi.org/10.1023/A:1015086831467>.

Salvador MA, de Brito JIB. 2018. Trend of annual temperature and frequency of extreme events in the MATOPIBA region of Brazil. *Theoretical and Applied Climatology*. Theoretical and Applied Climatology, 133(1–2): 253–261. <https://doi.org/10.1007/s00704-017-2179-5>.

Santos JYG dos, Montenegro SMGL, Silva RM da, Santos CAG, Quinn NW, Dantas APX, Ribeiro Neto A. 2021. Modeling the impacts of future LULC and climate change on runoff and sediment yield in a strategic basin in the Caatinga/Atlantic forest ecotone of Brazil. *Catena*, 203(March). <https://doi.org/10.1016/j.catena.2021.105308>.

Schlenker W, Roberts MJ. 2009. Nonlinear temperature effects indicate severe damages to U.S. crop yields under climate change. *Proceedings of the National Academy of Sciences of the United States of America*, 106(43). <https://doi.org/10.1073/pnas.0910618106>.

Sillmann J, Kharin V V., Zwiers FW, Zhang X, Bronaugh D. 2013. Climate extremes indices in the CMIP5 multimodel ensemble: Part 2. Future climate projections. *Journal of Geophysical Research Atmospheres*, 118(6): 2473–2493. <https://doi.org/10.1002/jgrd.50188>.

Silva AF, Neto AR. 2019. *As Principais Culturas Anuais E Bianaais Na Agricultura Familiar*. In: Freire de Melo, R. & Voltolini, T. V. (Eds.) *Agricultura Familiar Dependente de Chuva No Semiárido*. Brasília.

Silva VDPR, Campos JHBC, Silva MT, Azevedo P V. 2010. Impact of global warming on cowpea bean cultivation in northeastern Brazil. *Agricultural Water Management*. Elsevier B.V., 97(11): 1760–1768. <https://doi.org/10.1016/j.agwat.2010.06.006>.

Sinclair ATR, Devi J, Shekoofa A, Choudhary S, Sadok W, Vadez V, Rufty T. 2017. Limited-transpiration response to high vapor pressure deficit in crop species. *Plant Science*. Elsevier Ireland Ltd. <https://doi.org/10.1016/j.plantsci.2017.04.007>.

Siqueira PP, Oliveira PTS, Bressiani D, Meira Neto AA, Rodrigues DBB. 2021. Effects of climate and land cover changes on water availability in a Brazilian Cerrado basin. *Journal of Hydrology: Regional Studies*. Elsevier B.V., 37(September 2020): 100931. <https://doi.org/10.1016/j.ejrh.2021.100931>.

Strand J, Soares-Filho B, Costa MH, Oliveira U, Ribeiro SC, Pires GF, Oliveira A, Rajão R, May P, van der Hoff R, Siikamäki J, da Motta RS, Toman M. 2018. Spatially explicit valuation of the Brazilian Amazon Forest's Ecosystem Services. *Nature Sustainability*. Springer US, 1(11): 657–664. <https://doi.org/10.1038/s41893-018-0175-0>.

SUDENE. 2017. *Delimitação do semiárido brasileiro*. Superintendência de desenvolvimento do nordeste.

Tanure TM do P, Domingues EP, Magalhães AS. 2024. Regional impacts of climate change on agricultural productivity: evidence on large-scale and family farming in Brazil. *Revista de Economia e*

Sociologia Rural, 62(1): 1–26. <https://doi.org/10.1590/1806-9479.2022.262515>.

Taylor KE, Stouffer RJ, Meehl GA. 2012. An overview of CMIP5 and the experiment design. *Bulletin of the American Meteorological Society*, 93(4): 485–498. <https://doi.org/10.1175/BAMS-D-11-00094.1>.

Teutschbein C, Seibert J. 2012. Bias correction of regional climate model simulations for hydrological climate-change impact studies: Review and evaluation of different methods. *Journal of Hydrology*. Elsevier B.V., 456–457: 12–29. <https://doi.org/10.1016/j.jhydrol.2012.05.052>.

Thrasher B, Wang W, Michaelis A, Melton F, Lee T, Nemani R. 2022. NASA Global Daily Downscaled Projections, CMIP6. *Scientific Data*. Springer US, 9(1): 1–6. <https://doi.org/10.1038/s41597-022-01393-4>.

Vogel E, Donat MG, Alexander L V., Meinshausen M, Ray DK, Karoly D, Meinshausen N, Frieler K. 2019. The effects of climate extremes on global agricultural yields. *Environmental Research Letters*. IOP Publishing, 14(5). <https://doi.org/10.1088/1748-9326/ab154b>.

Xavier AC, King CW, Scanlon BR. 2016. Daily gridded meteorological variables in Brazil (1980–2013). *International Journal of Climatology*, 36(6): 2644–2659. <https://doi.org/10.1002/joc.4518>.

Xavier AC, Scanlon BR, King CW, Alves AI. 2022. New improved Brazilian daily weather gridded data (1961–2020). *International Journal of Climatology*, (October 2021): 1–15. <https://doi.org/10.1002/joc.7731>.

Zilli M, Scarabello M, Soterroni AC, Valin H, Mosnier A, Leclère D, Havlik P, Kraxner F, Lopes MA, Ramos FM. 2020. The impact of climate change on Brazil's agriculture. *Science of the Total Environment*. Elsevier B.V, 740: 139384. <https://doi.org/10.1016/j.scitotenv.2020.139384>.

Zuluaga CF, Avila-Diaz A, Justino FB, Martins FR, Ceron WL. 2022. The climate change perspective of photovoltaic power potential in Brazil. *Renewable Energy*. Elsevier Ltd, 193: 1019–1031. <https://doi.org/10.1016/j.renene.2022.05.029>.